CHEMICALLY AMPLIFIED RESISTS FOR ELECTRON BEAM LITHOGRAPHY

by

HASNAH MOHD ZAID

A thesis submitted to
The University of Birmingham
for the degree of
DOCTOR OF PHILOSOPHY

Nanoscale Physics Research Laboratory
School of Physics and Astronomy
The University of Birmingham
March 2006

Abstract

This thesis describes the development of chemically amplified resists for electron beam lithography. The techniques and concepts of lithography are discussed and the motivations for the development of chemically amplified resists are examined. The experimental techniques used in this work are then described. Two groups of resists, derivatives of fullerene and derivatives of triphenylene, were tested for chemical amplification and the results obtained from the research are presented.

A systematic study of the response of several methanofullerenes and polysubstituted triphenylene derivatives before and after chemical amplification is presented. Films of the compounds were prepared by dissolving the resists in solvents such as chloroform and adding to the solution various concentrations of certain photoacid generators and crosslinkers, and spin coating the mixture on hydrogen terminated silicon wafers. The films were irradiated using 20 keV electrons. Post exposure bakes between 90 to 120 °C for 30 to 180 s were applied to the resists before development with non-polar solvents such as monochlorobenzene. Most of the chemically amplified resists showed sensitivity enhancement compared to their pure counterparts. Fullerene derivative, 3' H-cyclopropa [1, 9, 5, 6] fullerene-C60-Ih - 3', 3'- carboxylic [2-2-(2-hydroxyethoxy) ethoxyl ethyl] ester (a mixture of adducts) demonstrated the highest sensitivity enhancement with the incorporation of an epoxy novolac crosslinker and bis[4-di(phenylsulfonio) phenyl]sulfide bis(hexafluorophoshate) as photoacid generator with a sensitivity of ~8 $\mu C/cm^2$ and a resolution of ~24 nm. The polysubstituted triphenylene derivative, 2,6,10-trihydroxy-3,7,11-tri(pentyloxy) triphenylene, showed a sensitivity of ~5 $\mu C/cm^2$ when the crosslinker hexamethoxymethylmelamine and the photoacid generator triphenylsulfonium triflate were added to the compound. However, fine patterning in the resist was not very successful due to acid diffusion. An alternative triphenylene derivative similar to 2,6,10-trihydroxy-3,7,11-tri(pentyloxy) triphenylene, with epoxides incorporated into the structure showed better results with the photoinitiator bis[4-di(phenylsulfonio) phenyl]sulfide bis(hexa fluorophoshate). The chemically amplified C5/epoxide demonstrated a sensitivity of ~9 $\mu C/cm^2$ and a resolution of 40 nm. The etch durabilities of these chemically amplified resists for dry plasma etching with SF_6 are reasonably high, comparable to a conventional high durability novolac resist.

Acknowledgement

First and foremost, I would like to thank my supervisors, Professor Richard Palmer, for giving me the opportunity to work on this research, and Dr Alex P.G. Robinson, to whom I'm greatly indebted, for his patience, constant support and guidance.

This research would not have been possible without the support from the School of Chemistry at the University of Birmingham. In that note I would like to thank Professor Jon Preece and Dr Manickam and their group, for preparing the compounds needed for the study. I would also like to thank Professor Preece for taking the time to try to help me understand the chemistry of resists.

I would also like to convey my appreciation to other members of the nanoscale group, past and present, for sharing their knowledge and experience. To Dr Andy Parker for sharing his expertise on high resolution imaging on the SEM, to Dr Susanne Jacke for sharing her knowledge on the application of lithographic software, and last but certainly not least to Francis Gibbons who is always ready to share his ideas and to lend a helping hand. Thanks to all the other people in the group for making NPRL a place conducive for study.

Acknowledgement is also due to Rohm and Haas electronics for sponsoring a major part of the research, and Universiti Teknologi Petronas, Malaysia, for sponsoring my studies.

Finally, I would like to thank my parents and family who have always offered their support and encouragement throughout my studies. I dedicate this thesis to my husband Azman, for the love, encouragement and support he always gives me. Praise be with Allah, the Almighty, for making this possible.

"The ideals which have lighted my way, and time after time have given me new courage to face life cheerfully, have been Kindness, Beauty, and Truth."

- Albert Einstein

Contents

Abstract i

Acknowledgement iii

List of Figures vii

Abbreviations and Acronyms x

Commercial Resist Acronyms xi

Chapter 1: Introduction 1

1.1 Lithography 3

1.2 Photolithography 4

1.2.1 Contact exposure 5

1.2.2 Proximity exposure 6

1.2.3 Projection exposure 6

1.3 The Lithography Roadmap 13

1.4 Next Generation Lithography 15

1.4.1 Immersion lithography 16

1.4.2 Extreme Ultraviolet Lithography 18

1.4.3 Other Lithography Techniques 20

1.4.4 Electron Beam Lithography 23

1.5 New Electron Beam Technologies 26

1.5.1 MAPPER Lithography 26

1.5.2 PREVAIL 27

1.5.3 Low-Energy Electron Beam Proximity Lithography 29

1.6 Electron Beam Resists 32

1.6.1 Exposure of Electron Beam Resists 32

1.6.2 Electron solid interaction 33

1.6.3 Characteristics of Resists 35

1.6.4 Current Resists 39

1.7 Chemically Amplified Resist 47

1.7.1 Chemically Amplified Electron Beam Resists 49

1.7.2 Factors that affect the responses of CARs 53

1.7.3 Techniques to improve CARs performance 61

Chapter 2: Experimental Techniques 66
2.1 Compounds, Crosslinkers and Photoacid Generators 67
2.1.1 Derivatives of Fullerene 67
2.1.2 Derivatives of Triphenylene 69
2.1.3 Crosslinkers 70
2.1.4 Photoacid Generators 71
2.2 Sample Preparation 72
2.2.1 Substrate Preparation 72
2.2.2 Spin Coating 73
2.2.3 Post-application Bake 73
2.3 Exposure 74
2.3.1 The Scanning Electron Microscope 74
2.3.2 Sensitivity Test 79
2.3.3 Resolution Testing 80
2.4 Resist Development 81
2.4.1 Post-exposure bake 81
2.4.2 Development 81
2.5 Sample analysis 82
2.5.1 The Surface Profiler 82
2.5.2 Response Curve 83
2.6 Etch Durability 85
2.6.1 Plasma Asher 86
2.6.2 Normalised etch durability 87
Chapter 3: Chemical Amplification of Fullerene Derivatives 88
3.1 Film Preparation 89
3.2 Sensitivity 90
3.2.1 Chemical amplification using PAG03-01 90
3.2.2 Chemical amplification using PAG03-01 and CL03-01 92
3.2.3 MF04-01 and MF04-02 94
3.2.4 Chemical amplification of MF03-04 95
3.2.5 Other Fullerene Derivatives 97

3.3 Delay effects 98
3.4 Etch Resistance 99
3.5 Resolution 100
3.6 Conclusions 102
Chapter 4: Chemical Amplification of Triphenylene Derivatives 103
4.1 Film Preparation 104
4.2 Sensitivity 104
4.2.1 C5/C5 104
4.2.2 C5/C0 105
4.2.3 Sensitivity vs PAG and crosslinker concentration 106
4.2.4 Sensitivity dependence on PEB conditions 107
4.3 Resolution 109
4.4 Etch Resistance 111
4.5 Conclusions 111
Chapter 5: Chemically Amplified Triphenylene Epoxide 113
5.1 Sensitivity 114
5.1.1 Sensitivity of C5/Epoxide 114
5.1.2 Sensitivity of C5/Epoxide + Photoacid generator 116
5.1.3 Sensitivity of C5/Epoxide + Photoinitiator 116
5.1.4 Sensitivity of C5/Epoxide + C5/C0 + Photoinitiator 119
5.1.5 Sensitivity vs Beam Energy 120
5.2 Resolution 120
5.3 Etch Resistance 122
5.4 Conclusions 123
Chapter 6: Discussion and Outlook 124
6.1 Discussion and Conclusion 125
6.2 Future Work 127
Appendix A 129
C_{60} Derivative Acronyms 129
Polysubstituted Triphenylene Derivative Acronyms 130
References: 131

List of Figures

1.1	Moore's Law for the scaling of semiconductor devices in the IC	2
1.2	The principles of lithography	4
1.3	Contact exposure	5
1.4	Near field (Fresnel) diffraction of light in proximity exposure	7
1.5	Schematic diagram of projection photolithography	8
1.6	Far field (Fraunhoffer) diffraction of light in projection photolithography	8
1.7	Exposure using phase-shift mask	11
1.8	Off-axis illumination	12
1.9	Exposure using mask with optical proximity correction	13
1.10	Immersion lithography replaces air with water to increase the value of NA	17
1.11	Schematic representation of the EUV lithography system	19
1.12	Schematic diagram of the MAPPER concept	27
1.13	PREVAIL electron optics	28
1.14	Principle of operation of the LEEPL system	30
1.15	Simulation showing electrons interactions in a resist at 2 keV and 10 keV	31
1.16	Exposure of resist by backscattered electrons resulting in proximity effects	34
1.17	Response curves for (a) positive resist and (b) negative resist	36
1.18	Chain scission of poly(methyl methacrylate)	40
1.19	Chemical structure of hydrogen silsesquioxane	41
1.20	Structure of calixarene derivatives	43
1.21	Chemical structure of a catechol derivative	44
1.22	A fullerene derivative with a functional group attached to the fullerene cage	45
1.23	Chemical structure of polysubstituted triphenylene derivatives	47
1.24	Chemical amplification schemes	48
1.25	Structure of calixarene derivative TOMCA4	51
1.26	Chemical equilibrium between acetal-protected-PHS and PHS	52
1.27	Tert-butoxycarbonyl group-protected poly(p-vinylphenol) type polymer	53
1.28	Effect of molecular size on resolution and line edge roughness	54
1.29	Chemical formulas of diaryliodonium and triarylsulfonium salts	55
1.30	T-top formation observed in chemically amplified positive resists	59

1.31	Set-up of electric-field-enhanced PEB	61
1.32	Simulations showing electrons interactions in a resist at 5 keV and 10 keV....	62
2.1	Chemical structures of fullerene derivatives investigated in the study..........	68
2.2	Chemical structures of triphenylene derivatives investigated in the study......	69
2.3	Chemical structure of triphenylene epoxide...	69
2.4	Chemical structures of the crosslinkers used in the study..........................	70
2.5	Chemical structures of the photoacid generators used in the study	71
2.6	Chemical structures the photoinitiators used in the study	71
2.7	The Philips FEI XL30SFEG SEM	74
2.8	A magnetic lens..	75
2.9	Cross-section through an electrostatic lens..	76
2.10	Raytrace of electrons in an SEM	77
2.11	The coordinate system of a sample with respect to that of SEM	80
2.12	The Dektak3ST Profiler	82
2.13	Response curves of (a) positive tone resist and (b) negative tone resist.........	84
2.14	The Plasmalab 80 Plus Etcher	85
2.15	Determination of the etch ratio of the resist..	86
3.1	Film thickness vs spin speed (RPM) for various concentrations of MAF5	89
3.2	Response curve of MF02-01	91
3.3	Response curve of MF02-01+PAG...	91
3.4	Response curves of MF02-01+PAG+HMMM and pure MF02-01..............	93
3.5	Optical micrograph of CA MF02-01 showing swelling and 'feathering'........	93
3.6	Pattern defined in CA MF03-01	94
3.7	Response curves of MF03-04 and PAG03-01/ PAG04-01 and CL05-01.....	95
3.8	Response curve of CA MF03-04 at various ratios of CL05-03+PAG04-01.....	96
3.9	Response curves of MF03-04+PAG04-01+CL05-03 and pure MF03-04.......	97
3.10	Response curves of various fullerene derivatives +PAG04-01+CL05-03	98
3.11	Exposure spots on samples subjected to delay in cleanroom environment	99
3.12	Exposure spots on samples subjected to delay in vacuum	99
3.13	SEM micrograph of patterns defined in CA MF03-04 resist	100
3.14	SEM micrograph of lines defined in CA MF03-04 resist	101

4.1	Exposed and developed spots in CA C5/C5	105
4.2	Response curves of CA C5/C0 compared to that of pure C5/C0	106
4.3	Sensitivity of C5/C0+PAG+CL03-01 vs PEB temperature	108
4.4	Sensitivity of C5/C0+PAG+CL03-01 vs PEB time	108
4.5	SEM micrograph of array of dots defined in C5/C0	110
4.6	SEM micrograph of array of dots defined in C5/C0	110
5.1	Response curves of C5/C0 and C5/epoxide	114
5.2	Response curves of C5/epoxide, and C5/epoxide + PAG03-01	114
5.3	Response curves of C5/epoxide+PAG04-01 at various ratios	116
5.4	Chemical amplification scheme of the C5/epoxide	117
5.5	Response curves of the composite resist C5/epoxide+C5/C0+PAG04-01	118
5.6	Response curves of CA C5/epoxide vs beam energies	119
5.7	SEM micrograph of line patterns in CA C5/epoxide films	120
5.8	SEM micrograph of line patterns in CA C5/epoxide+C5/C0 films	121

List of Tables

Table 1.1	The ITRS Lithography Roadmap	14
Table 4.1	Sensitivity of CA C5/C0 vs PAG/CL concentrations	107
Table 6.1	Comparison of Resists	127

Abbreviations and Acronyms

CA	Chemically Amplified (indicating that a pure resist has had sensitivity component added)
CAR	Chemically Amplified Resist
DOF	Depth of Field
DPN	Dip Pen Nanolithography
DUV	Deep Ultraviolet
e-beam	Electron Beam
EBL	Electron Beam Lithography
EPL	Electron Projection Lithography
ECR	Electron Cyclotron Resonance Microwave Plasma Etching
EUV	Extreme Ultraviolet
eV	Electron Volt
IPA	Isopropanol
IPL	Ion Projection Lithography
LEEPL	Low Energy Beam Proximity Projection Lithography
MAPPER	Multi-Aperture Pixel-by-Pixel Enhancement of Resolution
MCB	Monochlorobenzene
MIBK	Methyl Isobutyl Ketone
NA	Numerical Aperture
non-CAR	Non-Chemically Amplified Resist
PREVAIL	Projection Reduction Exposure with Variable Axis Immersion Lenses
RPM	Revolutions per Minute
SCALPEL	Scattering with angular limitation in projection electron beam lithography
SEM	Scanning Electron Microscope
TMAH	Tetramethylammonium hydroxide

Commercial Resist Acronyms

PMMA	poly(methyl methacrylate)
SAL-601	(Shipley Advanced Lithography) Chemically Amplified EBL Resist (Rohm and Haas, formerly Shipley)

The abbreviations of the resist compounds presented in this thesis are given in Appendix A.

1

Introduction

Electron beam lithography is one of the most promising lithographic techniques for nanoscale patterning, thanks to its flexibility and nearly unlimited resolution capability, able to fabricate sub-50 nm features. However, while it is able to achieve resolutions that are simply not possible using conventional optical lithography, its low throughput rate has always been a disadvantage. A dramatic increase in resist sensitivity is one way to achieve an economically feasible throughput. The concept of chemical amplification of photoresists to boost their sensitivity was introduced in 1982 and is now well accepted by the lithographic community. [1] Chemically amplified resists have become technologically important to increase throughput not only for photolithography but for other lithography techniques. [2] In this chapter, the concepts of photolithography and alternative lithography techniques are described. Current electron beam lithography technology systems are discussed as well as electron beam resists and their characteristics. A review of the current status of electron beam resists and chemically amplified resists is presented. Finally, issues in chemically amplified resists and techniques to overcome them are reviewed.

It was Gordon Moore, in 1965 who predicted that the number of transistors in an integrated circuit would double every 18 months. [3] The famous Moore Curve, as shown in figure 1.1, has proven very accurate at projecting future processing power, [2] as the device density of modern computer components (i.e. the number of transistors per unit area) continues to grow exponentially. [4] A smaller device means a reduced distance for an electron to travel, thus increasing switching speed and improving efficiency. Extrapolation of the curve indicates that the size of minimum features will be less than 50 nm in the next decade which would be unrealizable using conventional lithography. Nanotechnology is seen as the next logical step for continued advances in computational architecture.

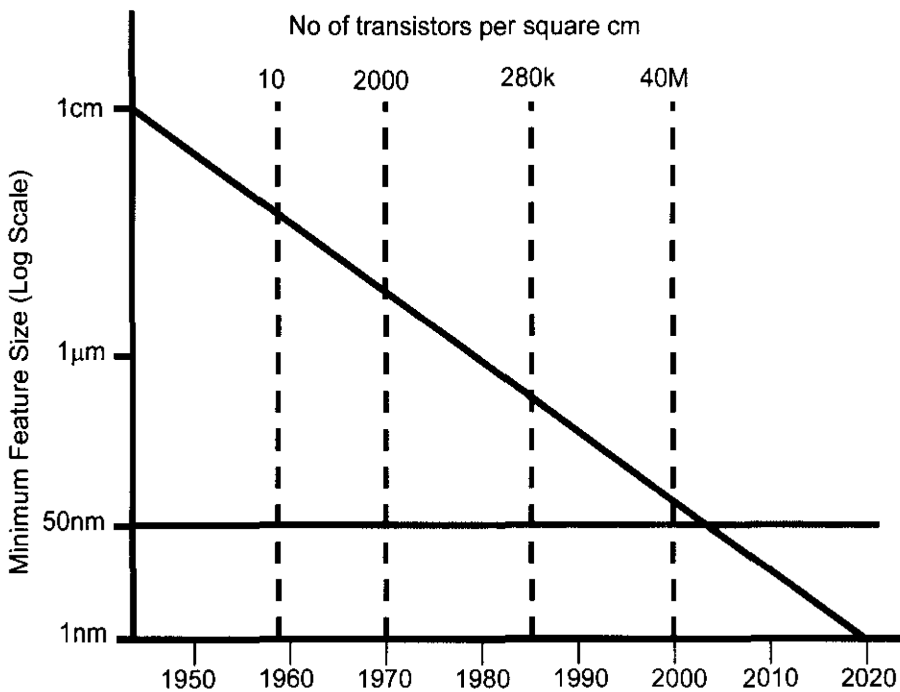

Figure 1.1 *Moore's Law for the scaling of semiconductor devices in the IC. The line at 50nm minimum feature size calls for nanoscale technologies.*

The term *nanotechnology* refers to technological developments on the nanometer scale, usually 1 to 100 nm. The two fundamentally different approaches to nanotechnology are called

'top down' and 'bottom up'. 'Top-down' refers to making nanoscale structures by removing material from the bulk using machining and etching techniques, whereas 'bottom-up', or molecular nanotechnology, applies to building organic and inorganic structures atom-by-atom, or molecule-by-molecule. The means to develop the ability to manipulate atoms and molecules was suggested by Richard Feynman in his talk '*There's Plenty of Room at the Bottom*' in 1959. [5] Nanotechnology, as applied today, mainly utilises 'top-down' techniques. Examples of this approach include the various lithographic techniques such as photolithography, ion and electron beam lithography, and X-ray lithography, which are used to pattern protective masks on the surface (resists) before removing material via etching, adding material via evaporating or sputtering, or altering material properties via doping.

1.1 Lithography

Lithography is the process of transferring patterns to a substrate. It can be used, for example, to fabricate integrated circuits. A beam of radiation, such as photons or ions is projected onto a suitable resist material coated on a wafer, causing chemical changes in the resist. For instance the solubility of the resist in a certain solvent may change. [6] In photolithography, a photopolymer is exposed to visible light or UV radiation through a mask. The solubility of the exposed area of the polymer is increased (positive tone resist) or decreased (negative tone resist) and the exposed, or unexposed, resist is removed respectively, using a developing chemical, producing the desired pattern on the substrate for further processing.

The principle of operation of lithography is shown in figure 1.2. A radiation sensitive material, known as a resist, is coated onto the substrate as shown in figure 1.2(a). The resist is then exposed to a beam of radiation through a mask which shadows certain areas of the resist, as in figure 1.2(b). The exposed areas of the resist undergo chemical alteration. In the case of a positive resist, its solubility is increased relative to the unexposed resist allowing it to be

removed by a developer solvent, while the exposed areas of a negative resist become less soluble and are left behind upon development as shown in figure 1.2(c). [7]

The final objective of the lithographic process is the accurate replication of the pattern originally specified by the device designer onto the substrate. Its success depends on the physics and chemistry of resist exposure and development, and the ensuing pattern transfer.

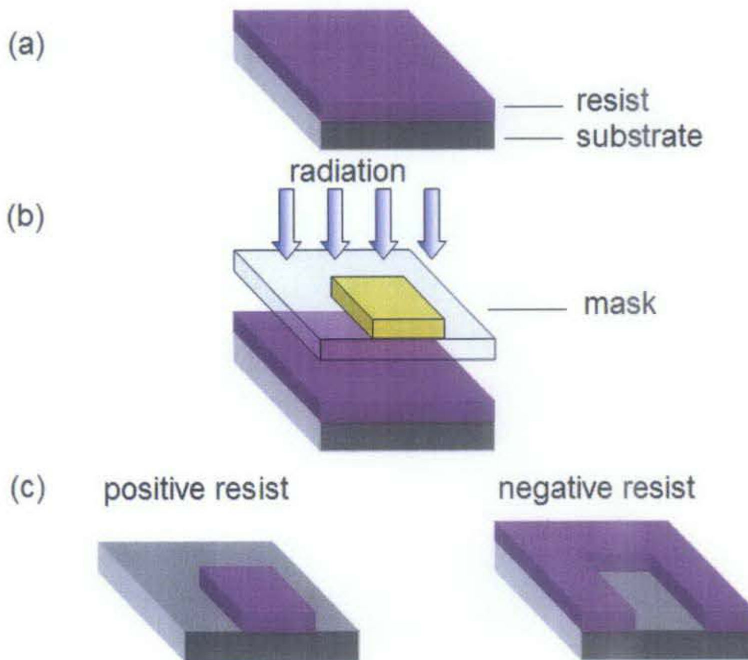

Figure 1.2 *The principles of lithography. (a) The substrate is coated with a radiation sensitive resist. (b) The resist is irradiated through a mask causing chemical modifications in the exposed areas. (c) In a positive tone resist, the exposed areas are removed upon development while in a negative tone resist, the exposed areas are retained.*

1.2 Photolithography

Photolithography (also known as optical lithography) has been the technique of choice for the fabrication of microdevices for more than 50 years, and still is the workhorse for volume manufacturing of integrated circuits. [8] It is based on the fact that many polymers are altered by exposure to light.

Light (visible or near-UV) is projected through a mask, defining the desired pattern, and then focused onto a photoresist on the wafer. The pattern defined in the polymer film on the substrate is then used as a mask for further processing of the substrate. There are three primary exposure methods: contact, proximity, and projection.

1.2.1 Contact exposure

In contact exposure, the wafer image is formed by placing the photoresist-coated wafer in contact with the mask and exposing it to light through the mask. [9] The mask used is a transparent glass plate with light-blocking patterns formed, for instance, by a metal coating. The pattern produced on the wafer is the same size as that on the mask. Due to the contact between resist and mask, very high resolution is possible since, as shown in figure 1.3, it is not affected by diffraction. However, this method causes contamination of the mask by the resist

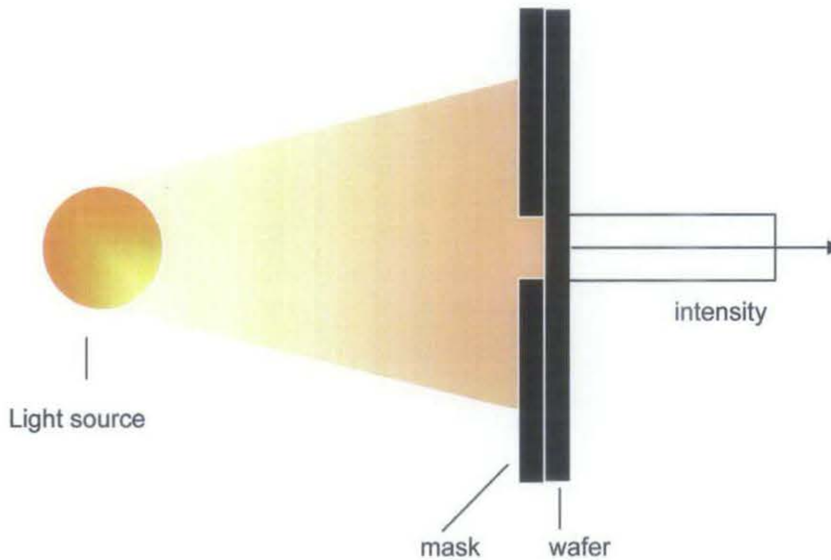

Figure 1.3 *Contact exposure is not affected by diffraction. The light intensity distribution projected through the mask is shown to be uniform. After [10]*

and tends to trap debris between the resist and mask, causing damage to the mask and defects in the resist. Furthermore, uniform contact between mask and wafer is difficult due to surface structures and warping of wafer. Mask fabrication is also difficult since the patterns on the mask are of the same size as the desired final features. Due to these problems, contact exposures are rarely used.

1.2.2 Proximity exposure

In proximity exposure, a small gap, 10 to 25 μm wide, is maintained between the wafer and the mask during exposure. As in contact exposure, this method also has a 1:1 magnification ratio, (ie the size of the pattern imaged on the wafer is the same as that on the mask). The gap helps to reduce wear and tear to the mask due to contact. However the resolution of the method is not as good as contact printing due to near field (Fresnel) diffraction. Diffraction is an inevitable consequence of the wave nature of light, and is responsible for the spreading of light as it passes through an opening with a dimension close to (or less than) the order of its wavelength. Some of the exposing light propagates at divergent angles causing a larger area of the resist to be exposed, as shown in figure 1.4.

Other than diffraction, there are a few other disadvantages of proximity printing. Although problems with trapped dust and particles are reduced due to the gap, they are not totally eliminated. Besides that, alignment is difficult due to wafer warp, which causes a variation in the distance L between mask and wafer. As in contact exposure, 1:1 mask fabrication is difficult.

1.2.3 Projection exposure

The third method of exposure is projection exposure. This method avoids mask damage entirely with a total separation between mask and wafer. In projection lithography, an image of the

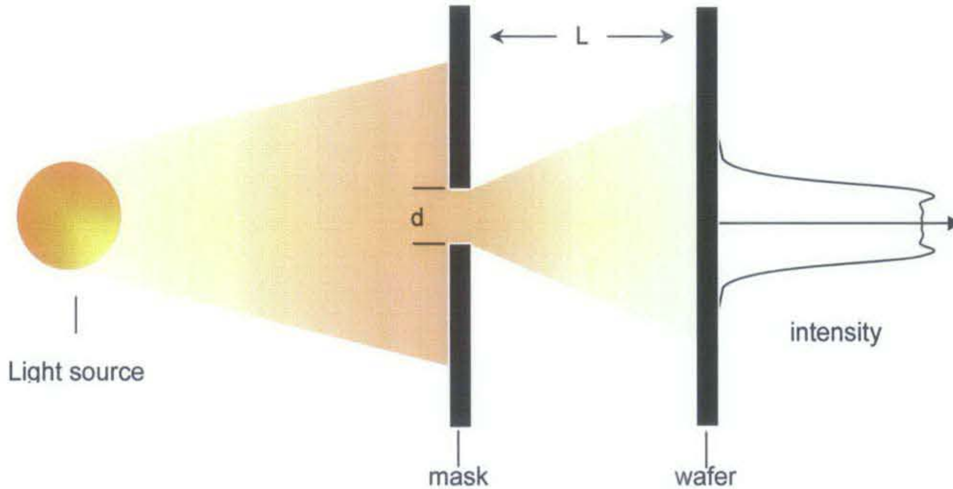

Figure 1.4 *Near field (Fresnel) diffraction of light through an opening, d, when $L < d^2/\lambda$ in proximity exposure. The light intensity distribution shows the diffraction effect. After [10]*

patterns on the mask, usually demagnified by 4 or 5 times, is projected onto the resist-coated wafer, which is many centimetres away, using a system of lenses [9] as shown in figure 1.5.

A stepper system with a high speed stage that moves the wafer is used. Instead of a full field exposure, where the entire wafer is exposed at once, as in contact and proximity exposure, a stepper exposes only part of the wafer at a time and repeats the process until the entire wafer is exposed. [6] Furthermore, the demagnification of the pattern allows less constraint on the mask pattern accuracy, since the final patterns are 4 or 5 times smaller than those on the mask, and therefore any defect or variation on the patterns would be significantly reduced.

The problem with projection photolithography is that as sizes of exposed details approach the wavelength of the exposing radiation, diffraction effects at the edges of the patterns become prominent. [6] The large separation between mask and wafer, L, causes far field (Fraunhoffer) diffraction, as shown in figure 1.6.

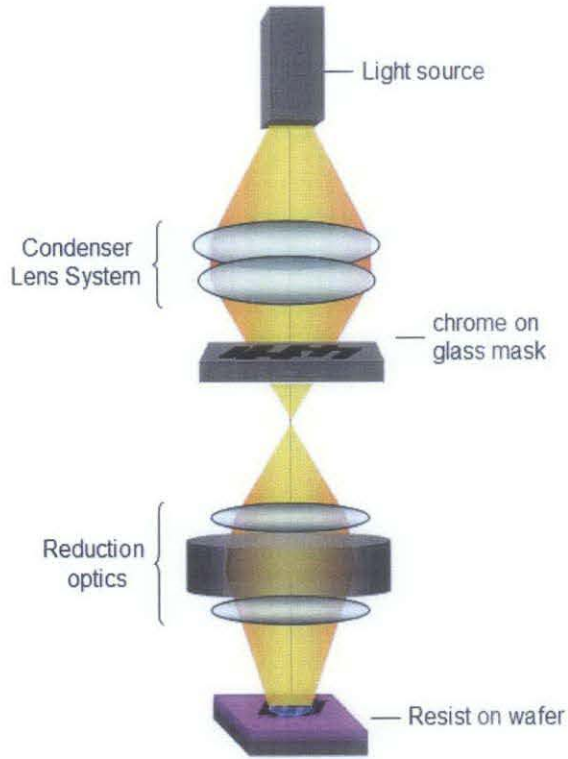

Figure 1.5 *Schematic diagram of projection photolithography*

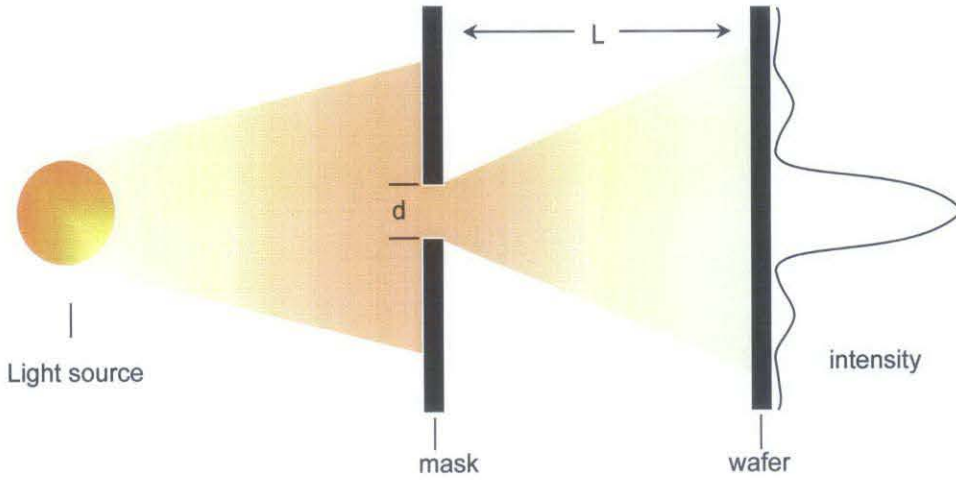

Figure 1.6 *Far field (Fraunhoffer) diffraction of light through an opening d when $L > d^2/\lambda$ in projection photolithography. The light intensity distribution shows the diffraction effect. After [10]*

The limits and performance of projection photolithography can be characterized by two equations. The minimum resolved feature size, d_{min}, or resolution, is given by the equation

$$d_{min} = k_1 \frac{\lambda}{NA}, \quad (1.1)$$

where λ is the wavelength of the exposing light and k_1 is a characteristic constant of the specific lithographic process, which typically has a value in the range of 0.5 to 1.0. [6] The value of k_1 generally depends on the lithographic equipment, resist, process parameters, the type of mask and the pattern being imaged. *NA* is the numerical aperture of the optical system, which is equal to the sine of the angle subtended by the objective lens of the system multiplied by the refractive index of the surrounding medium (~1 for air). [11] The *NA* of optical lithography systems today ranges between 0.5 and 0.6. [12] Based on equation (1.1) and the values of k_1 and *NA*, the minimum feature would be approximately equal to the wavelength of the light used.

The depth of focus, *DOF*, or the range over which the image is adequately sharp, is given by the equation

$$DOF = k_2 \frac{\lambda}{NA^2}. \quad (1.2)$$

Here, k_2 is another characteristic constant of the specific lithographic process, and is usually about 1.0. Depth-of-focus is important in defining whether an optical projection system is physically realizable. [2] A large value of *DOF* is desirable since it increases the tolerance of the process to deviation of the substrate surface from perfect planarity, which can be caused by previously created surface structures or wafer warping, amongst other things.

Referring to equation 1.1, we can see that a better resolution can be achieved by either increasing the numerical aperture (*NA*) or reducing the wavelength, or both. In immersion lithography, which will be discussed further in section 1.4.1, *NA* is increased by replacing the medium surrounding the objective lens with that of a higher refractive index. In other cases, increasing the *NA* of the lens system would require either an increase in the diameter of the lens

or reducing its focal length which would mean an increase in lens size and mass. Not only would this result in an increase in complexity of the overall lens system which provides correction for optical aberration, [11] but an increase in lens size would mean an increase in cost. Furthermore, since the *DOF* is inversely proportional to the square of *NA*, a resolution improvement achieved by increasing *NA* would be accompanied by a relatively larger decrease in *DOF*. Therefore, reducing wavelength is usually a better option.

In the past, resolution improvement in optical lithography has typically been accomplished by decreasing the wavelength of light used. The progression from using g-line (436 nm) to the i-line (365 nm) light source, to using deep ultraviolet of wavelengths 248 and 193 nm, has improved the imaging resolution from 1 μm to sub-100 nm. [13] Deep Ultraviolet Lithography (DUV) can generate devices as small as 65 nm. However, reducing wavelength also decreases the depth of focus although to a lesser extent than increasing *NA*. To counteract this, the proportionality constants k_1 and k_2 have been improved by applying better resists, resist processes and "wavefront engineering", or resolution enhancement technologies (RETs), [2] which have been used to improve lithographic performance at or below the diffraction limit. The three main types are phase shifting masks, off-axis illumination and optical proximity correction.

The earliest form of phase shifting mask (PSM) is the alternating PSM, which is a mask with layers of material with the desired refractive index and thickness added to it, causing the phase of the light passing through it to shift by 180°. PSM helps to increase the resolution of patterns through constructive and/or destructive interference, and amplitude modulation, to increase intensity contrast and prevent exposure of resists in the regions that should not be exposed. Figure 1.7 illustrates the principle of the PSM and compares it to that of conventional mask. It is shown that in the case of conventional mask, the constructive interference of light from adjacent patterns causes a loss of contrast for close features. With the use of PSM, the destructive interference between the phase-shifted light from adjacent patterns minimizes the

light intensity in the dark region, improving both contrast and resolution. It is shown that PSM improves the resolution by a factor of 2, that is, reducing k_1 to 0.25. [14]

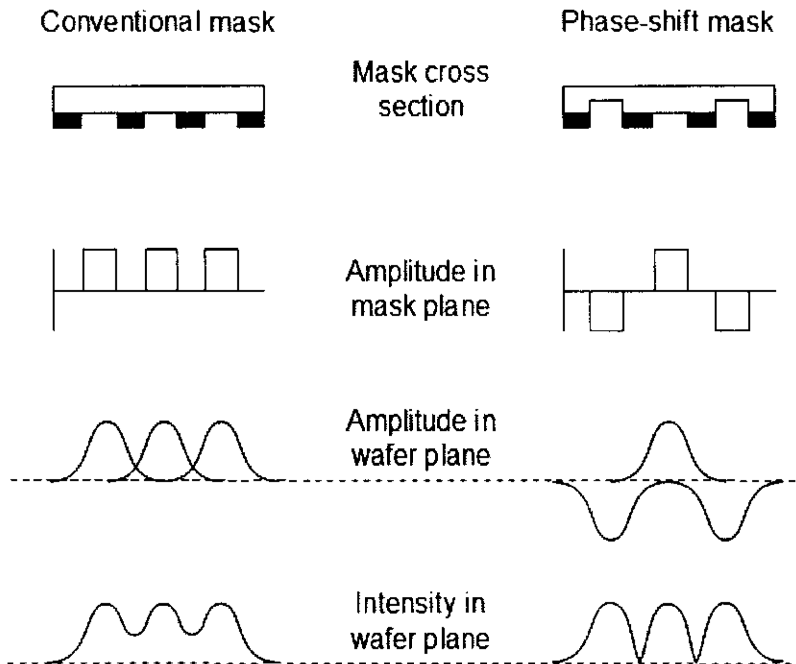

Figure 1.7 Schematic diagram comparing exposure using conventional mask (left) and phase-shift mask (right). After [14]

With off-axis illumination (OAI), the exposing light is set at an angle from the normal axis so that the zeroth order of diffraction and one of the first diffracted orders are allowed to pass through the entrance pupil of the imaging optics. Since the zeroth order of a diffracted light contains only the intensity of illumination and no spatial information, at least the first diffracted orders are required for pattern imaging. In conventional on-axis illumination as shown in figure 1.8, both first diffracted orders have to enter the aperture of the lens to produce an image. For sufficiently small dimensions, the diffracted angle would be such that all the beam except for the zeroth order are diffracted outside the lens. With off-axis illumination, the smaller angle of incidence for the zeroth and one of the first diffracted orders to enter the lens

allows imaging of smaller features. However, this method is limited by the fact that the illumination must be adjusted according to the mask pattern since different mask patterns will have different diffraction patterns.

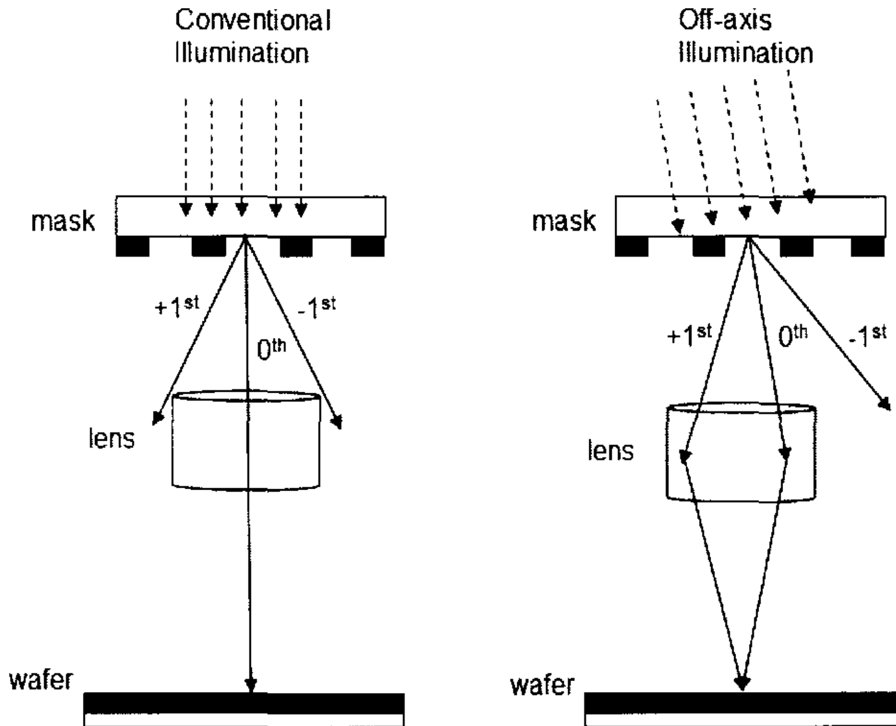

Figure 1.8 *Off-axis illumination improves resolution by allowing the zeroth and only one of the first diffracted orders to pass through the imaging lens.*

Optical proximity correction (OPC) is a method where the mask pattern is intentionally distorted so as to correct the proximity effect in the final image. Corrective features are added to the mask to counteract the divergence of the produced pattern from the original mask. For example, as shown in figure 1.9, corner rounding can be corrected by adding, or removing squares or "serifs" to the corners, and shortening of image can be corrected by lengthening the pattern on the mask. The addition of these sub-resolution features helps to improve the final image, making it closer to the desired pattern, as illustrated in the figure. However, the addition

of these correction features on the OPC mask increases its complexity and its cost. In addition, the complexity of the mask makes it susceptible to defects.

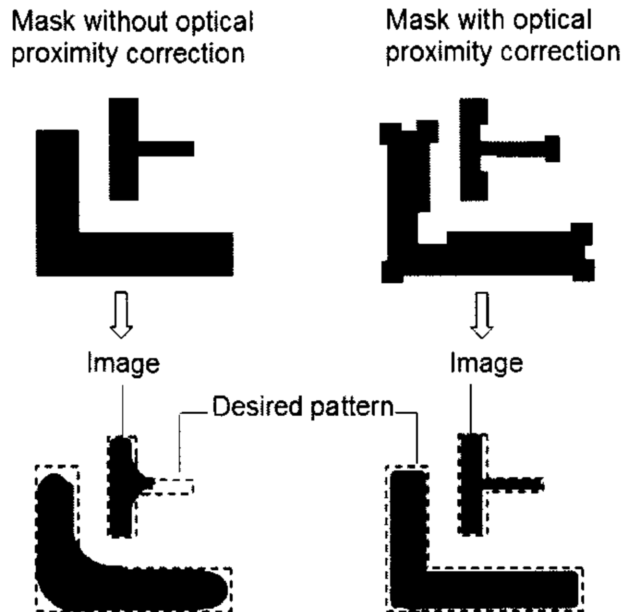

Figure 1.9 *Mask with optical proximity correction produces image closer to the desired pattern represented by the dotted lines.*

1.3 The Lithography Roadmap

One useful way to discuss the future of lithography is the 15 year International Technology Roadmap for Semiconductors (ITRS). The ITRS is an assessment of the semiconductor industry's technology requirements by the industry manufacturers and suppliers, government organisations, consortia and universities, and is updated yearly. The objective of the ITRS is to ensure advancements in the performance of integrated circuits [15] and to identify the technical capabilities that need to be developed for the industry to continue trends such as increased scaling to ensure a continuation of Moore's Law. Table 1.1 is taken from the roadmap and shows how the feature size of ICs is expected to evolve.

In table 1.1, the "technology node" is the latest lithography process, and is defined in terms of the half-pitch (HP). DRAM is the dynamic random access memory and MPU is a microprocessor unit. [15] Half-pitch is the distance between cells in a DRAM memory chip. The table indicates that minimum feature sizes of 35 nm with 65 nm pitch are expected in 2007.

TABLE 1.1 The ITRS Lithography Roadmap. After [15]

Year of production	2004	2007	2010	2013	2016	2018
Technology node	HP90	HP65	HP45	HP32	HP22	
DRAM ½ pitch (nm)	90.0	65.0	45.0	32.0	22.0	18.0
MPU resist gate (nm)	53.0	35.0	25.0	18.0	13.0	10.0
MPU gate precision (nm)	3.3	2.2	1.6	1.2	0.8	0.6

A higher resolution is always desired, as it means more complex integrated circuits containing larger numbers of components per unit area of substrate material can be produced. Smaller devices mean a reduced interconnect length, reducing the distance electrons have to travel and thus signal delay. For example in microprocessors, the minimum gate length of the transistors determines the speed of information processing of the chips. [16] Power dissipation due to heat is also reduced with reduced size. However, as the feature size decreases, the leakage current for a given voltage increases, thus increasing heat generation. Smaller features also mean lighter and more portable devices. In sensors, the sensitivities are increased with reductions in size due to the corresponding increase in surface area. [17,18] In terms of economy, the reduction in size means a reduction in material used and ultimately a reduction in cost, since, if the cost per wafer is maintained, there will be a significant reduction in cost per component. In general, miniaturization leads to systems with improved capability and lower prices.

So far, photolithography has shown remarkable progress in improving resolution to answer the demands of Moore's law and the semiconductor roadmaps via the reduction of radiation wavelength to 193 nm and the application of wavefront engineering. However, each shift in wavelength had to be accompanied by expensive efforts to develop appropriate light sources and imaging optics. The wavefront engineering used to improve resolution requires an increase in production cost due to mask complexity, especially in OPC and PSM. Even then, further reduction of feature sizes to meet the ITRS roadmap would require further wavelength reduction. 157-nm lithography used to be the likely answer. Unfortunately, the development of lithography using this wavelength faces several issues. The lens and mask material used at other wavelengths are unsuitable for use with 157 nm radiation. At this wavelength, the only suitable lens material is CaF_2 (calcium fluoride), the supply of which is believed to be inadequate for volume production. [19] Moreover, CaF_2 lenses have poor longevity, [20] and the effect of birefringence, a phenomenon of double refraction of light as it passes through an optically anisotropic medium such as CaF_2, is more prominent at this low wavelength. [19] The other problem is to develop a cost-effective mask pellicle, which is the soft material used to protect the mask from contamination; since the organic material used for other wavelengths do not provide the necessary transmittance and longevity. Furthermore, there is a lack of resists suitable for this wavelength. The limits of photolithography and issues of cost and throughput have motivated the development of alternative techniques of lithography.

1.4 Next Generation Lithography

Due to the limits of photolithography, several alternative lithography techniques are in development. Some techniques, such as x-ray and extreme ultraviolet lithography, use much shorter wavelengths to provide a substantial reduction of diffraction effects. Particle beams, such as electron beams, and beams of ions, like He^+, also have a very short wavelength, and

able to produce much finer features. Because of their low wavelengths, which are in the nanometer range or below, the effect of diffraction is negligible at the required feature size. Other techniques include immersion lithography which is an extension of photolithography, and nanoimprint and dip-pen lithography which employ mechanical means of pattern transfer. All of these techniques have been developed to further improve the minimum feature size.

1.4.1 Immersion lithography

Immersion lithography is a technique for improving the resolution of optical lithography by increasing the numerical aperture of the optical system. The numerical aperture, NA, which is the cone half-angle subtended by the entrance aperture of the system viewed from the point the optical axis intersects the imaging plane, is given by

$$NA = n \sin \theta , \tag{1.3}$$

where n is the index of refraction of the medium surrounding the lens as shown in figure 1.10(a). In conventional lithography, where the medium is air (n is approximately equal to 1), the maximum physical value of NA is 1. In immersion lithography, the air-filled gap between the lens and the wafer is replaced with a liquid of refractive index, $n > 1$, increasing the numerical aperture, NA, as shown in figure 1.10(b).

From equation 1.1, and 1.3, we can see that the resolution limit can be improved by an increase in numerical aperture, which is proportional to the value of n. The immersion liquid should have an index of refraction >1, have low optical absorption at 193 nm, be compatible with photoresist and the lens material, be uniform and non-contaminating. Ultrapure water is currently one of the most suitable candidates. Simulations have shown the capability of printing features smaller than 45 nm at λ = 193 nm, and smaller than 35 nm at λ = 157 nm. [21] Its refractive index increases at shorter wavelength, reaching 1.44 at 193 nm, while its absorption remains low. [22] A resolution of 38 nm has been achieved using 193-nm imaging and NA of 1.26. [22]

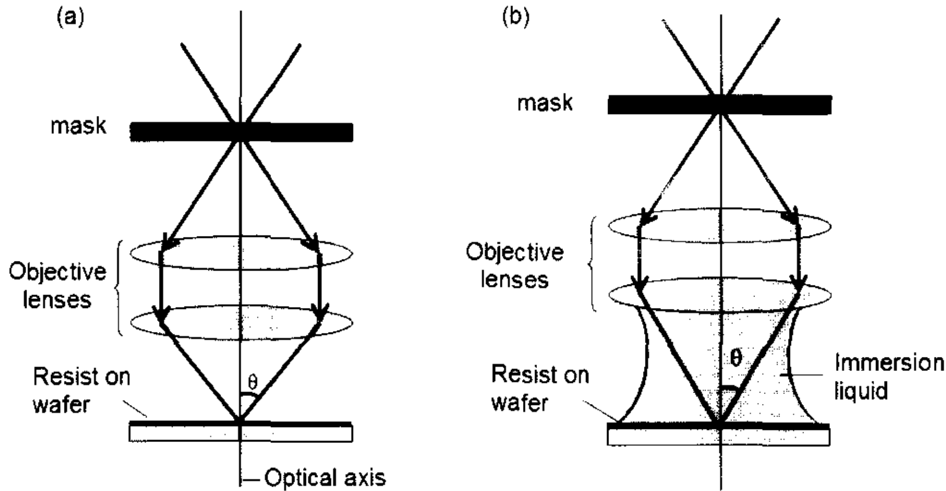

Figure 1.10 *The numerical aperture, NA is defined as n sin θ in (a) where n is the refractive index of the medium surrounding the lens. (b) In immersion lithography air is replaced with an immersion liquid such as water to increase the value of NA.*

However, there are some issues with immersion lithography that are still to be addressed. It is difficult to maintain a consistent bubble free liquid between the lens and the wafer. The impact of bubbles, which depends on their size, location and density, will affect the imaging of patterns by scattering, obstructing, or redirecting the light. [23] A method to remove bubbles and prevent them from reforming as the wafer stage moves for step and repeat, or step and scan process, has to be developed. The temperature of the immersion liquid also needs to be maintained since a variation in temperature would cause a variation in n and therefore image distortion. The rapid movement of the stage while in contact with the liquid could produce heating. Another problem is particle contamination, which is much higher in liquid as compared to in air. The immersion liquid should also be compatible with the lens and the photoresist used. Future extension of liquid immersion lithography would depend on the ability to identify or engineer a more suitable immersion liquid and the technology to maintain a consistent, bubble-free and contamination-free liquid in the space between the lens and wafer. [22]

1.4.2 Extreme Ultraviolet Lithography

In Extreme Ultraviolet Lithography (EUV), resolution is improved by reducing the wavelength, using 13.4-nm radiation. These photons can be produced by either a synchrotron or laser-produced-plasma (LPP). Most current EUV source use LPP since synchrotrons facilities are more costly. [24] LPP sources use a pulsed laser beam focused onto a target to produce light with a broad emission which includes the EUV wavelength. Since solid metal targets produce a lot of debris, a target using clusters of xenon is usually used. [24] The LPP produces a point-like source converting 0.8% to 3.8% of the incident laser power into EUV light of the required wavelength. The principle of operation of EUV lithography is similar to projection photolithography, but due to its short wavelength, EUV radiation is absorbed in virtually all materials, so the imaging systems are entirely reflective. Instead of lenses, it is focused by multi-layer mirrors (Bragg reflectors) [25] as shown in figure 1.11. Multilayer mirrors are surfaces coated with alternating multilayer thin films of dissimilar optical constants, such as molybdenum and silicon, such that they provide constructive interference in the direction of reflection.

The condenser is a system of mirrors which collect the EUV from the source and adjust the beam so that it illuminates the mask uniformly. The EUV mask consists of high reflectance multilayer coated substrates with patterns made of an EUV absorbing metal layer. [24] The reflected beam then goes through a system of reduction mirrors before exposing the resist on the wafer. Since the short wavelength of EUV is strongly absorbed by air, exposure has to be done in an ultra high vacuum system. [25]

Although EUV enables printing of feature sizes less than 100 nm due to its short wavelength, and even though the high throughput tool may be capable of 32 nm resolution, [25] there are some drawbacks to this technique. The shape of the multiple-layers mirrors used requires a fabrication accuracy that is hard to realize due to the extremely tight tolerance on the

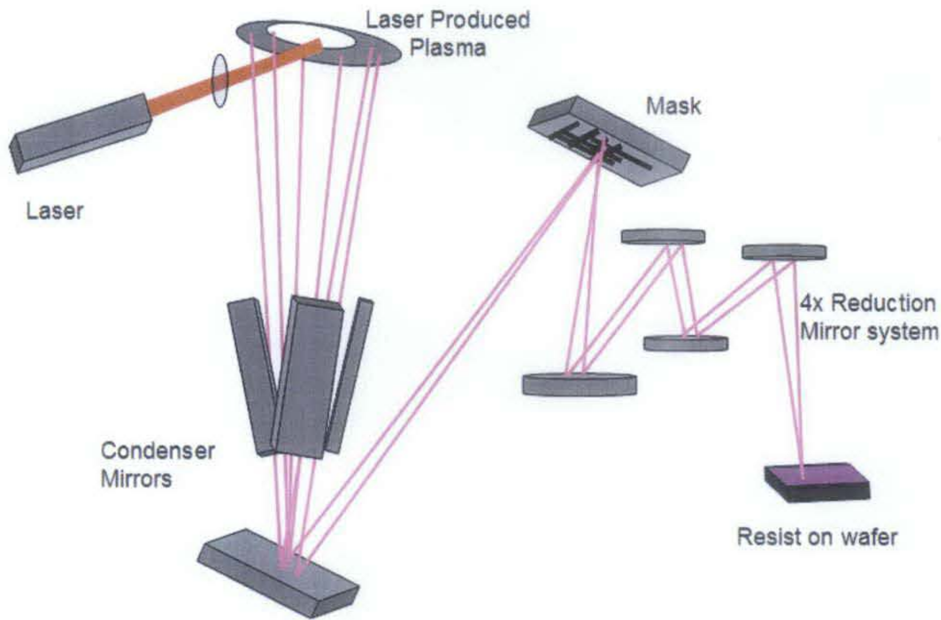

Figure 1.11 Schematic representation of the EUV lithography system.

pattern and surface-roughness. The layers of films on the mirrors themselves, which could number tens or hundreds, have to be deposited accurately to thicknesses of only a few nm. Transmission efficiency is also poor due to the power absorbed in each of the reflecting surfaces which usually have between 50 to 60% reflectivity. The multi-layer substrate used, which is almost impossible to repair, requires a very low defect level, which is hard to achieve. It is very difficult to repair a damaged region in the mask, which is a planar reflector with a heavy metal absorber patterned on its surface. [2] Besides that, debris from the plasma source can cause contamination. It is also hard to find a suitable resist material since it is hard to find a sufficiently transparent material and thus an extremely thin resist, that is, 100 nm or below, is required. [26]

1.4.3 Other Lithography Techniques

Numerous replacements for photolithography have been studied. However, most of these techniques have problems with cost, throughput, and/or practicality. Some notable techniques include dip-pen lithography, imprint, ion projection lithography (IPL) and x-ray lithography.

(a) Dip-Pen Nanolithography

Dip pen nanolithography (DPN) is a scanning probe nanopatterning technique in which an atomic force microscope (AFM) tip is used to deliver molecules to a surface via a solvent meniscus. In DPN, the AFM tip acts as a "nib" of a pen, a solid-state substrate as "paper" and molecules with a chemical affinity for the solid-state substrate as "ink". Capillary transport of molecules from the AFM tip to the solid substrate is used to directly "write" patterns consisting of a small collection of molecules onto the substrate. [27] This direct-write technique offers high-resolution patterning capabilities for a number of molecular and biomolecular 'inks' on a variety of substrates, such as semiconductors and metals.

The main advantage of DPN is its simplicity, and ability to achieve resolution comparable to more expensive and sophisticated competitive lithographic methods. However, DPN has major drawbacks which include its very slow speed writing, inherent to the AFM motion. Moreover, the 'ink' needs to be replenished periodically, which involves dismounting the AFM probe, interrupting the writing process.

(b) Nanoimprint Lithography

Nanoimprint Lithography (NIL) is a method of transferring patterns by mechanical means. NIL uses a hard mould, that contains nanoscale features defined on its surface, to emboss a resist cast under controlled temperature and pressure conditions, creating a thickness contrast in the resist. [28] There are several variants of nanoimprint lithography, with slight process differences with one another. In Thermoplastic Nanoimprint Lithography, a thin layer of

imprint resist, a thermal plastic polymer, is spin-coated onto the substrate. Then the mould, or template, is pressed against the resist and the assembly is heated until the polymer film melts and conforms into the patterns on the template. After being cooled down, the template is separated from the substrate, leaving behind a patterned resist. In Photocurable Nanoimprint Lithography, a transparent template is pressed into a low viscosity photocurable resist liquid such that it conforms to the topology of the template. Then, instead of heating as in the Thermoplastic Nanoimprint, the resist is irradiated with UV light to cure it, producing a relatively rigid polymer network. [29] In the Step-and-Flash Imprint Lithography, the substrate is coated with an organic transfer layer and a transparent template is aligned to the coated substrate. Then, a low-viscosity photopolymerizable solution is dropped into the gap between the template and substrate so that the solution spreads out and fills the gap. The template is then pressed against the substrate and UV light is irradiated through the back of the template to cure the photopolymer and solidify it. Then the template is removed, leaving the cured, patterned photopolymer resist. [28]

Although NIL has proved to be successful in nanopatterning, and is capable of 14 nm pitch lines, [29] it has several limitations as a flexible lithographic technique. First of all, the pattern can be degraded during removal of the mould from the resist. Furthermore, NIL requires perfect planary of both substrate and template for precise pattern transfer. Fabrication of a good quality 1× template is also a challenge. The direct contact between template and resist results in fast wear and contamination. Since the features of the mould physically deform and displace the polymer, except in the Step-and-Flash method, larger features on the mould would displace more polymer material over larger distances. Therefore, larger features would be more difficult to imprint. Besides that, the high viscosity of the fluid and the complexity of the mould pattern can result in an incomplete pattern transfer. [28]

(c) Ion Projection Lithography

Ion Projection Lithography (IPL) is very similar to electron projection lithography (discussed in section 1.4.4) except that, instead of electrons, it uses lightweight ions, such as H^+, H_2^+, H_3^+, or He^+, to expose the photoresist. The ions are accelerated by an electric field and the beam usually operates between 50 to 150 keV. [30] The ions pass through a patterned stencil mask and are focused and projected on to the wafer by electrostatic lenses. The wavelength of ions is extremely short; H^+ with energy 150 keV has a wavelength $<10^{-4}$ nm; and thus diffraction can be ignored. As the ions penetrate the resist, they lose a large proportion of their energy to the electrons in the molecules of the resist and substrate, so their path is almost straight line enabling good resolution. Feature sizes of 65 nm have been achieved with IPL and a throughput of 50 to 120 wafers per hour of 200 mm wafers has been estimated. [30]

However, IPL has some major disadvantages. The only viable mask is a stencil mask, with holes in the mask to allow ions to pass through. This severely circumscribes the available patterns, not allowing for instance, annular structures (donut shapes) in a single mask. To form closed paths on the wafer, two masks are required with extremely tight alignment. The high energy ion beams can induce erosion and damage to both mask and wafers. Absorbed ions cause mask heating that leads to distortion to the patterns in the mask. Furthermore, ion beams require vacuum operation which limits access to the lithography machine. [30]

(d) X-Ray Lithography

The X-ray exposure system is similar, in principle, to photolithographic contact printing, with an x-ray beam, of wavelength between 0.4 to 4 nm, being used to expose the sensitive material instead of a light beam. The x-ray beam is usually generated by a synchrotron radiation source. A mask, made of a thin membrane which allows x-ray to pass through, such as silicon nitride, with patterns made of x-ray absorbing material, such as gold, is used. [31] In x-ray proximity lithography, the mask is held within a few microns of the resist-coated substrate, allowing large

areas to be exposed, and is thus suitable for mass production of circuits. Features as small as 20 nm have been demonstrated. [32] One problem with x-ray lithography is that, since the mask is placed very close to the substrate, its pattern must be the same size as the final desired features on the chips, making mask fabrication more difficult and expensive. The mask must also be very thin to be transparent to the radiation, and requires extremely tight alignment. Mask damage would also occur quickly due to the high energy of x-ray radiation. In addition to that, the cost of x-ray lithographic tools, which include the synchrotron x-ray source and the mask, is very high. [33]

1.4.4 Electron Beam Lithography

In electron beam lithography (EBL), electrons are used to write a pattern in an electron sensitive resist coated on the substrate. The technique consists of scanning a beam of electrons across a surface covered with a resist film, thus depositing energy in the desired pattern into the film. [34] The main advantage of EBL over other methods of lithography is its very high resolution [34] which is due to the very small spot size of the electron beams, and the ability to create arbitrary patterns rather than requiring a mask. The wavelength of the electron beam is so small that diffraction is negligible. The de Broglie wavelength of an electron is given by the equation

$$\lambda = \frac{hc}{eV}, \tag{1.4}$$

where λ is in meters and the accelerating voltage V is in Volts. For example, electrons accelerated at 10 – 100 keV would have a wavelength of 0.0123 – 0.0039 nm. Therefore, the theoretical resolution is not limited by diffraction. Arbitrary patterns are possible because the electron beam can be steered using electrostatic and electromagnetic fields which can be generated from a virtual (computer) mask.

The most important current use of EBL is in photomask production. Masks are made by coating a chrome clad glass plate with e-beam sensitive resist layer, which is subsequently exposed and developed to generate the required pattern on the mask. In contrast to optical lithography systems, electron-beam lithography systems are not limited by diffraction, but instead, their ultimate attainable resolution is limited by beam-solid interactions, beam diameter which in turn is affected space charge, and the resist used. There are two basic types of electron beam exposure equipment - "direct write" and "projection systems". [35]

(a) Direct Write

Direct write EBL systems are the most common. Most direct write systems use an electron beam with small diameter, that is moved with respect to the wafer to expose the wafer one 'pixel' at a time. The electron beam is focused to a fine spot at the surface of the resist, and is scanned electronically to trace out the desired pattern in the resist film, [34] blanking the beam to move from one structure to the next. Direct write systems can be classified as raster scan or vector scan. In raster scan, the beam travels over the entire substrate, turning on and off depending whether the area is to be exposed or not. With the vector scan, the beam scans selected areas only. After a certain area is completely scanned, the beam is turned off and moved to another area that needs to be exposed. The raster scan is more common since it is simpler and cheaper. However it is comparatively slow. The vector scan, on the other hand, is faster, but since it requires more complicated hardware and software, is more expensive. Direct write is a method that can be used to generate submicron patterns, but, since the process takes a long time, it is not suitable for industrial mass production of circuits.

(b) Projection systems

Electron projection lithography (EPL) is basically similar to optical lithography but, instead of a quartz mask with chromium patterns, uses a solid membrane with holes (stencil mask) to

pattern the electron beam. [12] Electrons are absorbed in the solid parts of the mask. The short wavelength of the electron beam allows EPL systems to achieve extremely small feature sizes, significantly less than 50 nm. The projection system can expose a large area in a short time, but patterns can only be reproduced from an appropriate mask fabricated by some other method. As mentioned earlier, stencil masks limit the possible patterns, since they do not allow, for instance, annular structures in a single mask, so at least two masks are required to form closed paths on the wafer. Another problem with EPL is that the electrons absorbed in the mask cause it to heat up and distort. One of the first EPL tools, Scattering with Angular Limitation Projection Electron beam Lithography (SCALPEL), used masks with scattering contrast to overcome the mask heating problem. The SCALPEL mask was made up of thin membrane of low atomic number material which allows electron to pass through, and patterns made up of a high atomic-number material which is transparent but scattered electrons at large angles, to be subsequently stopped by a separate aperture plate. [36] However, there were some problems with the SCALPEL technology. The mutual repulsion of electrons, or space charge effect, led to the defocusing of the beam. When low beam current was used to reduce space charge effects, it resulted in a very low throughput (~1.5 wafers per hour per μA of current). [37] Furthermore, although the mask membrane was transparent to the electrons, some small energy loss did occur which led to image blur, affecting the resolution. When the beam current was increased for higher throughput, the space charge effects added to the image blur. If the beam size was enlarged to increase the effective electron field at the wafer (another way to increase throughput) it compromised the support of the mask design and reduced pattern placement performance. Hence, generally, the major problem for SCALPEL was throughput.

1.5 New Electron Beam Technologies

In spite of EBL's ability to achieve high resolution, throughput is a serious challenge. To address this issue, a number of techniques which enhance throughput have been proposed. These techniques include the "multiple aperture pixel by pixel enhancement of resolution" (MAPPER), Projection Reduction Exposure with Variable Axis Immersion Lenses (PREVAIL) and Low-Energy Electron Beam Proximity Lithography (LEEPL).

1.5.1 MAPPER Lithography

The "multiple aperture pixel by pixel enhancement of resolution" (MAPPER) lithography uses a concept which combines electron projection lithography and microcolumn technology. The system consists of a Tantalum disc electron source with collimator and deflectors, and a lens array, as shown in figure 1.12. The electron beam from the electron source is split up into 13000 electron beams separated by 2 μm, arranged to form a rectangular slit with a width of 26 mm, the same width of a field in an optical stepper. [38]

During exposure, the electron beams are deflected over 2 μm perpendicular to the wafer stage movement, exposing a full field of 26 mm x 33 mm with one scan. [39] Each of the electron beams has its own optical column to avoid a central cross-over. The beams are focussed on the wafer by miniature electrostatic lens array. The pitch between the lenses is 150 μm. The beams are switched on and off by light signals generated in a data system that contains the chip patterns, one light signal for each electron beam. In a test set-up used for exposure tests using 10 keV electrons, 30-nm lines at 140 nm pitch was realised. However, in order to limit resist heating and backscattering effects for high throughput, an electron energy of 5 keV will be used. A throughput of approximately ten wafers per hour has been estimated. [38]

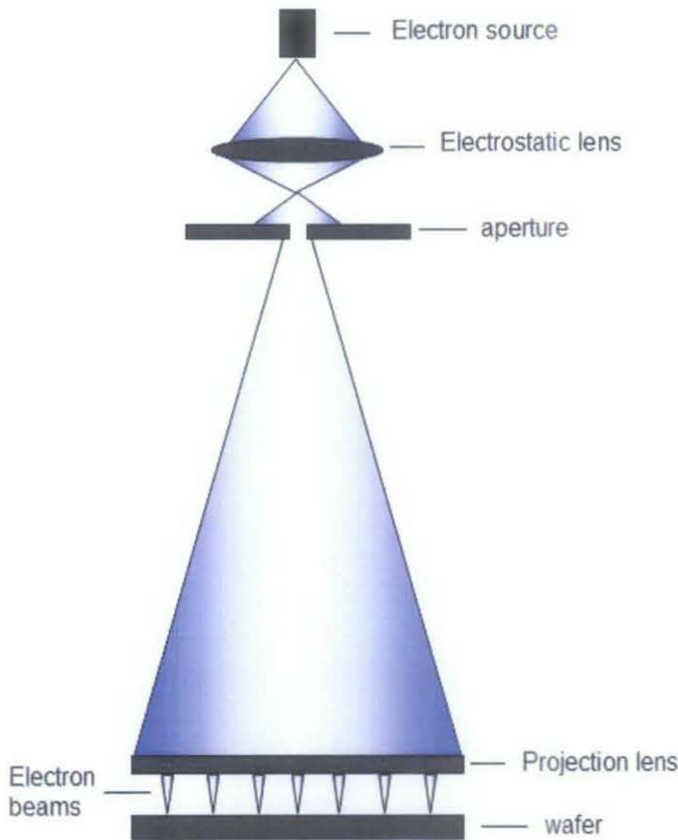

Figure 1.12 *Schematic diagram of the multi electron beam test set-up of the MAPPER concept. After [38]*

1.5.2 Projection Reduction Exposure with Variable Axis Immersion Lenses

Projection Reduction Exposure with Variable Axis Immersion Lenses (PREVAIL), shown in figure 1.13, is a technique explored by researchers in the IBM Microelectronic Division and Nikon Corporation. The main problem with most electron lithography systems is that the field size is limited by off-axis aberration. Off-axis aberration is a blurring of image due to electrons which are too far from the optical axis not being focused to the same point as the other electrons passing through the same electron lens. Due to the small field size, most systems would require mechanical stitching of the pattern subfield by aligning the mask and wafer. This

'stitching' process is limited by stage speed, resulting in low throughput. PREVAIL uses variable axis lenses to avoid off-axis aberration and therefore increases the field size and thus the throughput. [40] In PREVAIL, the electron optical axis is electronically shifted along a predetermined curvature and the beam is deflected to follow the curvilinear variable axis, as depicted by the bent beam path in figure 1.13. This is achieved by the superposition of various magnetic deflection fields. [41]

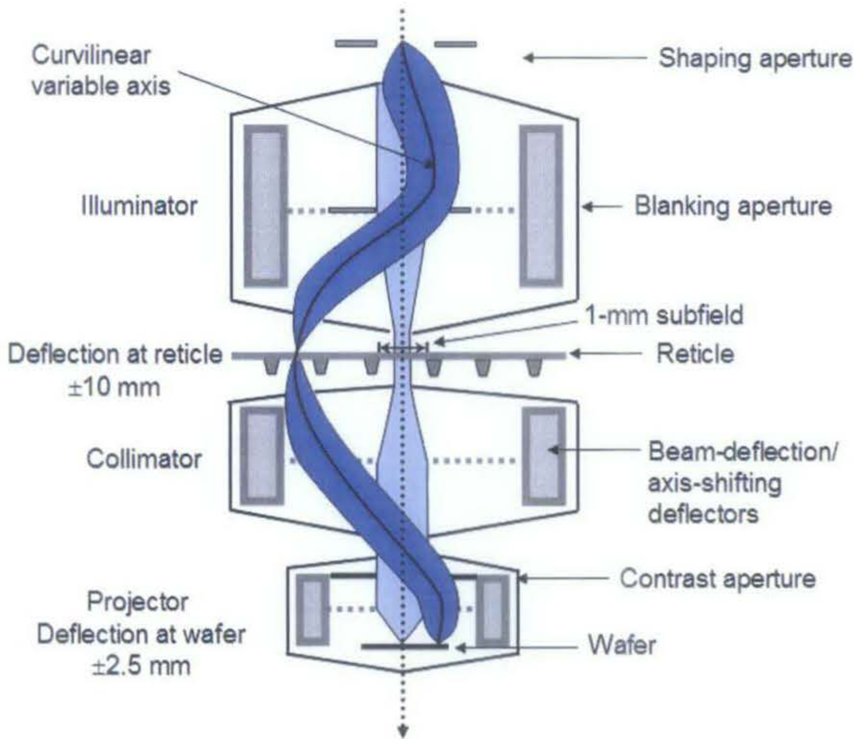

Figure 1.13 PREVAIL electron optics. After [40]

The electron-beam column consists of an electron source, a first lens system to generate a square-shaped beam to allow exposure of a square subfield on the wafer, an illuminator lens system to provide illumination of the individual square subfield of the mask, a collimator which consists of beam-deflection and axis-shifting deflectors to scan the beam and

to control exposure timing, and a projector lens system to project the mask subfields, reduced in size, onto the wafer.

The stencil mask is made of 2-μm-thick membrane, 'opaque' areas through which the electrons pass through with sufficient lateral scattering to be absorbed by the contrast aperture, and 'holes' through which the electron pass without interaction and reach the wafer for pattern exposure. Any annular shapes require a complimentary subfield pattern and double exposure, as with other stencil mask techniques. The mask is mounted on a movable stage in the chamber, between illumination and imaging section, while the wafer is mounted on a similar stage below the imaging section.

In the proof-of-concept of the system, patterns were exposed by illumination at 10 mm from the physical column axis in the mask plane and 2.5 mm off the axis at the wafer plane, to verify the elimination of off-axis aberration. The fabrication of 80-nm lines and space patterns in a 300-nm-thick resist was demonstrated. [41,42] It was also shown that the PREVAIL system, with an optical field of 5 mm at the wafer plane, was able to produce a throughput of twenty-eight 200-mm wafer per hour, compared to one 200-mm wafer per hour throughput of a system with stationary beam.

1.5.3 Low-Energy Electron Beam Proximity Lithography

Low-Energy Electron Beam Proximity Lithography (LEEPL) uses a parallel beam of low-energy electrons and proximity projection. Its exposure system is similar to X-ray proximity lithography, where the mask is placed close to the wafer, with the X-ray beam replaced with a beam of electrons at low energy. The use of low energy electrons increases the resist sensitivity and greatly minimizes the proximity effect as explained in section 1.6.2. A thermal field emission electron gun is used as a source of electrons with energy 2 keV and a condenser lens forms a well-collimated electron beam of about 1 mm in diameter [43,44] as shown in figure 1.14.

The beam illuminates a stencil mask and patterns of the same size as the mask are transferred to the resist on the wafer by scanning the beam over the mask plane using a set of main deflectors. In addition to the main deflectors, there are fine tuning deflectors, which tilt the beam at a pivotal point in the mask plane and allow for correction of mask distortion. The stencil mask is made in a 0.5-μm-thick silicon membrane. Due to the low energy of the electrons, the mask used in LEEPL does not require an absorbing metal layer of high atomic number which had been a major cause of mask distortion [43] in other projection systems.

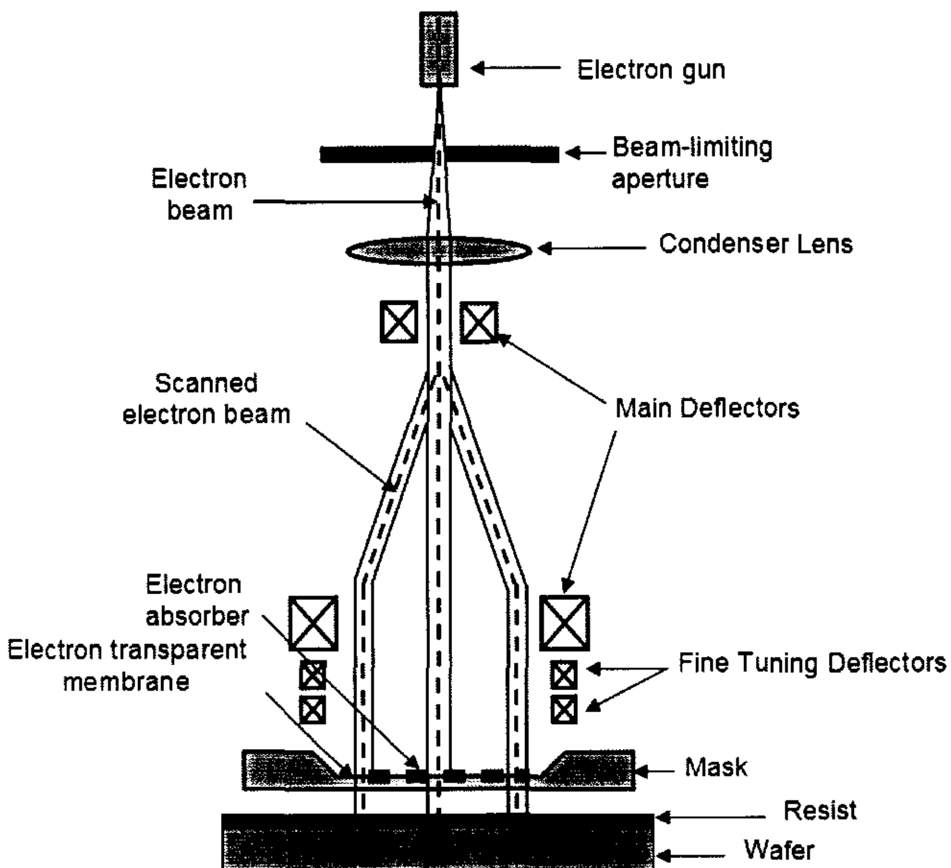

Figure 1.14 Principle of operation of LEEPL system. After [43]

The use of a low-energy beam virtually eliminates radiation damage to masks and wafers. Furthermore, it has been shown that mask heating due to electron absorption causes a maximum mask distortion of 10 nm, without any special cooling system (if the beam power is maintained at not more than 6 mW). [43] The forward scattering of low energy electrons in the resist does however create a spheriodal exposure region whose diameter is larger than the original beam diameter, which affects the spatial resolution. This behaviour can be shown in the simulations [45] as shown in figure 1.15 which compares the electron trajectory for 2 keV and 10 keV electrons as they enter the resist.

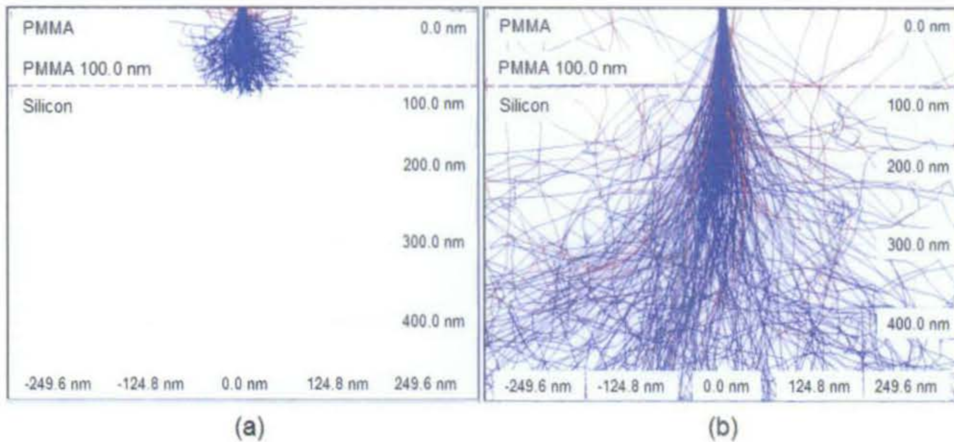

Figure 1.15 *Simulations showing electron interactions in a resist at (a) 2 keV and (b) 10 keV energy. The resist used is 100 nm of PMMA. The blue lines represent primary electrons and the red lines backscattered electrons.*

In figure 1.15(a), the 2 keV electrons remain mostly in a spherical region within the resist, with very little backscattering. On the other hand, the higher energy electrons in figure 1.15(b) form a thinner path through the resist (less forward scattering), but with many more backscattered electrons. Nevertheless, after taking into account all the possible contributions which would affect the resolution, the system resolution is estimated to be below 50 nm, and, at a total exposing power of 6 mW, the wafer throughput to be thirty to forty 300-mm wafers per hour. [43,44]

1.6 Electron Beam Resists

Electron beam resists are the recording and transfer media for electron beam lithography, with a function similar to film in photography. They are usually polymeric materials that are modified by exposure to electrons. Following exposure, the resist is developed by immersion in a suitable solvent which would remove either the exposed or unexposed areas of the resist. After development, the resist pattern is most often then used either as a mask for subsequent deposition of a material, such as dopants or a metal layer, or as an etch mask during etching of the underlying material to alter its topology. Therefore, as well as sensitivity to electrons, the resist must be able to protect the underlying substrate during subsequent processing, that is, it should be mechanically stable to allow high quality deposition and durable enough to resist etchants.

For pattern recording, the resist must be capable of easy application to give uniform and reproducible film thickness, sufficiently sensitive to the exposing radiation to be economically useful and have adequate resolution. For subsequent process steps, it must have strong adhesion to the substrate, be durable, and have a sufficiently high melting point so as to allow deposition and etching, but also be easily and completely removable after the subsequent processing. [35]

1.6.1 Exposure of Electron Beam Resists

There are two types of resist, positive tone and negative tone. In the former, the exposed areas are removed by a suitable developer, whereas the unexposed areas are removed for a negative resist. Typically a positive tone resist would be used when the retained area is more than 50% of the overall area, and negative tone for less than 50%.

When an electron strikes the resist, it can cause a number of different reactions. For instance, two molecules may crosslink forming a larger less soluble molecule (negative tone).

Alternatively, a polymer chain may be broken into smaller fragments (chain scission) increasing solubility (positive tone). Both reactions can happen at the same time, but in most materials, one reaction dominates over the other. After irradiation, there is a net increase or decrease in the solubility of the resist [35] resulting in either positive or negative tone. Electron irradiation can also cause an extensive rupture of the main chain to form volatile fragments so that no development is required, as in self-developing resists, [35] which can only be positive tones. Another type of reaction is a change in polarity, bringing about a dual tone resist. An example is the mixture of poly(4-*t*-butoxycarbonyl oxystyrene) and an 'onium' salt. Exposure leads to a polar compound which would produce a positive tone image if developed in polar solvents, and a negative tone one if developed in non-polar solvents. [35]

1.6.2 Electron solid interaction

Although the resolution of electron beam lithography is not limited by diffraction, it is very much limited by the scattering of electrons which occur when they enter the resist and penetrate further into the substrate. The two types of scattering are forward and back- scattering. Forward scattering occurs when electrons are deflected by small angles as they enter a resist. These small angle deflections lead to an overall increase of the beam diameter which results in the exposure of a larger area in the resist, reducing resolution. The extent of the diameter increase depends on both the beam energy and resist thickness. Since forward scattering causes the beam diameter to increase as the electron penetrates further into the resist, its effect can be reduced by using thinner films. Forward scattering can also be reduced by increasing the beam energy. This effect has been illustrated in the simulation shown in figure 1.15.

Backscattering is a process whereby electrons are deflected at large angles and occurs mostly in the substrate, which typically has a higher atomic number than the resist. Backscattering can be reduced by using electrons with lower energy, or using substrates with lower atomic weight. Backscattered electrons sometimes return into the resist at very large

distances from the point where they first entered it, causing the proximity effect, a phenomenon where certain areas of a resist receive a larger dose than intended, due to backscattered electrons from neighbouring areas, as shown in figure 1.16. The proximity effect is one of the most serious problems experienced in EBL. It leads to over exposure in some areas and unwanted exposure in others. However, this effect can be mitigated by adjusting the electron dose and pattern size and shape until the desired image is obtained. Several software packages allow the necessary dose corrections to be calculated, such as CAPROX, produced by Raith GmbH. [34]

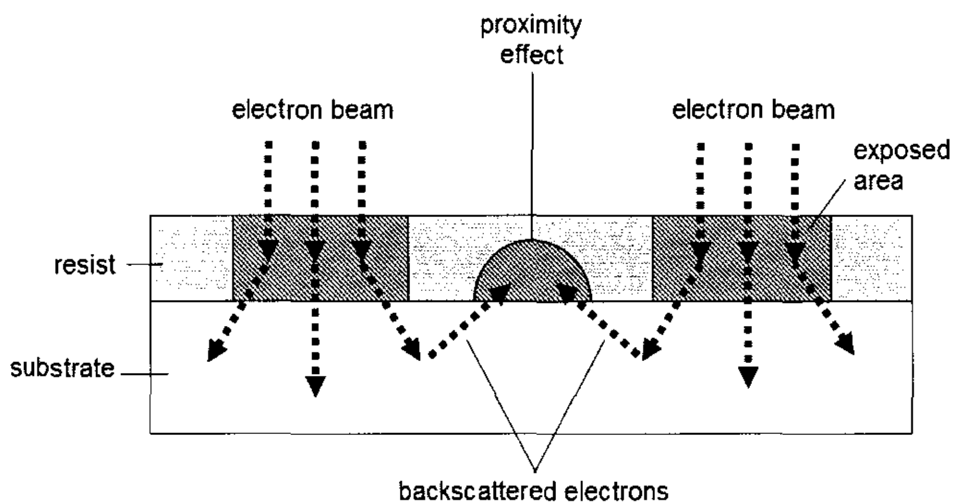

Figure 1.16 Exposure of resist by backscattered electrons from neighbouring areas results in proximity effect.

When the electrons in the electron beam enter, or are backscattered into, the resist they can deposit energy in the film. These electrons can collide inelastically with the electrons in the molecules of the resist or substrate, dissipating much of their energy in the form of secondary electrons. These secondary electrons have energies in the 2 to 50 eV range and are responsible for the majority of exposure of the resist. [34] They lead to an effective widening of the beam diameter, affecting the resolution but since their range in resist is only a few nanometers, they contribute little to the proximity effect.

1.6.3 Characteristics of Resists

There are a number of characteristics that determines whether a resist is useful, the main ones being sensitivity, resolution, contrast, and etch resistance.

(a) Sensitivity

The sensitivity of a resist is a measure of the dose of electrons required to expose it. A high sensitivity resist is generally desirable because less time is required to expose patterns. The sensitivity can be determined by plotting the thickness of resist after development against the exposure dose. This is also called the response curve, and is shown in figure 1.17. When a resist is exposed to radiation, its solubility gradually changes. For a positive resist, it becomes more soluble, so the thickness after development would decrease with dose. For a negative resist, the solubility decreases, so the retained film thickness increases with dose. To plot the response curve, areas on the resist are exposed to a range of electron doses, and then developed. The dose, D, of electrons received by an area of the film is given by equation:

$$D = \frac{It}{A}, \tag{1.5}$$

where I is the sample current of electrons in amps, t, the exposure time in seconds and A, the area of the exposure site in square centimetres. The retained film thickness in the exposed areas is measured using a surface profiler and is plotted against the dose received by that area, on a log-linear scale. The sensitivity of a positive resist is defined as the dose necessary to clear all of the film from the substrate (D_2 in Figure 1.17(a)), while for a negative resist it is defined as the dose at which 50% of the resist thickness is retained (D_3 in figure 1.17(b). [46]

The sensitivity of a resist depends on several factors. In most positive resists, the sensitivity increases with the molecular weight of the resist polymer. [35] This is due to the fact that only a few chain scissions are necessary to substantially alter the solubility of a high molecular weight polymer. A larger molecule would also have a larger cross section and hence

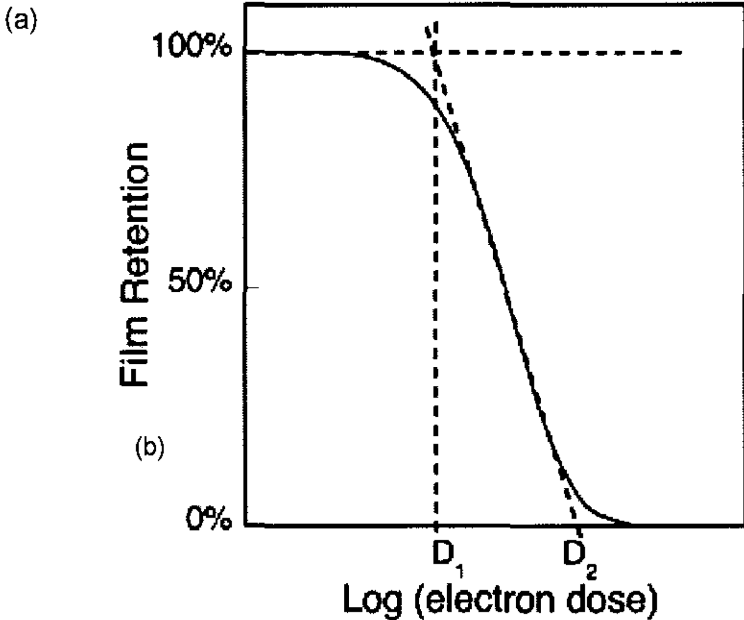

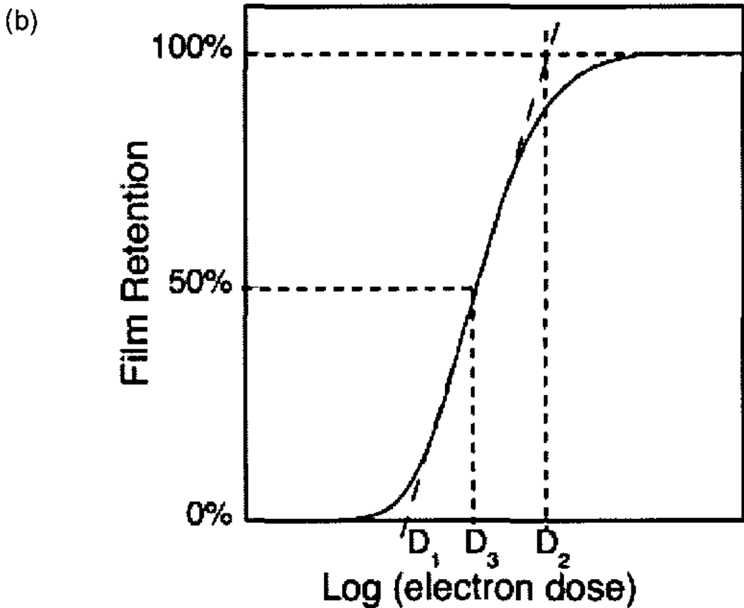

Figure 1.17 Response curves of a resist upon electron irradiation and development for (a) positive resist and (b) negative resist.

a higher probability of electron interactions. The sensitivity is also affected by the electron energy. An electron with lower energy is more likely to interact with the resist layer rather than reaching the underlying substrate. Therefore, the required exposure dose is reduced. Hence, as long as the electron has enough energy to expose even the bottom of the resist film (thereby ensuring that the pattern is not undercut, and hence removed, on development), the sensitivity is higher at lower electron energy. Another factor that affects the sensitivity of the resist is the atomic weight of the substrate. The heavier the atoms of the substrate, the higher the electron cross section and therefore the greater the level of backscattering, returning the electrons back into the resist, which also leads to an apparent increase in the sensitivity of the resist. [35]

(b) **Resolution**

The resolution of a resist is usually indicated by the minimum feature size that can be resolved by the resist. However, it can also be defined as the minimum half pitch of dense lines and spaces, which is a more useful measure of lithographic use. [12] In practice, the smallest possible linewidth achievable would depend on not only the resist, but the lithographic system and processing conditions. The beam size and current of the system can determine minimum feature size. Resolution also depends on the electron energy. As the electron energy is increased, the effect of forward scattering become less pronounced, as shown in the simulation in figure 1.15, producing wall profiles that are more nearly vertical, thus better resolution may be achieved. [34] However, a greater electron energy produces more back scattering leading to proximity effects which would affect the resolution of dense features. As already explained in section 1.6.2, the use of thinner resist reduces the effects of forward scattering, and thus increases the resolution. [47] Although lower energy electrons undergo more forward scattering compared to high energy ones, the range of scattering depends on the electron energy. For example, at electron energy 5 keV and below, both forward and backscattering are significantly reduced. Therefore, using sufficiently low energy electrons can also improve resolution. As the

energy is increased from 5 keV to 20 keV, the effect of both forward and backscattering significantly increases the exposed resist area, while at 20 keV and above, the almost straight path of the electrons leads to the improvement of resolution.

(c) Contrast

The contrast of a resist is a measure of how fast its solubility changes when it is exposed to radiation. It is defined as the slope of the response curve shown in figure 1.17. In the curve, D_1 is the largest dose at which a positive resist retains its original thickness, and D_2 the smallest dose for it to be completely removed, so the contrast, γ, is defined as

$$\gamma = \frac{1}{\log_{10}\left(D_2 / D_1 \right)}, \tag{1.6}$$

which is the slope of the response curve. [35] For a negative resist, the contrast is still similarly defined, with D_1 being the largest dose at which the film is completely removed, and D_2 the smallest dose where it retains its original thickness. A resist with high contrast would transition from unexposed to exposed over a small range of doses, indicated by a more vertical slope on the graph. A low contrast resist would have a wide range of doses over which the resist is only partially exposed. A high contrast resist is usually desirable since it tends to have more vertical feature sidewalls upon development compared to lower contrast resist. This is due to the lower current at the edge of the electron beam, causing a lower dose received at the edge of the pattern. For a high contrast resist, the effect is negligible, however, for a lower contrast one, the partially exposed resist at the edge of a pattern results in a sloping wall.

(d) Etch Resistance

To achieve its function, a resist must be able to protect the underlying substrate during subsequent processing. One of the processes used to alter the substrate is etching, a technique that removes substrate material from the uncovered areas. A good resist should be highly

resistant to the etching process to allow high aspect ratio to be realised. Besides, poor etch resistance causes an uneven film surface during etching that can be transferred on to the substrate. An important parameter in etching is the etch selectivity. This is the ratio between the etch rate of the material to be etched (the substrate) and the etch rate of the mask material (the resist). An ideal etch would be one where the substrate is removed whilst the resist is unaffected. A sample can be etched using a corrosive liquid (wet etch), gas or plasma (dry etch), or a beam of ions. Etching by wet chemicals is isotropic and can result in undercutting. Dry etching, such as reactive ion etching, can be highly anisotropic, resulting in a more faithful transfer of pattern.

1.6.4 Current Resists

Resists are grouped into two main categories, positive and negative tone, according to whether the exposed areas are removed, or retained, after exposure. Initially, electron beam resists were composed of electron sensitive polymers such as poly(methacrylates) or poly(sulphones) which readily form smooth, amorphous films by spin-coating. Examples of positive-tone electron beam resists include PMMA (Poly(methyl methacrylate)), PBS (Polybutene-1-sulphone) [35] EBR-9, and ZEP, [34] while negative-tone resists include polystyrene, [35] HSQ (Hydrogen SilsesQuioxane) [48,49] and SU-8. [50]

(a) PMMA (poly(methyl methacrylate))

PMMA was one of the first materials used for electron beam lithography. [34] It has been shown to provide resolution that is among the highest in any lithographic application. It is a commonly used positive resist and has demonstrated features down to <5 nm. [51] Exposure to electron irradiation causes a chain-scission producing low-molecular weight polymer fragments which are soluble in a developer [52] as shown in figure 1.18.

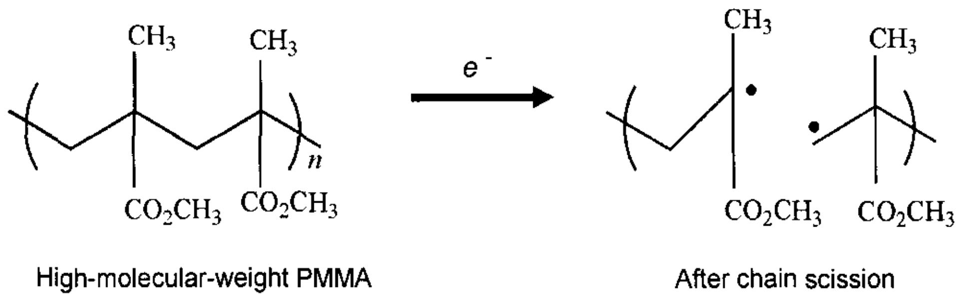

Figure 1.18 Chain scission of poly(methyl methacrylate). After [52]

Its sensitivity is ~10 μC/cm^2 at 2 keV, falling to 90 μC/cm^2 at 20 keV. Structural modification by the incorporation of highly electron-withdrawing groups had produced PMMA derivatives with sensitivities as low as 1 μC/cm^2 at 10 keV. [53] When exposed to more than 10 times the optimal positive dose, PMMA will crosslink, forming a negative resist. Its negative-tone resolution has been shown to be about 10 nm. [54] Despite excellent sensitivity and resolution, PMMA suffers from poor resistance to corrosive etching conditions, compared to novolac-based photoresists, [52] as discussed in section 1.7.1.

(b) Hydrogen SilsesQuioxane

Hydrogen SilsesQuioxane (HSQ) can be described as a siloxane-based polymer wherein every silicon atom is bound to three oxygen atoms and one hydrogen atom with the exception of the terminal silicon atom, where one of the oxygen atoms is replaced by an H group. [48,49] Alternatively, HSQ can be described as caged oligomer structures with the general formula $(HSiO_{3/2})_{2n}$ as shown in figure 1.19. HSQ is a high-resolution negative-tone inorganic resist for electron beam lithography. Isolated 6-nm-wide lines and 27 nm period gratings using 50 keV electrons have been demonstrated. [55] HSQ also shows negative-tone resist behaviour for X-ray, and photolithography with wavelengths from 157 nm and below. [56] In extreme ultraviolet (EUV) lithography, HSQ has been shown to have a sensitivity of 11.5 mJ/cm^2 and a

resolution of 26 nm. [57] Although HSQ is capable of high resolution and has demonstrated etch durability comparable to novolac resist, [58] its sensitivity in EBL is only ~200 μC/cm^2 at 50 keV [48] making it unsuitable for high throughput applications.

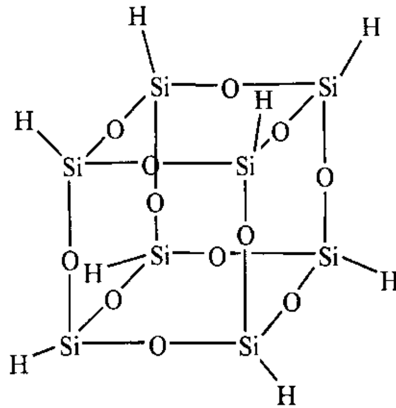

Figure 1.19 Chemical structure of Hydrogen SilsesQuioxane. After [59]

(c) Other polymer resists

Another example of positive-tone resist is PBS, poly(butane-1-sulfone), which was developed by Bell Laboratories, RCA and IBM. [52] It has been widely used in photomask production due to its high-sensitivity of 1 to 2 μC/cm^2, and has a resolution down to ~500 nm. However, as the industry progressed to smaller feature sizes, this resolution was not good enough, and since its performance with regards to etch resistance and CD linearity was poor, [52] PBS was no longer acceptable. ZEP, another chain-scission positive-tone resist, developed by Nippon Zeon, consists of a copolymer of α-chloromethacrylate and α-methylstyrene. It has a sensitivity of 15 to 30 μC/cm^2 at 25 keV. Despite its resolution being almost as high as PMMA, enabling lines of widths 10 nm with pitch 50 nm to be fabricated in the resist, [60] ZEP does not fully satisfy the industry's requirements in terms of etch resistance and contrast. A new nanocomposite resist incorporating a fullerene derivative into ZEP520 increased its resolution and etch resistance with a slight decrease of sensitivity. [60,61]

In general, most polymers crosslink upon sufficient electron irradiation, [35] so they can be used as negative-tone resists. However, not all of them have the sensitivity, resolution or other properties required for commercial application.

(d) Molecular resists

Although most conventional resists are polymer-based, as in PMMA and HSQ, there are some problems with them, such as line edge roughness, which is the deviation of a feature edge from a smooth, ideal shape and usually measured in terms of the root-mean square of the edge deviation from a best fit straight line, [62] and pin-holes, which are minute holes or defects with diameters as small as a few nm. Furthermore, the resist resolution is limited by the size of the polymer molecule, usually defined in terms of the radius of gyration, which is the average distance of the chain segments from the center of the gravity, at least several nanometers for most polymers. This constraint is especially significant in negative-tone resists, where irradiation causes polymerization or crosslinking of molecules, resulting in larger insoluble molecules so that the resolution does not even approach the molecular size. [35] These problems might be avoided by using low molecular weight resists. These relatively new resists include calixarene derivatives, [63-65] catechol, [66] fullerene and its derivatives, [67-69,78] and resists based on liquid crystals, such as triphenylene derivatives. [70-71] These mainly negative tone resists are able to provide high resolution due to their low molecular size and weight. However, not all molecular compounds can be used as resists since most of them tend to crystallise upon spin coating, forming rough surfaces, making them unsuitable for resist application.

(i) Calixarene Derivatives

Calixarenes are macrocyclic molecules comprising of phenolic units linked by methylene bridges to phenolic hydroxyl groups as shown in figure 1.20. They have small molecular size

(~1 nm) and a sensitivity in the ~mC/cm^2 range. [72] Calixarenes have high melting point (~300 °C) and are stable in air. The phenol derivative in calixarene causes it to have high durability to plasma etching. Several derivatives of calixarene have demonstrated negative tone e-beam resist properties. [63-65]

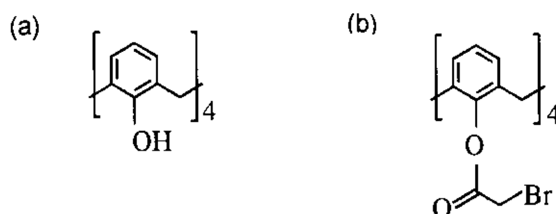

Figure 1.20 *Structures of two calixarene derivatives, (a) calix[4]arene and (b) tetra(bromoacetoxy)calix[4]arene. After [73]*

Ruderisch et al demonstrated that the sensitivity of calix[4]arene, as shown in figure 1.20(a) can be improved by the introduction of allyl, acethyl or bromoacetyl groups at the lower rim. [73] The highest sensitivity was achieved with the use of a bromoacetyl group, as shown in figure 1.20(b). The tetra(bromoacetoxy)calyx[4]arene has a sensitivity of 1.5 mC/cm^2 when irradiated with 25 keV electrons.

Manako et al [65] studied high purity calixarenes (an absence of metal contaminants (Na, Mg, K, Fe)) and found that these derivatives demonstrated high contrasts suitable for high-resolution patterning. It was also shown that the residual resist thickness was greatest for high-purity resist. The unpurified calixarene contains components and chain polymers which are more easily decomposed, resulting in molecules like hydrocarbons and carbon-oxides which evaporate, decreasing the resist thickness. The sensitivity of the resist increases with increasing molecular weight for the negative resist. [65]

The calixarene derivative, hexaacetate *p*-methylcalixa[6]rene (MC6AOAc) is a high resolution resist with a sensitivity of ~5 mC/cm^2 when irradiated with electron beams with energy 50 keV. Lines of width ~10 nm were defined in a 60 nm thick film of M6AOAc using

30 keV electrons. The dry etch durability of MC6AOAc is approximately equal to that of silicon. [74]

(ii) catechol

Another family of low molecular weight resists, which also have cyclic ring structures, are catechol derivatives. The general chemical structure of a catechol is shown in figure 1.21. It was found that this derivative, with three catechol groups linked by three CH_2 units, acts as a positive-tone photoresist material. [75] This derivative is an amorphous compound and can form smooth films. Another derivative, also with three catechol groups, hexahydroxy cyclotribenzylene, protected with p-t-butoxy carbonylmethyl groups, works as a positive tone electron beam resist with a high sensitivity and contrast, and high durability to CF_4 plasma etching. [76] It has a poor resolution, however, allowing a 90-nm space pattern at 10 $\mu C/cm^2$ under 50-keV electron beam.

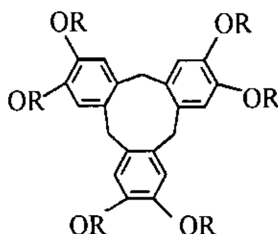

Figure 1.21 Chemical structure of a catechol derivative. R can be COOtBu, $CH_2COOtBu$, or CH_2COOH. After [66]

(iii) Fullerene (C_{60}) derivatives

Fullerene (C_{60}) is a closed hollow spherical cage comprising of sixty carbon atoms arranged in interlocking hexagons and pentagons. [77] The application of fullerene as a negative resist was first studied by Tada and Kanayama [67] who verified that electron beam irradiation on fullerene C_{60} films reduced its solubility in organic solvents such as monochlorobenzene,

showing that this material could be used as a negative electron beam resist. Its small molecule (<1 nm diameter) enables the resist to have a resolution of at least 20 nm. The resist has a sensitivity of ~10 mC/cm^2 and very high dry-etch durability. [67] However, the C_{60} film is unsuitable for spin coating due to poor solubility in all solvents, and must be deposited on the substrate by vacuum sublimation, making it difficult for industrial application. Furthermore, its sensitivity is two orders of magnitude lower than that of PMMA.

Robinson et al [47,68,78] demonstrated that chemical modification of C_{60} by adding functional groups to the C_{60} cage can significantly enhance the resist properties. Methano derivatives of the C_{60} (methanofullerenes) were formed by attaching a functional group to the fullerene cage via a three-carbon ring called a methano bridge as shown in figure 1.22. These derivatives dissolve readily in chloroform and smooth films of resists can be easily prepared by spin coating from their solutions. Films of nine different C_{60} methanofullerene monoadducts, exhibited negative tone resist behaviour with sensitivities between 8.2 to 0.85 mC/cm^2 when irradiated with a 20 keV electron beam, more than an order of magnitude higher than that of pure C_{60}.

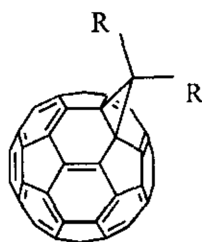

Figure 1.22 A fullerene derivative, with a functional group, R attached to the fullerene cage via a methano bridge.

It is believed that the addition of functional groups cause a considerable charge localization, and consequently bond weakening, making them more susceptible to electron beam damage, thus increasing their sensitivity. Raman spectra of exposed and unexposed films implied that, instead of polymerization, the e-beam irradiation of the fullerene derivatives leads

to cage fragmentation and the formation of a disordered network of graphite-like particles which are mechanically resistant to being washed away by the solvent and highly etch resistant. [78] In the case of derivatives with two polyether chains, the sensitivity was found to be linearly dependent upon the derivative mass. In addition, this derivates has high dry-etch durability with etch ratios twice those of a standard novolac-based resist. Features with widths of 20 nm were produced using these compounds.

The study of the derivatives of fullerene was further pursued by Tada et al [79] who also showed that the sensitivities of the methanofullerene resists were dependent on the methano bridge in the side chains. A derivative with two diels-alder side chains has a sensitivity about the same as that of C_{60}, while derivatives with one methano side chain showed sensitivities in the order of mC/cm^2. By synthesizing a multi-adduct methanofullerene, which had four to six side chains, the sensitivity of the derivative was further improved to 0.38 mC/cm^2 at 20 keV, two orders of magnitude better than that of C_{60}. [79]

(iv) Triphenylene derivatives

Triphenylene is a disc-shaped molecule with a planar structure and three-fold rotation. Its main structure consists of a polycyclic aromatic hydrocarbon made up of four fused benzene rings. Low molecular weight resists based on the triphenylene molecule have been studied by Robinson et al [70,71] and it was shown that these resists can be used as negative tone electron beam resists, with sensitivity between 1.5 and 6.5 mC/cm^2 at 20 keV with monochlorobenzene as developer. These polysubstituted triphenylene derivatives, shown in figure 1.23, which are liquid crystalline, readily form smooth films when spin coated using chloroform as a solvent without a need for a post application bake, a heating process applied to most resist after spin coating to remove the casting solvent.

One of the derivatives, the molecule 2,3,6,7,10,11-hexapentyloxytriphenylene (C5/C5) demonstrated high resolution capability, allowing 14 nm patterns to be realized in the resist at

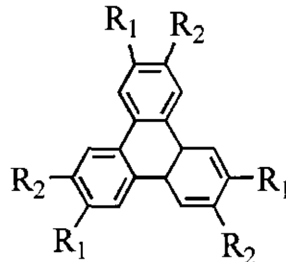

Figure 1.23 *Chemical structure of polysubstituted triphenylene derivatives.*
$R_1 = OC_nH_{2n+1}$, *and* $R_2 = OC_nH_{2n-1}$, *where n=0,1,2,3...*

30 keV beam energy. [71] The derivative has a very small molecular size (744 AMU). [70] The derivative C5/C5, also demonstrated positive tone behavior at doses lower than 250 $\mu C/cm^2$ and negative tone behaviour at higher doses when pentanol was used as a developer. [80] Furthermore, the resist has a high etch-durability, better than that of the conventional novolac based resist, SAL601, discussed in section 1.7.1, which is known as a dry-etch durable resist.

The primary objectives of e-beam lithography are high resolution and high speed (high sensitivity). Higher-voltage e-beam exposures could be the best solution to get the resolution and accuracy required in advanced masks due to their finer beam profile. However, the higher accelerating voltages lead to lower resist sensitivity because fewer electrons interact in the resist layer, but travel through to the underlying substrate. [52] Therefore, an enhancement of resist sensitivity is necessary to achieve an economically feasible throughput while maintaining the high resolution of electron beam lithography.

1.7 Chemically Amplified Resist

The concept of chemical amplification aimed to dramatically increase the sensitivity of a resist and was invented at IBM Research in 1980. [81] It is now well accepted by the lithography

community. Chemically amplified resists (CAR) have become technologically important because they have higher sensitivity, thus increasing wafer throughput. In chemically amplified resist systems, a catalytic species generated by irradiation induces a cascade of subsequent chemical reactions, providing a gain mechanism. [1,81]

The original chemical amplification scheme included cross-linking through ring-opening polymerization of pendant epoxide groups for negative resist, shown in figure 1.24(a), depolymerization for self-developing positive resist, and deprotection of pendant groups to induce polarity change for dual-tone imaging as shown in figure 1.24(b). All three of these reactions are acid-catalyzed. [82] As already mentioned in section 1.6.1, self-developing

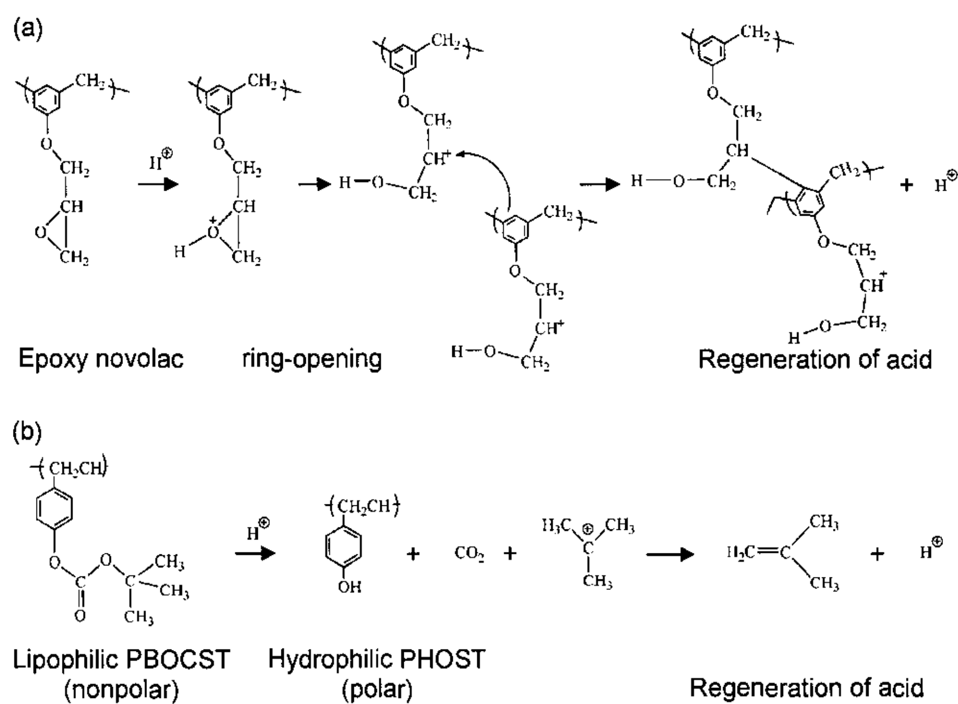

Figure 1.24 Chemical amplification schemes, (a) cross-linking through ring-opening polymerization of pendant epoxy group for negative-resist systems, and (b) deprotection of pendant groups to induce polarity change. After [82]

systems require no subsequent development due to the volatile products, however, they are not widely used since these products cause contamination to the lithography tools. Therefore some of these systems were later modified from self-development to thermal development, as in the depolymerization of polyphthalaldehyde. [82]

Acid-catalyzed reactions form the basis of many chemically amplified resist systems for microlithography applications today, either via cross-linking to reduce solubility for negative tone resists or deprotection reactions (removal of a solubility inhibitor) for positive tone resists applications. [83] Cross-linked resists generally offer more resistance to subsequent processing than non-cross-linked resists. [2]

CARs generally contain more than one component; for instance, a base polymer, a photo-acid generator (PAG), and sometimes a separate cross-linker. During exposure the photoacid generator is decomposed, releasing acid. The acid then diffuses during a post-exposure bake (PEB) and catalyzes cross-linking reactions to render the resist insoluble for negative resist or deprotection/chain-scission to render it soluble for positive resist. Many different chemical amplification schemes have been investigated, and various process conditions have been studied, to attempt to achieve resists with increased sensitivity, optimized resolution, and acceptable etch resistance, suitable for nano-scale lithography.

1.7.1 Chemically Amplified Electron Beam Resists

(a) Current Commercial CARs

The most widely used and studied chemically amplified resist family are the Shipley Advanced Lithography (SAL) resists produced by Rohm and Haas Electronics Materials (formerly Shipley). [84-92] The negative-tone SAL601 resist for instance, has three components; a base polymer, an acid generator, and a crosslinking agent. It has been shown to have a sensitivity of 4 $\mu C/cm^2$ and displays high-dry etching resistance similar to that of a conventional

diazoquinone based positive resist. [84] A minimum feature size of 20 nm isolated line was obtained in the resist, but required stringently controlled PEB conditions, and showed significant line edge roughness. [85] SAL601-ER7 consists of a novolak polymer contributing to high dry-etching resistance, a melamine resin as the crosslinker and a bromic triazine compound as the acid generator. [91] SAL605, the successor of SAL601, has the same basic chemistry but is about three times more sensitive. [86]

Another negative-tone chemically amplified resist is the epoxy novolak SU-8, which is composed of a Bisphenol A Novolak epoxy oligomer and a triarylsulfonium hexafluroantimonate salt as photoacid generator. [50] Its sensitivity ranges from 1 to 4 $\mu C/cm^2$ when irradiated with 20 keV electrons, depending on the PEB conditions. [93] The resist has been shown to resolve features as small as 30 nm using 40 keV electrons at minimum line dose of 0.03 nC/cm [50] and 75-nm wide lines using 50 keV electrons at a dose of ~3.6 $\mu C/cm^2$. [94] However, the resist has poor dry etch resistance around half of that of SAL601. [50]

A number of chemically amplified DUV resists, have been shown to work effectively for electron beam lithography. [95-97] UVIII, a positive tone photoresist from Rohm and Haas has a resolution of 60 nm at a dose of 40 $\mu C/cm^2$ and beam energy of 50 keV, [96] and sub-50 nm at 60 $\mu C/cm^2$ and 100 keV. [97] UVN-2 and UV-5, also from Rohm and Haas, also have high resolution capabilities in electron beam lithography. The negative-tone UVN-2 is a successor of UVN, a negative resist with a sensitivity of 20 $\mu C/cm^2$ at 50 kV which has an ultimate resolution of 70 nm isolated lines or 140 nm lines and spaces. UVN-2 allows 50 nm resolution of single line widths at 30 $\mu C/cm^2$ nominal dose. [95] UV-5 shows positive tone behaviour with a sensitivity of 12 $\mu C/cm^2$ and 50 nm resolution. The resist switches to negative-tone behaviour at higher doses, and shows negative-tone resolution of 90 nm at a dose of 500 $\mu C/cm^2$. [95]

Two chemically amplified resists from Clariant are the positive-tone AZPF514 and negative-tone AZPN114. AZPF514 is a sensitive resist, about 25 $\mu C/cm^2$ but unable to achieve resolution better than 150 nm. [97] AZPN114 also has a high sensitivity, about 30% better than SAL601, and a resolution of 30 nm. [98]

(b) Other CARs

Studies on chemical amplification of other resists have also been conducted. Sailer et al [99,100] have recently presented the chemical amplification of a class of calixarenes via cationic polymerization. A calix[4]arene derivative bearing four epoxides, tetrakis(oxiran-2-ylmethoxy)-tetra-*tert*-butylcalix[4]arene (TOMCA4), as shown in figure 1.25, was synthesised. The negative tone resist showed a sensitivity of ~3 mC/cm^2 at 25 keV, higher than those of calixarenes without the epoxides.

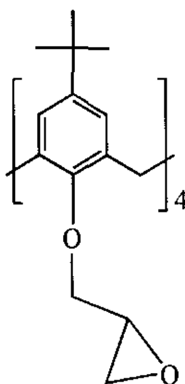

Figure 1.25 Structure of tetrakis(oxiran-2-ylmethoxy)-tetra-tert-butylcalix [4]arene (TOMCA4). From [100]

In the study, the concept of chemical amplification via ring opening of epoxy resins was applied. Here acid generated during PEB protonates the epoxide, inducing a ring opening and producing a carbocation. The carbocation, which is a positively charged carbon ion, reacts with other neutral epoxides resulting in a chain reaction of crosslinking events. A Cyracure photoinitiator (PI) which consists of mixed triarylsulfonium hexafluoroantimonate salts was

added to the derivative at PI:TOMCA4 ratio of up to 4:10. Depending on the photoinitiator concentration in the resist and PEB temperature, the sensitivity of the resist was improved by almost two orders of magnitude to ~15 $\mu C/cm^2$. Line-space patterns with a period of 80 nm and a linewidth of 40 nm were fabricated in the resist using a 30 keV electron beam. However, etch resistance tests showed that the etch rate of the resist is only slightly higher than that of silicon.

Saito et al [101] proposed a new chemically amplified system consisting of poly(hydroxysterene) (PHS) protected with a 1-ethoxyethyl group as base polymer and triphenylsulfonium triflate as PAG. The PAG concentration was 1.5 % of the base polymer and a PEB of 90 °C for 180 s was applied. As shown in figure 1.26, under acid catalysis, the acetal-protected-PHS (a-PHS) develops a chemical equilibrium with the soluble PHS. The equilibrium shifts to the right if water is present in the system. By adding a tertiary alcohol (2,4-dimethyl-2,4-pentandiol), to act as a water generating compound, to the resist, a chemically amplified positive electron beam resist was produced. The CAR exhibits a sensitivity of 1.7 $\mu C/cm^2$ under 50 keV electron beam irradiation. [101]

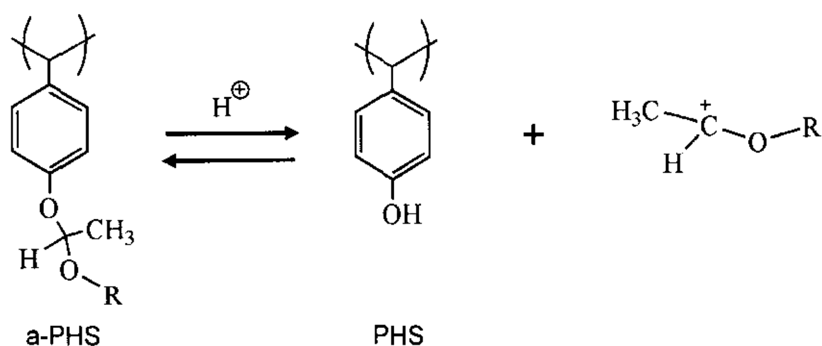

Figure 1.26 Chemical equilibrium between acetal-protected-PHS and PHS. After [101]

Another relatively new positive tone chemically amplified resist developed by Hashimoto et al [102] consists of a tert-butoxycarbonyl (*t*-BOC) group-protected poly(p-

vinylphenol) as shown in figure 1.27(a) as the matrix polymer, which is insoluble in aqueous alkaline solution, and a photoacid generator. Upon exposure to electron beam and post exposure bake, the generated acid causes a deprotection of the matrix polymer producing poly(*p*-vinylphenol) which is soluble in aqueous alkaline solutions, such as tetramethyl ammonium hydroxide solution. Three types of PAG were tested in the resist system, and 2-methyl-2-(benzenesulfonyl) propyophenone, shown in figure 1.27(b) was found to be most effective. A sensitivity of ~1.5 μC/cm^2 was obtained at 20 keV with PEB of 90 °C for 90 s. The resist demonstrates a high dry etch durability comparable to that of conventional photoresist, but is only capable of achieving 200-nm line-space patterns in 0.5-μm-thick resist film at 50 keV.

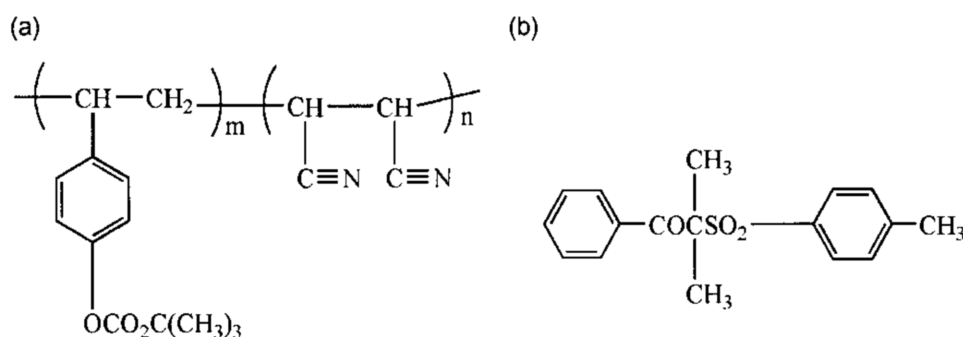

Figure 1.27 Chemical structures of (a) tert-butoxycarbonyl group-protected poly(p-vinylphenol) type polymer, and (b) 2-methyl-2-(benzenesulfonyl) propyophenone. After [102]

1.7.2 Factors that affect the responses of chemically amplified resists

Chemically amplified resists have been the subject of much research, aimed at achieving the best combination of properties. The effects of altering the molecular structures of various resists, increasing or decreasing PAG concentration in the system, and varying process

conditions have all been studied. Although CARs have the advantage of high sensitivity, there are several problems that need to be addressed.

(a) Molecular structure

The molecular structure of a resist can affect its sensitivity, resolution, contrast and etch resistance. [82] In the case of a conventional positive resist which functions on chain scission and negative resist systems which function by crosslinking, higher molecular weight materials are known to provide higher sensitivities. This could be due to better dissolution differentiation of higher molecular weight polymers, that is, a few chain scission or cross-linking events are enough to change their solubility. [1] Furthermore, higher molecular weight also means a higher cross-section for electron interactions.

However, in terms of resolution, polymer-size effects can cause variations in pattern sizes. [103] This effect is shown in figure 1.28. In the diagram, each circle represents one polymer molecule. The red area in figure 1.28(a) and (b) signifies the exposed part of the resist. Figure 1.28(b) and (c) show the retained resist after development for a negative and positive tone resist respectively. It is shown that some of the unexposed areas were retained in the negative tone resist, and removed in the positive tone one. Since the smallest dissolvable volume is one molecule, a smaller molecular size would offer better resolution and smoother line-edge.

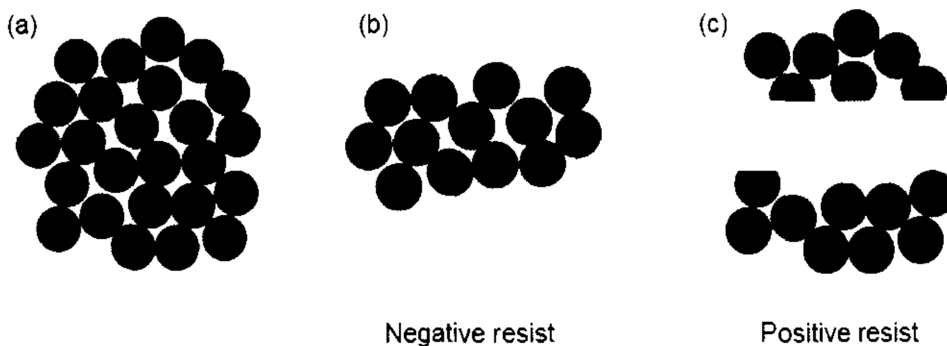

Figure 1.28 Effect of molecular size on resolution and line edge roughness.

(b) Photoacid Generator

The photoacid generator (PAG) is one of the key components of a chemically amplified resist. The type used and its concentration, affect the performance of the CAR. The PAG should have sufficient radiation sensitivity to ensure adequate acid generation, be free of metallic elements such as antimony or arsenic that are regarded as device contaminants, be fully compatible with the matrix resin to avoid phase separation and be stable to temperature to avoid premature thermal generation of acid. [104] The first PAGs used in CARs were from a class of materials called onium salts, which include diaryliodonium and triarylsulfonium salts. The chemical formulas are shown in figure 1.29.

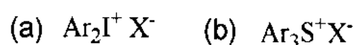

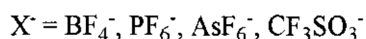

Figure 1.29 Chemical formulas of (a diaryliodonium salts and (b) triarylsulfonium salts. After [104]

When irradiated, the carbon-iodine or the carbon-sulfur bond in these salts ruptures, resulting in the formation of an acid. The advantages of these PAGs are their thermal stability up to 200 °C, their potential to be structurally modified to suit their purpose, and the wide variety of acids that can be generated, such as hexafluoroarsenic, hexafluoroantimonic and triflic acid, which is a strong organic acid. Other than the onium salts, which are ionic, there are also nonionic PAGs, such as nitrobenzyl esters and imino sulfonates.

The sensitivity of a CAR is usually enhanced by increasing the concentration of PAG in the resist formulation. However, this approach can have significant consequences. Petrillo et al, in their studies on a positive-tone chemically amplified photoresist, showed that, although as expected, the sensitivity of the resist increased as the PAG concentration was increased, several aspects of the process window including exposure latitude (the range of exposure dose over which acceptable image size tolerances can be maintained) and focus latitude

decreased. [105] Pawloski et al found that, as the concentration of the PAG was increased, the photoacid required to achieve the appropriate extent of deprotection to allow development also increased. [106] It was shown that resists with greater concentration of PAG required more photoacid to achieve the same deprotection as a resist with a lower concentration of PAG at identical processing conditions. The observation suggests that the diffusivity or catalytic activity of the photoacid within the resist is reduced when the concentration of PAG increases.

In most chemical amplification systems, the crosslinker and/or photoacid generator (PAG) are added to the resist matrix during sample preparation. The efficiency of the crosslinker and the PAG are highly dependent on the compatibility between the crosslinker and PAG and the polymer matrix. Poor compatibility can cause phase separation, non-uniform acid distribution, and component migration. Phase separation is a process that occurs when chemically dissimilar molecules coexist within a material such that the interconnection between the chemically similar molecules are stronger than the adhesive connection between the dissimilar molecules, causing a movement of molecules within the material and hence separation of the dissimilar molecules.

Alternatively, the photoacid generator could also be incorporated into the resist molecules to avoid incompatibility and enhance the sensitivity of the resist. [107,108] Wu et al have demonstrated a high-sensitivity chemically amplified negative resist by synthesizing a photoacid generating monomer containing a sulfonium group. It was reported that the resists exhibited excellent film formation behaviour due to the absence of phase separation. 260 nm features were obtained using a 4 keV electron beam at a dose of 10 $\mu C/cm^2$. [107]

(c) Post Application Bake

Post application bake (PAB) is the process of heating a resist sample before exposure, with the main purpose of evaporating the casting solvent that remains in the resist film after spin coating. Since the residual solvent can act as a reaction medium, it is expected that the acid-

catalyzed reaction would be sensitive to residual solvent content. Azuma et al [91] have shown that both resolution and sensitivity are affected by PAB temperature. Results of their studies on the CA negative resist SAL601, using Fourier transform infrared spectroscopy (FTIR) and gas chromatography/mass spectroscopy (GC/MS), showed that a difference in PAB temperature not only affects the degree of crosslinking in the exposed areas but also the dissolution rate in the unexposed areas. It was also found that the residual content in thicker resists was affected more by PAB temperature than thinner resists, which suggest that the residue remains mainly at the bottom of the resist. The presence of more residual solvent in thicker resists also contributes to its lower resolution. Schlegel et al [109] investigated acid mobility for two different resist systems under various process conditions and found that solvent traces in the film cause a very strong increase of the acid mobility and that a higher PAB temperature would leave a lower amount of residual solvent, shown by IR-spectroscopic measurements.

However, although higher PAB temperatures can improve resolution by reducing residual solvent, Ainley et al [110] reported, in their study using the negative tone CAR NEB-22, that a prolonged prebake temperature caused a decrease in resist sensitivity. This is expected, since the rate of acid diffusion is reduced with the reduction of residual solvent. On the other hand, it was also observed that a longer PAB time improved the exposure latitude slightly, ie, there was less variation in feature sizes with a variation in exposure dose.

(d) Post-exposure Bake

In chemically amplified resists, heating the resist sample after exposure, or post-exposure bake (PEB), is usually necessary to activate the catalytic reaction of the acid generated during exposure. The thermal energy applied during PEB enables the acid to defuse and initiate the crosslinking or deprotection reactions in the resist. [85] The rate of the reactions depends on the acid concentration, diffusion rate and the temperature. [104] Therefore, the responses of a CAR are affected by PEB temperature and time. The mobility of the acid during post exposure bake

is essential for the catalytic mechanism, but resolution will be lost if the diffusion range of the acid is of equal or greater magnitude as the critical dimension. The PEB process is very critical as a small temperature shift can significantly affect the pattern quality.

Manako et al [111] showed that the sensitivity of negative-tone CAR SAL601 increased, while resolution decreased, when the PEB temperature is increased, due to an increase in acid diffusion. Ainley et al [110] also reported an increase in sensitivity but decrease in resolution with higher PEB temperature whilst Yoshimura et al, [85] showed that the measured feature linewidths are proportional to the squareroot of the PEB time, all other exposure conditions remaining the same. Similarly, a study of chemically amplified HSQ, showed that increasing the PEB temperature increased the sensitivity, but reduced its contrast. [112] It is therefore important to control the PEB conditions when using chemically amplified resists, to achieve an optimal combination of the sensitivity, resolution and contrast.

(e) Airborne Contamination

CARs are sensitive to process conditions. Airborne base contamination and time in the vacuum system can strongly affect the resist performance. [82] Basic contaminants, such as ammonia and 1-methyl-2-pyrrolidinone in the air can neutralize the surface acid in the exposed area in the delay between the exposure and PEB steps. This results in an insoluble layer in the exposed area of positive tone CARs which causes T-top profiles, as shown in figure 1.30, and enlarged critical dimensions. [113]

Several methods have been identified to reduce susceptibility of CA resist to airborne contamination. The use of special activated carbon filters to remove airborne bases in the processing facility has been shown to reduce the T-top effect. [82] Other methods include overcoating the resist with a soluble protective film and minimizing the time interval between exposure and PEB. [83] Petrillo et al [114] studied the effect of applying a top antireflective coating on the lithographic performance of chemically amplified resists and found that the

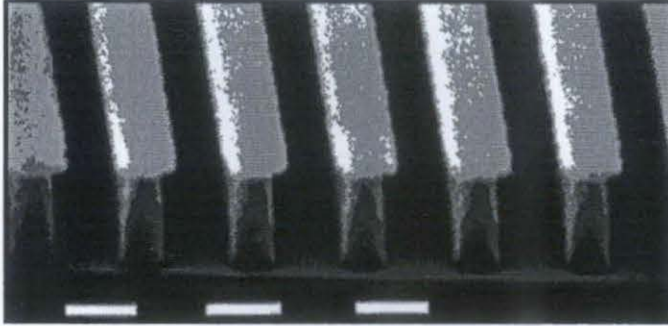

Figure 1.30 T-top formation observed in chemically amplified positive resists. After [82]

presence of the coating not only protects the resist from the environment, but also improved the resist profile and its resolution. It was shown that when base-free Aquatar, a top coat which consists of a polyacrylic acid, water, and an ammonium salt, with a pH of 3 was left on the resist sample during PEB, the t-top profile was removed. To be effective as a protective layer, the top coat material must be acidic so that it can neutralize any basic contaminants that come into contact with it.

(f) Acid Diffusion

Although chemically amplified (CA) resists have the advantage of high-sensitivity, they tend to have poor resolution. [52] Acid diffusion is essential for high sensitivity, but excess diffusion can reduce the resolution. [82] As mentioned earlier, the stability of CAR is not only affected by environmental contaminants, but also to post-application and post-exposure bake temperature variations. [52] It was shown that the diffusion of the catalytic acid in CARs follows Fick's law, [109] which states that the rate of diffusion of certain molecules across two regions is proportional to the difference in concentrations of the molecules between the two regions. [115] This implies that a higher acid concentration in the resist would increase acid diffusion. The study also showed that the range of acid diffusion is higher with higher PEB

temperature and time suggested that in order to control the diffusion range, the PEB temperature should be lower than the glass transition temperature. [109] The glass transition temperature is the temperature above which a polymeric substance softens and becomes rubbery. At this point, the molecular motion and the coefficient of thermal expansion increase. Acid diffusion generally increases considerably above this temperature.

The effect of post exposure delay was investigated using two negative-tone CARs, SUMITOMO NEB-22 A2 and TOK TDUR 908N [116] and it was found that the minimum feature size increased by more than 20 and 30% respectively after 24 h delay in filtered standard clean-room open air, demonstrating that acid had diffused from the exposed to unexposed areas. When the same resists were stored after exposure under nitrogen atmosphere, it was observed that critical dimension (CD) stability was maintained even after 24 h delay. This shows that, since in both cases the resists were stored in contaminant-free atmosphere, it is the absence of moisture that curbs the acid diffusion, in this case.

The influence of acid diffusion on the lithographic performance of chemically amplified resists [117] can also be examined by calculating the distribution of chemical amplification reactions and their dependence on acid distribution. It was shown that the reactions occur in a smaller region than the area the acid has diffused to, and that the effect of acid diffusion is greater on hole patterns than on line patterns in a positive-tone resist. This is because, in a hole pattern, the diffusion effect is two-dimensional, whilst in line patterns, it can be considered one-dimensional. Using a model explaining the effect of acid diffusion on resolution and sensitivity, it was calculated that the resolution can be expressed in terms of diffusion coefficient, D, and PEB time, t, as

$$\mathit{Re}\text{solution} \propto (\mathrm{Dt})^{-1\ 2}, \tag{1.5}$$

and the sensitivity expressed as

$$\mathit{Sensitivity} \propto 1/Dt, \tag{1.6}$$

which led to the correlation

$$Resolution \propto (\text{Sensitivity})^{-1/2}. \tag{1.7}$$

This trade-off between resolution and sensitivity can be applied for all chemically amplified resist. However, an improvement in resist material and control of PEB time can optimize the performance of the resist.

1.7.3 Techniques to improve CARs performance

The aforementioned problems with CARs have motivated many studies aimed at improving their performance. The main issues are poor resolution due to acid diffusion, poor etch resistance and the effect of contaminants during post exposure delay.

(a) Electric-field-enhanced PEB

One reported way of controlling the diffusion of acid is by applying an electric field during PEB. Cheng et al [118,119] reported an improvement of resist resolution and sensitivity by applying an external electric field to the resist film during PEB, a method called electric-field-enhanced (EFE) PEB. In this method, an alternating electric field is applied across the thickness of the resist, as shown in figure 1.31(a). The acid molecules, which are ions, are affected by the electric field, enhancing the photoacid drift in the vertical direction as shown in figure 1.31(b), thereby confining the lateral acid diffusion. [118] Experiments conducted on

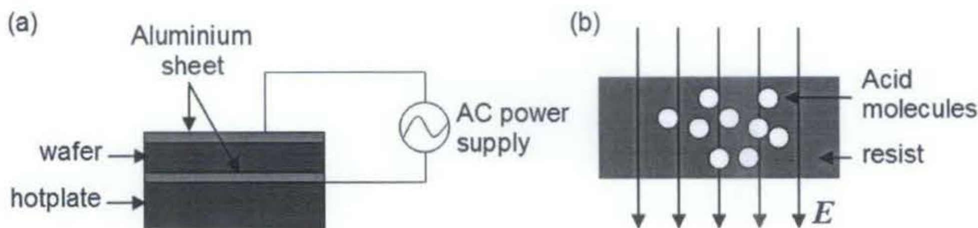

Figure 1.31 (a) Set-up of electric-field-enhanced PEB and (b) acid drifts in the vertical direction is enhanced by electric field. After [118]

UVIIHS and UVII-10 resist showed that the technique also reduced PEB time requirement by 30%, improved the sharpness of two-dimensional corners and increased the verticality of resist sidewalls. [119] Furthermore, the electric-field-enhanced PEB improves tolerance to overexposure and provides better critical dimension control. It was estimated that the lateral acid diffusion length was reduced by about 70-90 nm, or by 50%.

(b) Low voltage electrons

Using low voltage electrons for irradiation has been shown to be an effective means of avoiding the proximity effect (section 1.6.2). In exposures on test-patterns with dimensions of 150-nm, McCord and Newman [120] demonstrated that the proximity effect on silicon substrates is greatly reduced at 5 keV compared to that when 10 keV electrons are used. This is due to the reduction in backscattered electrons at 5 keV compared to 10 keV as shown in the simulation [45] in figure 1.32. This concept is used in the LEEPL system, discussed in section 1.5.3. The use of low energy electrons, not only reduces the proximity effect, but also since the electron interacts more within the resist layer, enhances the sensitivity of the resist. [120,121]

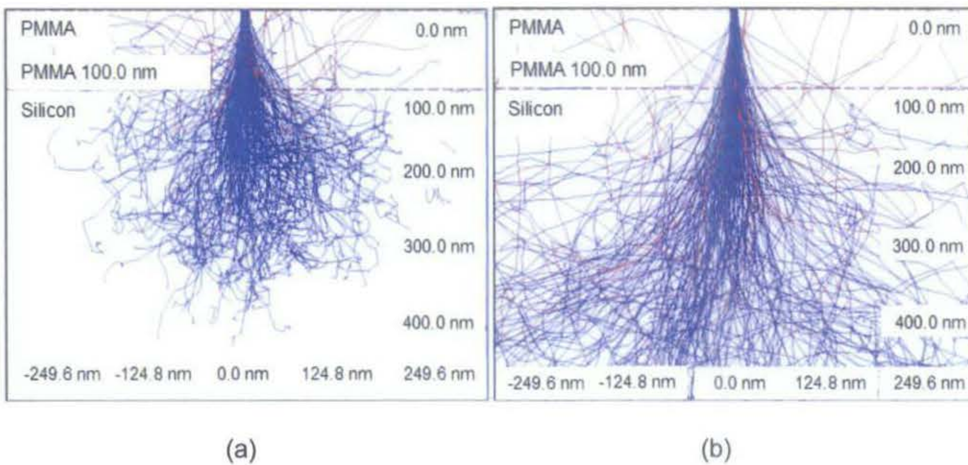

Figure 1.32 Simulations showing electrons interactions in a resist at (a) 5 keV and (b) 10 keV energy. The resist used is 100 nm of PMMA. The blue lines represent primary electrons and the red lines backscattered electrons.

Furthermore, damage on the substrate and mask are significantly reduced due to the low bombardment energy of the electrons.

(c) Ultrasonic Development

Ultrasonic development has been proposed as a method to improve the resolution and sensitivity of electron beam resists. It is suggested that it helps to overcome the intermolecular forces between resist molecules so that narrow lines are fully developed at lower exposure doses. [122] Additionally, agitation of the developer continuously brings fresh developer into contact with the resist enhancing the dissolution rate and reducing the development time. Swelling of the resist due to the penetration of developer into the film can therefore be reduced as the contact time with the developer is decreased. Yasin et al demonstrated an improvement in the sensitivity and contrast for PMMA, UVIII and calixarene resists, compared to conventional dip development for the same development time. [122] It was also observed that, for a given linewidth, ultrasonic development improved the exposure dose latitude.

(d) Incorporation of Additives

Incorporation of certain additives to resist systems can help to improve their performance. The etch resistance of a resist, for instance, can be improved by the incorporation of etch durability enhancers, such as fullerene. The etch durability of an organic resist is shown to be proportional to the percentage of carbon content in the resist. Ishii et al [123] showed that fullerene (C_{60} and/or C_{70}) incorporated into the positive e-beam resist ZEP520 improved the pattern contrast of the resist. Evaluation of etch resistance using electron cyclotron resonance (ECR) etching demonstrated that the etch durability of the resist also increased as the proportion of fullerene in the resist was increased. With higher etch resistance, thinner resist films can be used, which minimizes electron scattering effects, and in turn improves pattern resolution.

The effect of basic additives on a CA negative electron-beam resist, 1,3,5-Tris(2-(2-hydroxypropyl))benzene (Triol) was investigated by Migitaka et al. [124] It was shown that the addition of quinoline not only enhanced the resist contrast, but also improved the process latitude. Comparison of response curves of the resist with and without the additive indicated that quinoline induced a drastic change of dissolution rate, improving the contrast. It was also observed that the dependence of pattern-width on PEB temperature, was significantly reduced, allowing a larger process latitude. However, the addition of the base deteriorated the sensitivity of the resist.

Post exposure delay (PED) instability between exposure and post-exposure bake can be observed by the change in pattern dimensions. Incorporation of diphenylamine as base additive to CAR polyhydroxystyrene (PHS) was shown to improve resist stability in atmosphere. [125] It was observed that the change in pattern dimension due to contaminants in atmosphere was significantly reduced when the resist was kept in vacuum for more than 20 min after exposure. It was suggested that the base additive and the acid generated by the PAG of the resist system reached equilibrium after 20 min in vacuum making it more stable in atmosphere.

Most CARs provide some trade-off between resolution and amplification. It is a common occurrence in the design of CARs that an improvement of one characteristic is usually at the expense of another. A major challenge in resist design is to achieve the combination of high sensitivity, resolution, and dry etch resistance. The aim of this research is to develop high sensitivity chemically amplified resists for electron-beam lithography. Whilst electron-beam lithography is able to achieve high resolution, it is comparatively slow. The low throughput which has always been associated with EBL can be significantly reduced by using high-sensitivity chemically amplified resists.

The most common type of chemical amplification resists are based on acid catalysed deprotection or crosslinking of a polymer during a post-exposure bake (PEB). In chemically amplified positive-tone resist, the acid generated by a photoacid generator or photoinitiator during exposure increases solubility by catalytic deprotection of solubility enhancing functional groups or chain scission, whilst in a negative tone resist, the acid catalyses a crosslinking reaction. Most negative tone CARs consist of a resist matrix, a crosslinker and a photoacid generator. The objective of this research was to design a high sensitivity resist with good etch resistance while maintaining the high resolution required by lithography industry.

Two groups of resists - the derivatives of fullerene and the derivatives of triphenylene - were chosen for the study. These two families of molecular resists have shown potential for electron beam lithography and have been extensively studied by this group. [68-71] The small molecular sizes of the materials give the potential for high resolution to be achieved, enabling features of dimensions 10 to 20 nm to be fabricated. Furthermore, these resists also demonstrated high etch durability, 2 to 3 times higher than novolac resists such as SAL601, due to their high carbon content. However, the sensitivities of these resists, which are in the range of mC/cm^2, are too low for commercial application.

Chemical amplification of resists using crosslinkers and photoacid generators to enhance their sensitivities has been widely investigated. [1,52,99] The crosslinkers and/or the photoacid generator can also be incorporated into the resist structure itself. [107] For this research I proposed the chemical amplification of the fullerene and triphenylene derivatives to enhance their sensitivities by means of adding a photoacid generator (or photoinitiator) and a crosslinker to the molecular resists, as well as the incorporation of the crosslinking functionality into some of the resist molecules themselves.

2

Experimental Techniques

The equipment and techniques used in this research are discussed here. First, the two groups of resist materials studied for chemical amplification are introduced and described. The photoacid generators and crosslinkers employed in the chemical amplification process are then introduced. Various different pieces of equipment were involved in the study, both as experimental and as analytical tools. The main experimental tool, a scanning electron microscope adapted for lithography was used both for exposing the resists and analysis, and is described in depth. The experimental steps, including substrate and sample preparation, lithographic exposures, and sample development and analysis are explained. Plasma etching, which was used to transfer patterns defined in a resist to the silicon substrate, and other processing tools including the profiler and plasma asher, are also discussed.

2.1 Compounds, Crosslinkers and Photoacid Generators

Two groups of molecular electron beam resists – the derivatives of fullerene (C_{60}) and the derivatives of triphenylene – were chosen for chemical amplification. These resists, which have been studied extensively by the group, were available via the collaboration with the Nanoscale Chemistry Research Group in the School of Chemistry of The University of Birmingham. Initial tests were performed on materials which are available at the time and these results were then used to guide further synthesis efforts. Several commercially obtained crosslinkers and photoacid generators were employed in the studies.

2.1.1 Derivatives of Fullerene

Nine different fullerene derivatives resists were investigated. They are the methanofullerenes MF02-01, MF03-01, MF03-04, MF04-01, MF04-02, MAF1, MAF4, MAF5, and MAF9 as shown in figure 2.1. MF02-01 is a mixture of hexa, penta, and tetra adducts of fullerene with triphenylene based addends. MF03-01 and MF03-04 are hexaadducts with methyl and hydroxyl terminated malonyl ester addends, respectively. MAF1, MAF4, MAF5 and MAF9 are all monoadducts, also with malonyl ester addends. MAF1 has polyether tails and tetrahydropyran protective groups, MAF4 is hydroxyl terminated, MAF5 is methyl terminated and MAF9 is chlorine terminated. MF04-01 and MF04-02 are fullerene derivatives with epoxide groups added to the fullerene cages to aid crosslinking.

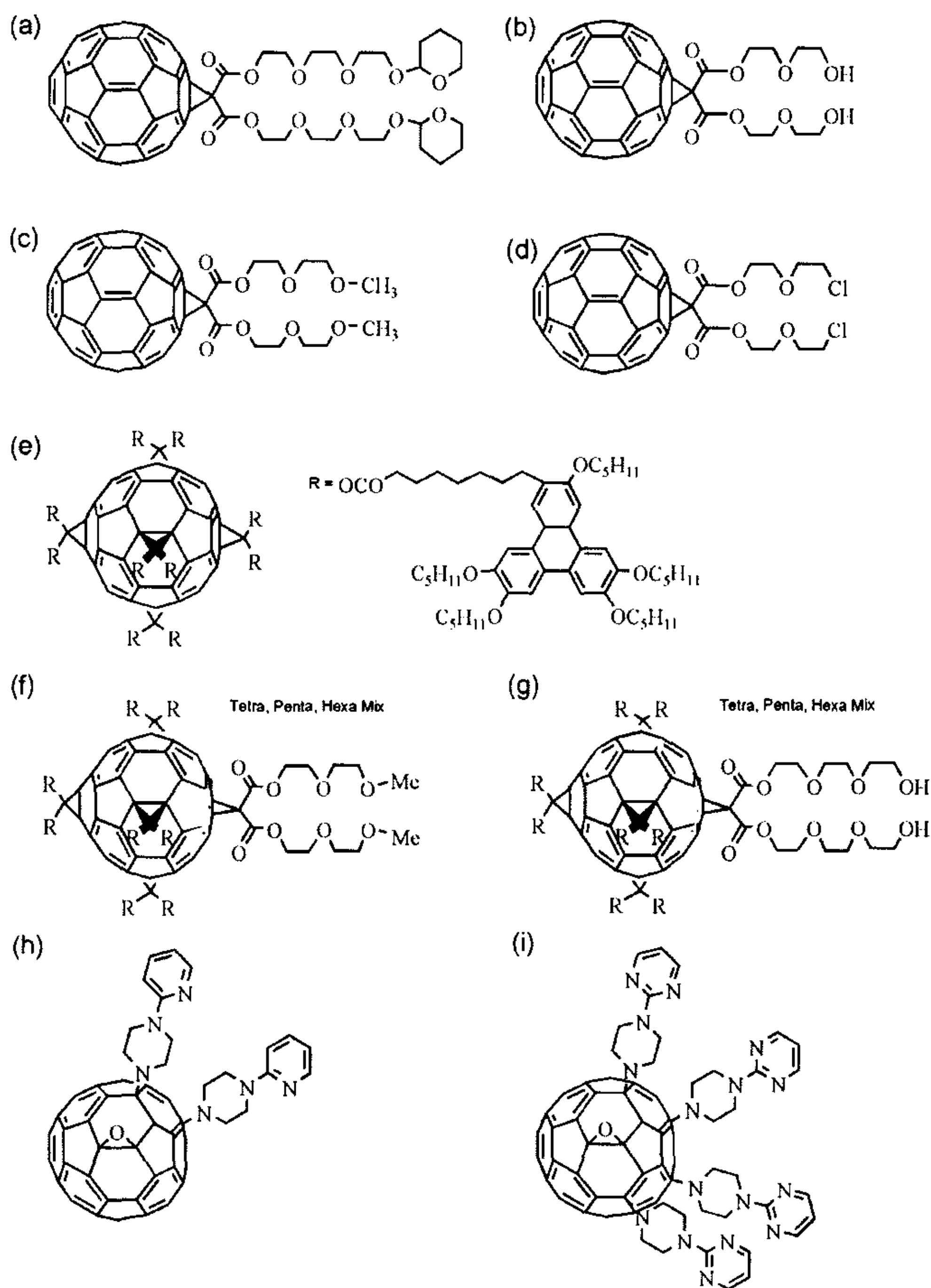

Figure 2.1 *Chemical structures of the fullerene derivatives investigated in the study (a) MAF1 (b) MAF4 (c) MAF5 (d) MAF9 (e) MF02-01 (f) MF03-01 (g) MF03-04 (h) MF04-01 (i) MF04-02.*

2.1.2 Derivatives of Triphenylene

Four polysubstituted derivatives of triphenylene were studied in the research. C0/C0 is a derivative of triphenylene with OH addends, known as hexa hydroxy triphenylene (figure 2.2(a)). Derivatives 2,6,10-trihydroxy-3,7,11-tri(pentyloxy)triphenylene (C5/C0) and 2,3,6,7,10,11-hexakis(pentyloxy)triphenylene (C5/C5) (figure 2.2(b) and (c)) were part of a homologous series of alkyl polysubstituted triphenylene derivatives previously studied by Robinson et al. [71]

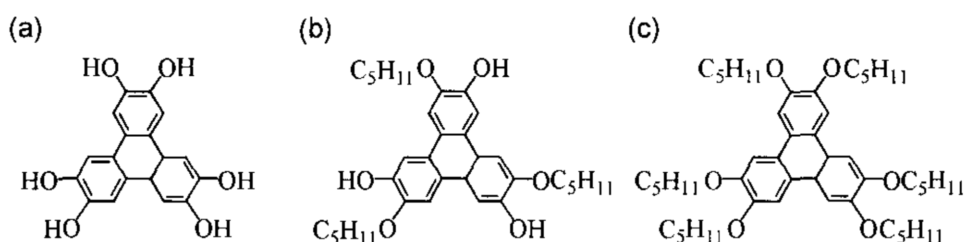

Figure 2.2 Chemical structures of the triphenylene derivates (a) C0/C0 (b) C5/C0 (c) C5/C5.

Also studied was 2,6,10-triethoxyoxirane-3,7,11-tris-pentyloxytriphenylene (C5/epoxide), which is similar to C5/C0 except that the OH groups are replaced by epoxy pendant chains to aid crosslinking as shown in figure 2.3.

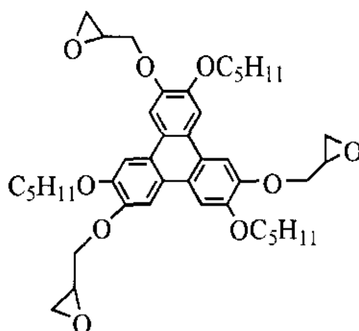

Figure 2.3 Chemical structure of C5/epoxide.

2.1.3 Crosslinkers

Eight types of crosslinker were tested in this study, shown in figure 2.4. They are the hexamethoxymethylmelamine (CL03-01), [2-hydroxy-5-methyl]-1,3-benzenedimethanol (CL04-01), 2,6-di(methoxy-methyl)-4-methylphenol (CL04-02), 3,3',5,5'-tetrakis (methoxymethyl)[(1,1'-biphenyl)-4,4'-diol] (CL04-03), cycloaliphatic epoxide resin (CL05-01), Cycloaliphatic epoxide resin dilutent (CL05-02), the epoxy novolac resin (CL05-03) and tetraglycidyl-meta-xylylenediamine (CL05-04). CL05-03 is an epoxy novolac crosslinker formed by the product of epichlorohydrin and phenol-formaldehyde novolac.

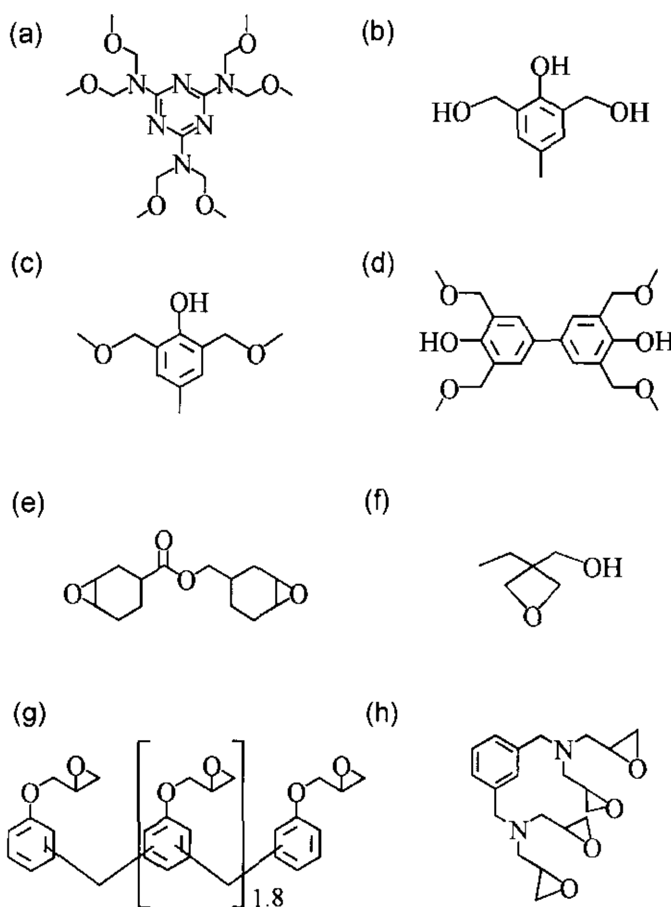

Figure 2.4 Chemical structures of the crosslinkers used in the study (a) CL03-01 (b) CL04-01 (c) CL04-02 (d) CL04-03 (e) CL05-01 (f) CL05-02 (g) CL05-03 and (h) CL05-04.

2.1.4 Photoacid Generators

The photoacid generator (PAG) is one of the key elements of a chemically amplified resist formulation. Two different groups of acid generators were employed in the study. The first group, shown in figure 2.5, include triphenylsulfonium triflate (PAG03-01), a PAG based on sulfonium salts and commonly used in chemical amplification resists [126-129] and 3,6-bis(2-methyl-2-morpholinopropionyl)-9-octylcarbazole (PAG04-03). The second group, commonly known as photoinitiators, include the bis[4-di(phenylsulfonio)phenyl]sulfide bis(hexafluorophoshate) (PAG04-01) and triarylsulfonium hexaflurophosphate salts (PAG04-02) are shown in figure 2.6.

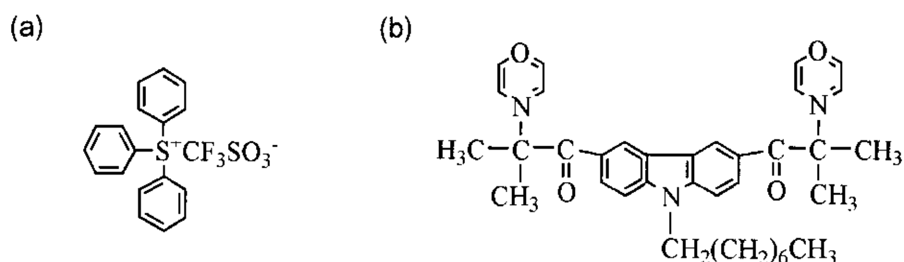

Figure 2.5 *Chemical structures of the photoacid generators (a) triphenylsulfonium triflate (PAG03-01) and (b) 3,6-bis(2-methyl-2-morpholino propionyl)-9-octylcarbazole (PAG04-03).*

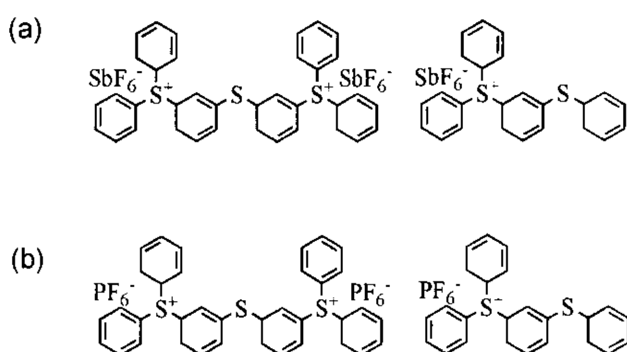

Figure 2.6 *Chemical structures of the photoinitiators (a) bis[4-di(phenylsulfonio) phenyl]sulfide bis(hexafluorophoshate) (PAG04-01) and (b) triarylsulfonium hexaflurophosphate salts (PAG04-02).*

2.2 Sample Preparation

Hydrogen terminated silicon was used as the substrate for most of the experiments, although silicon treated with hexamethyldisilazane (HMDS) was also utilized, as both provide hydrophobic surfaces needed for the resists studied. Since the solvents used in the resist preparation are mostly non-polar, better adhesion with the substrate is achieved with hydrophobic surfaces.

2.2.1 Substrate Preparation

Silicon (100) wafers were cut into 2 cm x 2 cm chips and were cleaned ultrasonically in deionized (DI) water to remove dust. They were then immersed in piranha solution, which is a mixture of hydrogen peroxide and fuming sulphuric acid (1:1), for 10 minutes. The piranha removes organic contaminants from the chips by oxidizing (burning) them, and metals by forming soluble complexes. After rinsing in DI water for 1 minute, the chips were immersed in a weak solution hydrofluoric acid. This removes the native silicon dioxide and hydrogen-terminates the silicon, producing a hydrophobic surface. After rinsing again in DI water for 1 min, the substrates were dried in a flow of dry nitrogen.

To treat the silicon with HMDS, each chip was heated on a hotplate at 120 °C for about 2 minutes to remove moisture before putting it on the vacuum chuck of a spin coater (described below). About 100μl of HMDS was then quickly dropped onto the chip before it cooled. The HMDS was allowed to react with the native silicon dioxide surface for one minute, forming a hydrophobic self-assembled monolayer. The sample was then spun at 1000 RPM for 30 s followed by 3000 RPM for 40 s to remove the excess HMDS.

2.2.2 Spin Coating

Spin coating is a technique for preparing smooth films. A resist is first dissolved in a suitable solvent (e.g. chloroform). A substrate is placed on the vacuum chuck of a spin coater and a calibrated amount of the resist solution is dropped onto the substrate. The chuck is then rotated at a given speed. Centripetal forces cause the droplet to spread out evenly across the chip whilst the solvent evaporates. A thin film of uniform thickness is therefore formed on the substrate.

The solvent is chosen such that it can dissolve the resist, the PAG and the crosslinker, and has the ability to wet the surface to be coated. It should also have a high evaporation rate so that it will dry quickly during spin coating. The thickness of the film depends on both the resist concentration and the rotation speed. The higher the concentration, the thicker the film, whilst a higher rotation speed will produce thinner films. For most of the films used in this report, a concentration of between 5 to 10 g of resist per L of solvent was used, and a rotation speed of 600 revolutions per minute (RPM) for 60 s was applied followed by a 10 s spin at 3000 RPM to ensure no solvent remained at the edges of the chip (which could otherwise then flow back and damage the film).

2.2.3 Post-application Bake

Post application bake (PAB) is the process of heating a resist sample before exposure, with the main purpose of ensuring complete evaporation of the casting solvent remaining in the resist film after spin coating. Unlike most commercial polymer based resists, evaporation of the solvent in our resist is relatively rapid, and thus the PAB process after coating on most of the resists in the study was unnecessary. However, for the purposes of comparison, PABs of between 100 to 120 °C for between 5 to 10 min were applied to some of the resist samples using a hotplate.

2.3 Exposure

2.3.1 The Scanning Electron Microscope

In this work, a scanning electron microscope (SEM) was used for both analysis and lithography. Throughout the project, a Philips FEI XL30SFEG SEM, as shown in figure 2.7, was used.

Figure 2.7 The Philips FEI XL30SFEG SEM used in the research.

(a) Imaging using the SEM

In a scanning electron microscope, a monoenergetic beam of electrons is generated by an electron gun. This electron source can be either thermionic or field emission. In a thermionic emission source, electrons are emitted from a conducting material by heating it, providing the electrons with enough thermal energy to overcome the surface material work function. The most common thermionic emitter is a tungsten filament, chosen due to its high melting point, and thus ability to absorb more thermal energy. Another common emitter is the lanthanum hexaboride (LaB_6) crystal. LaB_6 has the advantage of having a lower work function, emitting electrons at a lower temperature than tungsten, and producing a brighter beam. However, LaB_6

requires a higher vacuum to operate. In a field emission source, a strong electric field is applied across a sharp metal tip, allowing electrons to tunnel through and leave the source. [34] A field emission source provides a brighter beam compared to a thermionic source, and since the source size is smaller, the beam produced is narrower and has a smaller energy spread, resulting in better resolution. However, field emission sources require a much higher vacuum (10^{-9} Torr) to work. The Schottky field emission gun (SFEG) incorporates both thermionic and field emission by using a heated tungsten tip. SFEG produces a narrower electron beam with higher brightness, thus a higher resolution. The Philips FEI XL30SFEG SEM used in this study uses a Schottky emitter. [130]

Electrons can be focused either by magnetic or electrostatic lenses. A magnetic lens consists of two circularly symmetric iron polepieces with a copper winding in-between, as shown in figure 2.8.

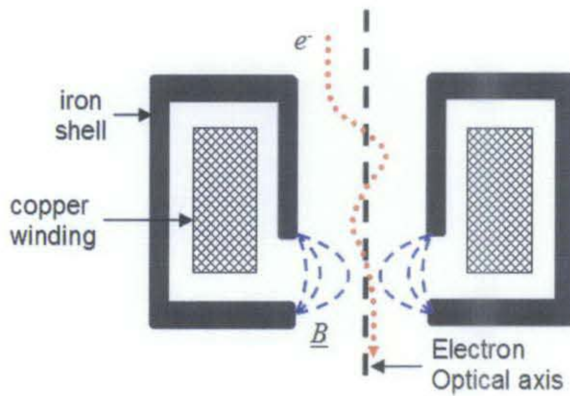

Figure 2.8 *A magnetic lens. The blue lines represent the magnetic field and the red line is the electron path.*

The force, $\underline{F}$, acting on the moving electron due to the magnetic field, $\underline{B}$, follows the right hand rule, in the direction towards the optical axis, such that,

$$\underline{F} = q\,\underline{v} \times \underline{B} \ , \tag{2.1}$$

where q is the electron charge and $\underline{v}$ is the velocity of the electron. This force causes electrons to move back towards the optical axis, resulting in a focusing action.

Electrostatic lenses generally consist of three consecutive elements like apertures, as shown in figure 2.9. Two of the elements are at ground potential while the inner one is held at some potential, V_f, which determines the lens strength. The electric field, $\underline{E}$, between the plates exerts a force, $\underline{F}$, on the electrons, such that

$$\underline{F} = \underline{E}\, q\,. \tag{2.2}$$

The electric force, $\underline{F}$, tends to pull electrons travelling away from the optical axis back towards it, focusing them. Although electrostatic lenses have the advantage of being able to adjust strength much more quickly than magnetic lenses, they have substantially more aberration than magnetic lenses. Aberration is a failure of a lens system to focus all the electrons passing through the lens to the same focal point, due to the different converging power at different points of the lens, resulting in the blurring of the image. Therefore, electrostatic lenses are usually used as condenser and deflector lenses where speed is essential and aberrations are less critical, while magnetic lenses are more commonly used as objective lenses, where sharp focussing is critical. [34]

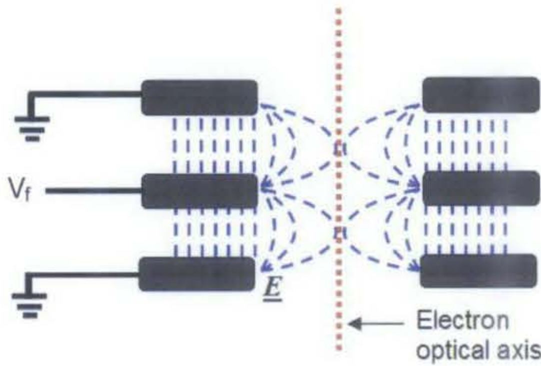

Figure 2.9 *Cross-section through an electrostatic lens. The blue lines represent the electric field, $\underline{E}$.*

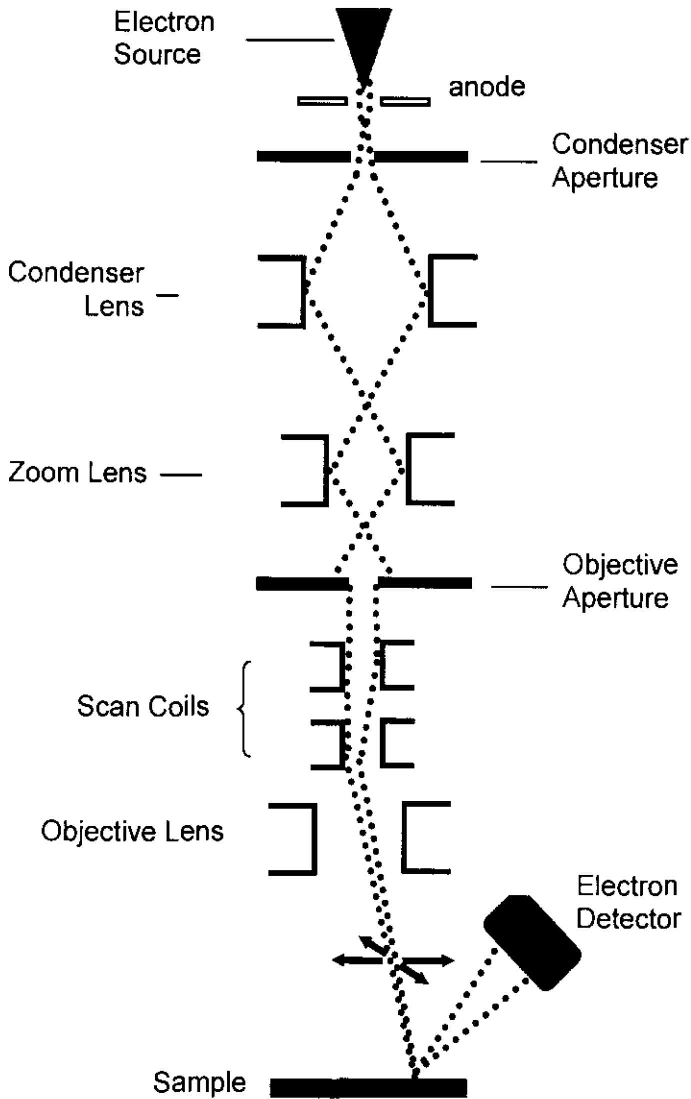

Figure 2.10 Raytrace of the electrons in an SEM as it is emitted from the cathode through the column onto the sample.

In figure 2.10, a ray diagram shows how the beam of electron travels through a typical SEM. The beam from the electron source passes through the condenser aperture which narrows the beam by stopping electrons which have travelled too far from the axis. The beam is then de-magnified by the condenser lens which forms the electrons into a well collimated beam and limits the current. [34] The zoom lens determines the area scanned by the beam at the sample

and thus the magnification of the image. Since magnification is the ratio of the size of the monitor screen to the size of the scanned area, it is increased by reducing the area scanned on the sample. The objective aperture further eliminates electrons deviated at large angles from the beam. The scan coils are used to deflect the electron beam in the x and y direction, scanning it across the surface of the sample, and can be done magnetically or electrostatically. Scanning is usually done in a grid fashion, called a raster pattern, in the direction determined by the voltages on the x and y coils, dwelling on points for a period of time determined by the scan speed. Finally, the objective lens focuses the scanning beam onto the sample.

When the tightly focused electron beam is scanned across a sample, the electrons strike the sample and interact with the atoms in the sample, producing backscattered electrons (incident electrons bouncing back after colliding with an atom), or secondary electrons, (electrons emitted from the atoms excited by the incident electrons). These electrons are collected by either a secondary electron detector (or a backscattered electron detector) located to the side of (or above) the sample. The image of the sample is then displayed on a television monitor by plotting the signal intensity received by the detector against the applied voltage on each of the scan coils. Secondary electrons, which have very low energy (~100 eV), can provide information on the topography of the sample surface because their intensities vary with the angle of the surface being probed. On the other hand, the energies of backscattered electrons are strongly affected by the atomic mass of the material they collide with, so a backscattered electron detector would provide more information on the chemical composition of the surface. As the electron beam scans over the entire sample, a complete image of the sample is displayed on the monitor.

(b) SEM as a lithography tool

The first electron beam lithography machines were developed in the late 1960s, based on the scanning electron microscope. [34] The technique consisted of scanning a beam of electrons

across a surface covered with a resist film sensitive to electrons, depositing energy in the desired pattern in the resist film. This was achieved by manually blanking or unblanking the beam as needed to expose certain areas of the resist.

To achieve high resolution patterns, an external lithographic pattern generator can be used to control the beam deflection of the SEM. In this study, a Raith Elphy Quantum pattern generator was utilised. The pattern generator works by applying the necessary voltage to the x- and y-scan coils, depending on the beam deflection required to create a certain pattern. The scan field is the area across which a pattern can be written without moving the sample stage. The area of the scan field determines the deviation of the beam from the optical axis. Large angle deviation tends to increase the beam diameter, so a large scan field is usually used for low resolution patterning while a smaller scan field is employed for high resolution. The software also takes over the stage control of the SEM, moving the sample to the next area to be scanned after a pattern is completed.

The dwell time of a beam on certain areas is determined by the resist sensitivity and the beam current. Since the electron dose is proportional to the beam current and dwelltime, as stated in equation 1.6, the dwell time must increase for a less sensitive resist or a lower beam current, and vice versa.

2.3.2 Sensitivity Test

After a resist film was prepared by spin coating, its sensitivity was measured. The resist-covered substrate was broken into 8 samples of 10 mm x 5 mm. Alignment marks were made on the sample, using a diamond scribe, and it was placed into the SEM. The ends of the alignment marks were carefully located without irradiating other areas of the sample and the image on the SEM was carefully focussed on the alignment mark. The beam was then blanked. The position of the beam on the sample was moved to a fresh part of the substrate and subsequent exposures were done on un-irradiated areas of the resist film. To determine the

sensitivity of a resist, a pattern of squares was exposed on the sample, with each square receiving a different electron dose, controlled by varying the exposure duration. The magnitude of the current could also be varied to control the dose applied to each area. To determine the sensitivity, the resists were developed and analysed as discussed in sections 2.4 and 2.5.

2.3.3 Resolution Testing

Fine patterning was done using a Raith pattern generator. The scan field size was chosen and an appropriate magnification selected. Calibration of field size, skew and rotation was performed, in every case using a sample featuring an array of gold squares on silicon with known dimensions, positioned next to the sample. The sample coordinate system (expressed in uv) is then connected to the xy coordinated system of the SEM, as shown in figure 2.11. To do this the left lower corner of the sample was set as the origin for pattern exposure and the lower right corner is then used to calculate a rotational correction. The beam was then focused on an area

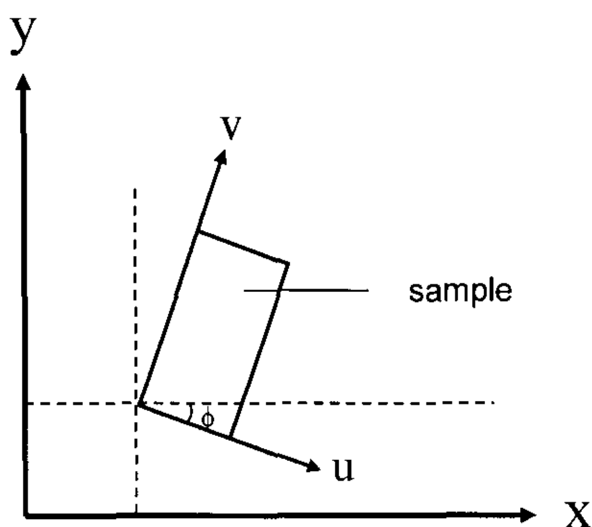

Figure 2.11 The uv coordinate system of the sample with respect to the xy coordinate system of the SEM.

of the sample close to the area to be patterned and the pattern generator took over control of the SEM scan coils in order to expose the resist.

Patterning was done at high electron energy (30 keV) to reduce forward scattering and so achieve higher resolution. When a pattern was completely exposed, the beam was automatically blanked, and the sample was moved to the next area to be patterned, or removed from the SEM for further processing.

2.4 Resist Development

After exposure it is necessary to develop the pattern defined in the resist. For a positive tone resist this means removing the exposed areas of the film whilst for a negative tone resist the unexposed areas are removed. This process was usually done immediately after exposure to avoid any contamination or post-delay effects, except when the effects of a delay were being investigated.

2.4.1 Post-exposure bake

In the case of chemically amplified resists, a post-exposure bake (PEB) is usually necessary to activate the photoacid generator (PAG) in the resist. After exposure, the samples were heated on a hotplate at a temperature between 90 and 120 °C for a duration of between 30 and 120 s. The sensitivity and resolution of the resist depend on both the PEB time and temperature and thus it was necessary to determine optimal PEB conditions.

2.4.2 Development

To develop the exposed film, the sample was immersed in a suitable solvent, immediately after the PEB process, until the exposed or the unexposed areas, depending on the tone, were

removed. In most of our resists, monochlorobenzene (MCB) was used although other developers such as anisole, mixtures of MCB and isopropanol (IPA) (MCB:IPA[1:1], mixtures of IPA and water (IPA:H_2O[3:7]), ethyl-3-ethoxy proprionate and ethyl alcohol were also investigated. The development time could vary between 2 and 120 s, depending on the developer and the resist. Ultrasonic development was used only when stated. The sample was then rinsed in an inert liquid, usually IPA or DI water, to stop development, and dried using a dry nitrogen gas flow.

2.5 Sample analysis

After development of the exposed resist film, the defined pattern was analysed using a variety of techniques, to determine sensitivity, contrast and resolution. Following this analysis the sample was then sometimes processed further to evaluate the durability of the compounds against the etching step which would follow pattern definition in commercial usage.

2.5.1 The Surface Profiler

A surface profiler was used to measure the thickness of the resist before and after exposure. Several different types of surface profiler exist. In this work, we used a Dektak3ST from Veeco, shown in figure 2.12, which is a contact profiler.

Figure 2.12 The Dektak3ST Profiler used in the research.

The surface profiler is a high precision instrument capable of measuring the topography and thickness of a sample with a vertical resolution of approximately 5 nm. A contact surface profiler uses a diamond tipped stylus in contact with the sample, and moves the sample horizontally under the tip. The stylus is connected to the core of a linear variable differential transformer (LVDT). [131] As the sample moves, the tip is deflected vertically by the surface topography, and electrical signals, due to the corresponding motion of the core of the LVDT, and proportional to the vertical displacement of the tip, are produced. A two-dimensional contour of the sample is thus recorded. The tip is held down on to the sample with a known force between 1 – 40 mg in order to accurately measure the topography of the surface.

A low force of 5 mg was usually used to measure the thickness of the resist to avoid the stylus from digging into the relatively soft resist film. Because of the low force it was necessary to use a slow scan speed, so that the stylus did not bounce off the surface. In the case of very soft resist films, an even smaller force had to be used.

The horizontal resolution of this surface profiler is determined by the scan length and the scan speed, which determine the number of data point per scan. A highest resolution of ~6 nm between data points can be achieved with a scan length of 50 μm and the lowest scan speed. Although both the vertical and horizontal resolutions are not as good as an atomic force microscope (AFM), they are more than sufficient for this study which requires thickness measurement of resist areas with ~100 μm dimensions. Furthermore, the profile of a surface can be determined much faster and over much larger areas using a surface profiler as compared to an AFM.

2.5.2 Response Curve

Several characteristics of the resist can be determined from their response curve, which plots the thickness of the resist retained after development as a function of the exposure dose in a log

linear graph. The tone, the sensitivity and contrast of a resist can be determined from the response curve as shown in figure 2.13.

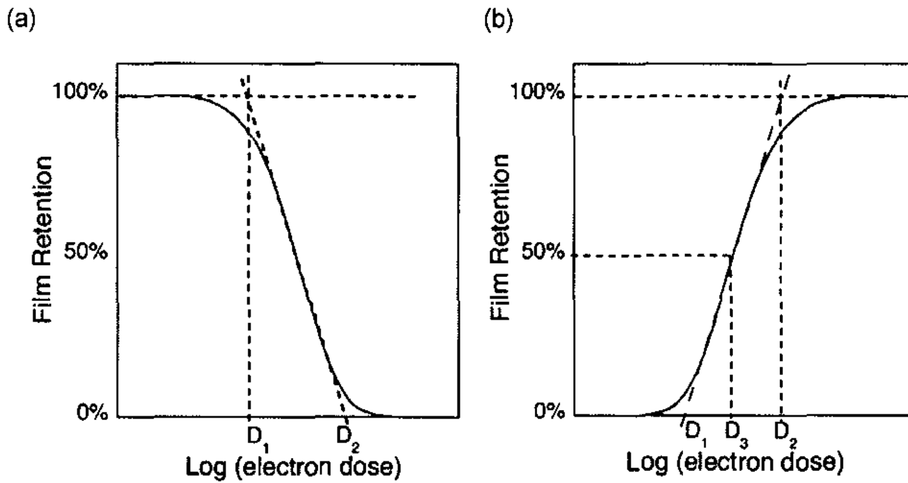

Figure 2.13 Response curves of (a) positive tone resist and (b) negative tone resist.

This shows a typical response curve of a positive tone resist (a) and the response curve of a negative tone resist (b). The sensitivity of the positive tone is, traditionally, the minimum dose that removes all of the resist, depicted by D_2 in figure 2.13(a) while that of the negative tone is the dose when 50% of the resist is retained, depicted by D_3 in figure 2.13(b).

The contrast of the resist, which demonstrates the rate of change of its solubility with exposure dose, can be calculated using equation 2.1, which represents the slope of the graph.

$$\gamma = \frac{1}{\log_{10}\left(D_2 / D_1\right)} \quad (2.1)$$

2.6 Etch Durability

After a sample has been exposed, developed and profiled to measure its sensitivity, the etch durability can be determined. The equipment used in this study was a Plasmalab 80 Plus Etcher from Oxford Instruments, shown in figure 2.14.

Figure 2.14 The Plasmalab 80 Plus Etcher used in the research

To determine the etch durability of a resist, the film thickness of a processed resist sample, together with a control sample, were measured. A commercial resist with a known high etch durability, in this work SAL-601, was used as a control sample so as to allow comparison of different etchs. The samples were etched simultaneously with an electron cyclotron resonance microwave plasma (ECR) process using sulphur hexafluoride (SF_6) as the etchant for a preset time (1 - 30 min). The sample and the control were profiled to determine the etch durability.

The etch durability of a resist is usually expressed in terms of its etch ratio, which is the ratio of the etch rate of resist to the etch rate of the substrate, determined by measuring the original thickness of the resist before etching, t_1, and the height of the etched pattern, t_2, as

shown in figure 2.15. When the resist is totally removed after etching as in figure 2.15(a), the etch ratio, ER, is such that,

$$ER = \frac{t_1}{t_2}. \tag{2.2}$$

However, if some resist remains on the substrate after etching, as in figure 2.15(b), an ashing step is required after profiling the resist to determine how much resist was actually removed.

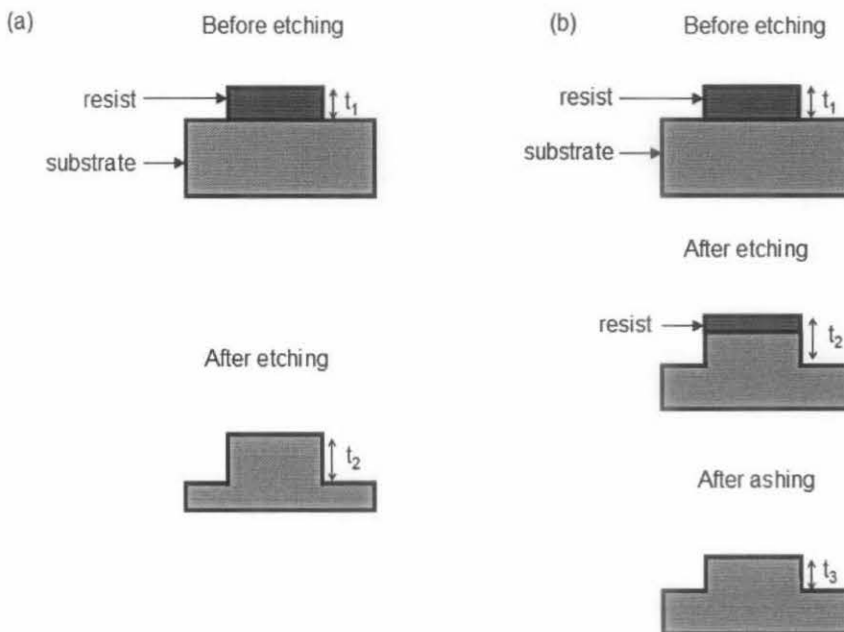

Figure 2.15 *Determination of the etch ratio of the resist. In (a) the etch ratio of the substrate is equal to the ratio of the thickness of the resist before etching,* t_1*, to the height of the pattern after etching,* t_2 *and in (b) the etch ratio is* $= t_1 - (t_2 - t_3) / t_3$.

2.6.1 Plasma Asher

An asher uses an oxygen plasma to remove organic residues (such as resist) from a sample without damaging the substrate. In this study, a Plasma Processor 100-E from Technics GmbH, was used. The substrate was placed in the oxygen plasma between 5 to 20 min, and radicals

from the plasma react with the resist, oxidizing it and removing it from the substrate, without significantly affecting the substrate itself.

This process is only necessary when etching a sample with a thick resist or one which is highly etch resistant such that some resist remains on the substrate after etching, as shown in figure 2.15(b). The ashing step helps to determine how much resist and substrate has been etched, in which case, the etch ratio, ER, is given by,

$$ER = \frac{t_1 - (t_2 - t_1)}{t_3}. \quad (2.3)$$

2.6.2 Normalised etch durability

In order to make comparison between different etch runs, where process parameters, and hence the etch durability vary somewhat, the control sample was used to normalise the results presented. To do this a 'standard' etch durability of SAL601, SED_{SAL601}, was set to be 3 times that of silicon, based on the average etch durability achieved for SAL601 in the various etch runs. The etch durability of a resist is defined as its resistance to etching compared to the silicon substrate - the inverse of etch ratio. The normalised etch durability of the resist investigated, NED_{resist}, was calculated using equation 2.4.

$$NED_{resist} = \left(\frac{ED_{resist}}{ED_{SAL601}} \right) \times SED_{SAL601}, \quad (2.4)$$

where ED_{resist} and ED_{SAL601} are the actual etch durability of the investigated resist and that of SAL601 respectively, for a particular etch run. In each case, the normalised etch durability has been presented, whilst the raw data is given in an endnote.

3

Chemical Amplification of Fullerene Derivatives

This chapter discusses the results of chemical amplification of several fullerene derivatives using a number of crosslinkers and photoacid generators. The sensitivities of several derivatives have been greatly improved by the incorporation of crosslinkers and photoacid generators. The chemically amplified MF03-04 resist has a sensitivity of 8 $\mu C/cm^2$ when exposed to 20 keV electrons, three orders of magnitude better than pure MF03-04 resist, while maintaining a resolution below 30 nm. The sensitivity dependence on the photoacid generator and crosslinker concentrations, and on post exposure bake conditions, were investigated. Effects of post exposure delays on the performance of the chemically amplified resists were also studied.

Chemical amplification of several fullerene derivatives described in chapter 2, using crosslinkers and photoacid generators was investigated. Five different crosslinkers, shown in figure 2.4, and two different photo acid generators, shown in figure 2.5 and 2.6 were tested.

3.1 Film Preparation

To prepare films of the resist, the derivatives were dissolved in chloroform at concentrations of 0.1 to 1 g per litre (g/l). The solution was dispensed (100 μl) by pipette onto hydrogen-terminated silicon which was then rotated at speeds of between 500 to 1500 RPM using a spin coater. The thickness of the resulting films depended on both the solution concentration and spin speed. Figure 3.1 illustrates how the thickness changes with solution concentration, and spin speed, for the fullerene derivative MAF5. The thickness of the resist film can be reduced by decreasing the resist concentration and/or increasing the spin speed.

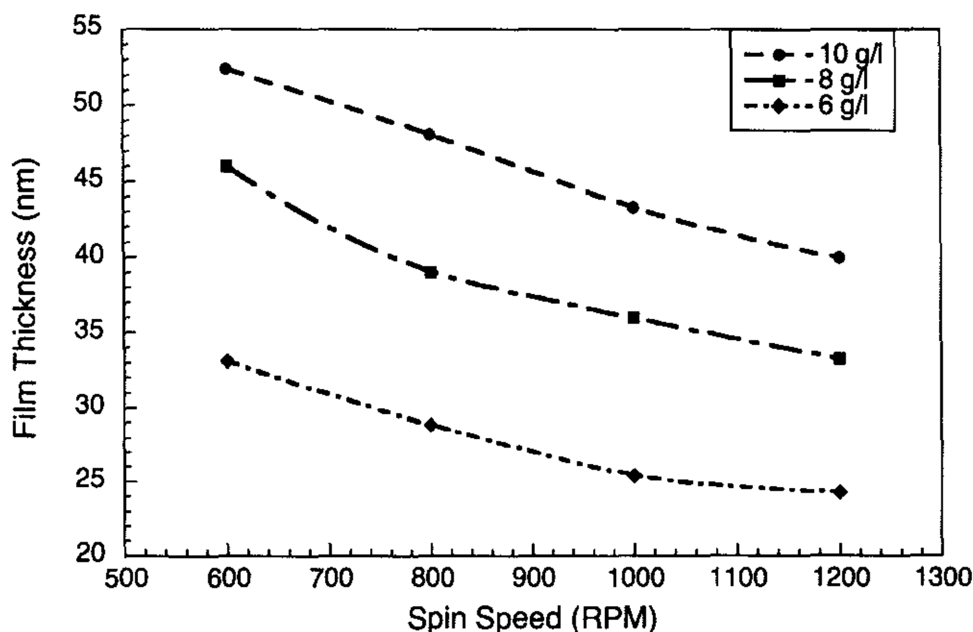

Figure 3.1 The film thickness vs spin speed (RPM) for various concentrations of MAF5.

Chloroform ($CHCl_3$) was used as the casting solvent for all the derivatives studied. It was also a suitable solvent for the crosslinkers and photoacid generators used.

3.2 Sensitivity

Chemical amplification of several resists was attempted by adding a photoacid generator, and by adding both a photoacid generator and a crosslinker. The sensitivities of the resists were determined following the processes described in section 2.3.2.

3.2.1 Chemical amplification using photoacid generator PAG03-01

The methanofullerene MF02-01, a mixture of hexa, penta, tetra adducts of fullerene with triphenylene addends, is shown in figure 2.1(e). Pure MF02-01 was exposed using 20 keV electrons, developed in monochlorobenzene (MCB), rinsed in isopropanol (IPA) and dried with nitrogen. The residual film thickness after processing was measured using a surface profiler. A log-linear plot of thickness against exposure dose is shown in figure 3.2. The resist demonstrates negative tone behaviour, with sensitivity ~ 460 $\mu C/cm^2$.

The photoacid generator PAG03-01 was added to MF02-01 at 1 g per g of derivative, and the composition was spin coated from chloroform. After irradiation, the film was baked at 100 °C for 240 s, developed in Ethyl Alcohol and rinsed in IPA. The response curve is shown in figure 3.3. Although there was some film thickness reduction, the resist was not entirely removed. Similar results were seen with several other developers including Acetone, TMAH, MCB, cyclohexanone and cyclopentanone. When PAG03-01 was added at concentration of 0.1 g per g of derivative, no positive resist behaviour was observed and the negative tone sensitivity was as that for pure MF02-01. Since positive tone behaviour occurred only when substantial PAG was added, it was inferred that the "positive behaviour" could be due to leeching of the PAG in the highly PAG loaded resist.

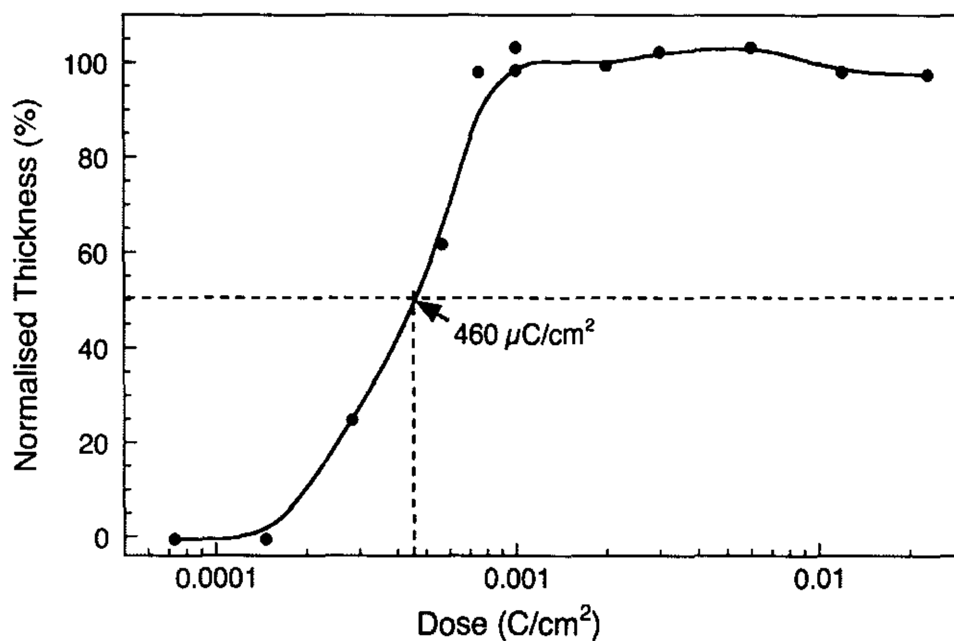

Figure 3.2 Response curve of MF02-01 after irradiation at 20 keV and development with MCB.

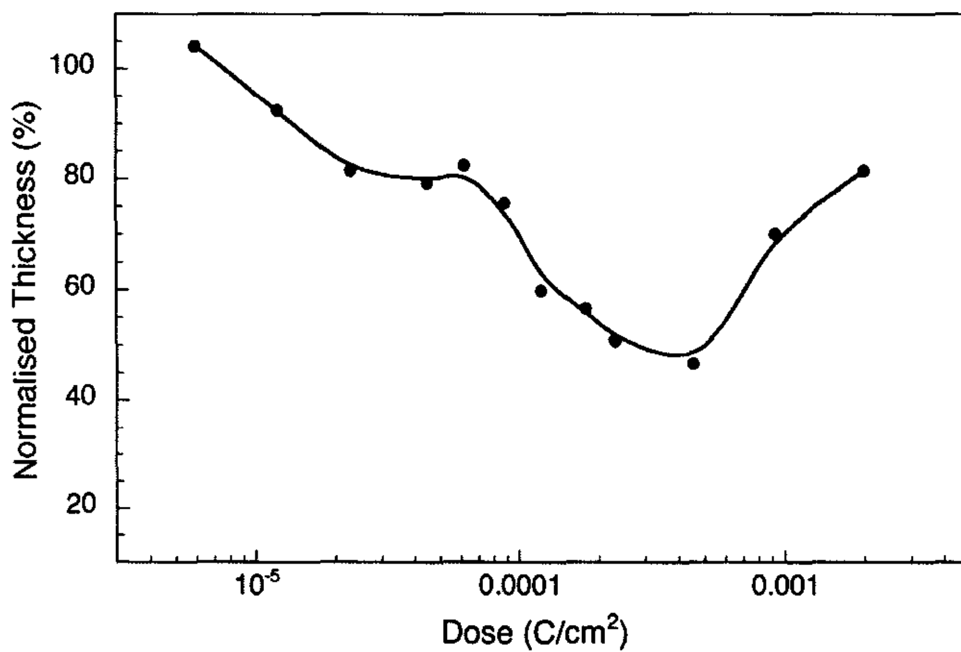

Figure 3.3 Response curve of MF02-01+PAG03-01[1:1] after irradiation at 20 keV and development with ethyl alcohol.

The monoadduct fullerene derivative MAF5, shown in figure 2.1(c), has previously been investigated by this group [69] and shown to be a high resolution resist with a sensitivity of ~3 mC/cm^2. However, chemical amplification of the compound by combining it with PAG03-01 was unsuccessful, so no further tests were carried out.

3.2.2 Chemical amplification using PAG03-01 and CL03-01

The responses of three derivatives, MF02-01, MAF5 and MF03-01, were investigated when combined with PAG03-01 and crosslinker CL03-01. Several films with different ratios of PAG03-01 and CL03-01 per g of derivative were prepared. Resists were exposed at 20 keV, baked at 100 °C for 60 s and developed for 10 s in MCB. It can be seen from the response curves in figure 3.4 that all three resists demonstrated sensitivity enhancement. The resist MAF5 with incorporation of both PAG03-01 and CL03-01 showed a sensitivity of ~150 μC/cm^2. However, this sensitivity would not be high enough for industrial application. The derivative MF03-01, shown in figure 2.1(f), has the same addends as MAF5, but six times as many. As a hexadduct it should have more crosslinking sites, and as expected, a higher sensitivity was achieved. A combination of MF03-01, PAG03-01 and CL03-01 at PAG and crosslinker concentrations of 0.23 and 0.5 g per g of derivative respectively, showed a sensitivity of ~12 μC/cm^2. The resist combination of MF02-01, PAG03-01 and CL03-01, at PAG and crosslinker concentrations of 0.14 and 0.6 g per g of derivative respectively, showed the best performance with a considerable sensitivity enhancement to 3.2 μC/cm^2.

Although the sensitivities of chemically amplified MF02-01 and MF03-01 were encouraging, close inspection revealed some problems with the resists. Swelling and 'feathering' of the edges in CA MF02-01, as shown in figure 3.5, made it unsuitable for commercial use. Patterns written in CA MF03-01, on the other hand, were smeared as shown in

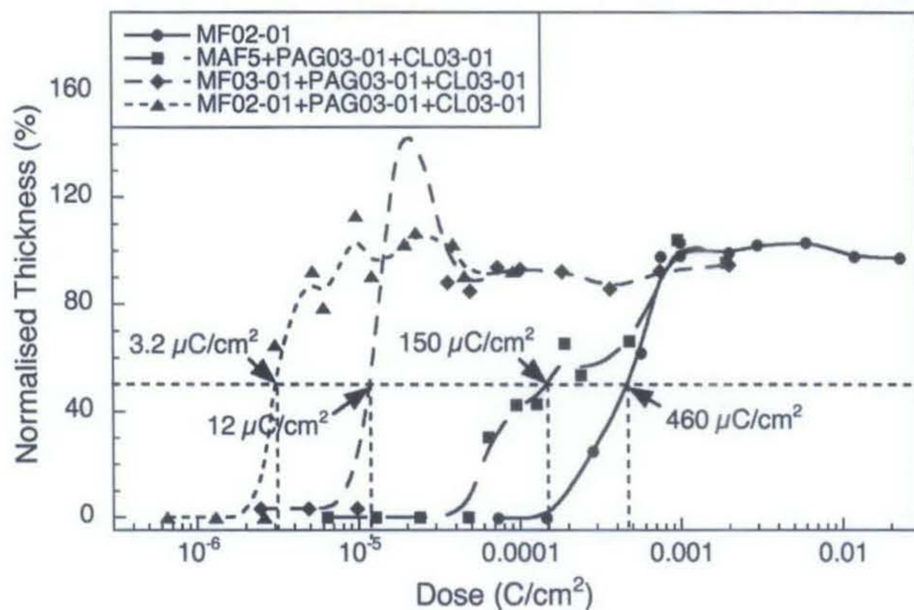

Figure 3.4 *Response curve of CA MAF5, CA MF03-01 and CA MF02-01, compared to that of pure MF02-01, on exposure to 20 keV electrons, PEB at 100 °C for 60 s and development in MCB.*

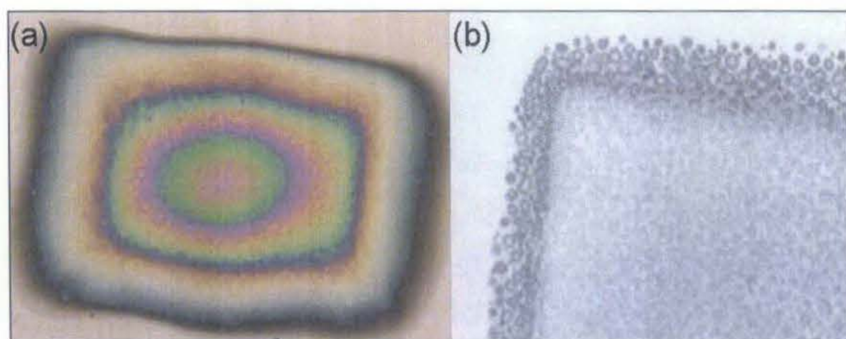

Figure 3.5 *Optical micrograph of an exposed spot in CA MF02-01 showing (a) swelling and (b) 'feathering' of edges.*

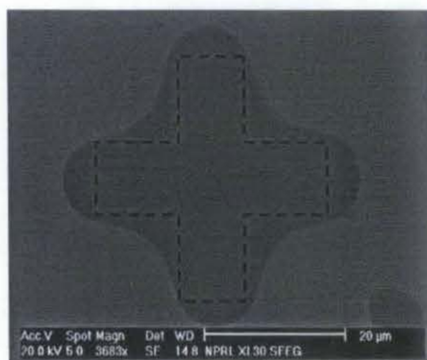

Figure 3.6 *Pattern defined in CA MF03-01 resist at a dose of 320μC/cm^2. The dotted cross showed the written pattern.*

figure 3.6, which could be due to the photoacid, or one of its reaction components, out-gassing from the resist and diffusing laterally over the surface of the material. (The effect being microns greater than typical acid diffusion).

3.2.3 MF04-01 and MF04-02

Epoxide functional groups are often used to improve crosslinking in chemically amplified resists [82,132]. MF04-01 and MF04-02, shown in figure 2.1(h) and (i), have epoxy groups on the C_{60} cage. MF04-01, whilst soluble in chloroform, did not form films on either hydrogen terminated silicon or on silicon dioxide (SiO_2). The same phenomenon was observed when PAG03-02 was added to the resist, so further studies on the derivative were not carried out.

MF04-02 was spin coatable, both pure and with PAG03-02 and CL05-01 added. Samples were exposed at 20 keV, with doses as high as 3 mC/cm^2, and PEB of 100 °C for 60 s. MCB was used to develop the samples, but no patterning of the samples was observed at any dose. Thus the resist was not studied further.

3.2.4 Chemical amplification of MF03-04

The methanofullerene MF03-04, shown in figure 2.1(g), is similar to MF03-01 but with hydroxyl termination of the addends. The sensitivity of pure MF03-04 was found to be ~550 μC/cm². Adding the photoinitiator PAG04-01, shown in figure 2.6(a) and crosslinker CL05-01 (figure 2.4(e)) to the derivative at PAG and crosslinker concentrations of 0.6 and 1 g per g of derivative, and at 0.5 and 4 g, gave a sensitivity of ~300 and 150 μC/cm² respectively, as shown in figure 3.7. When PAG03-01 was substituted for PAG04-01, the sensitivity increased slightly to ~120 μC/cm².

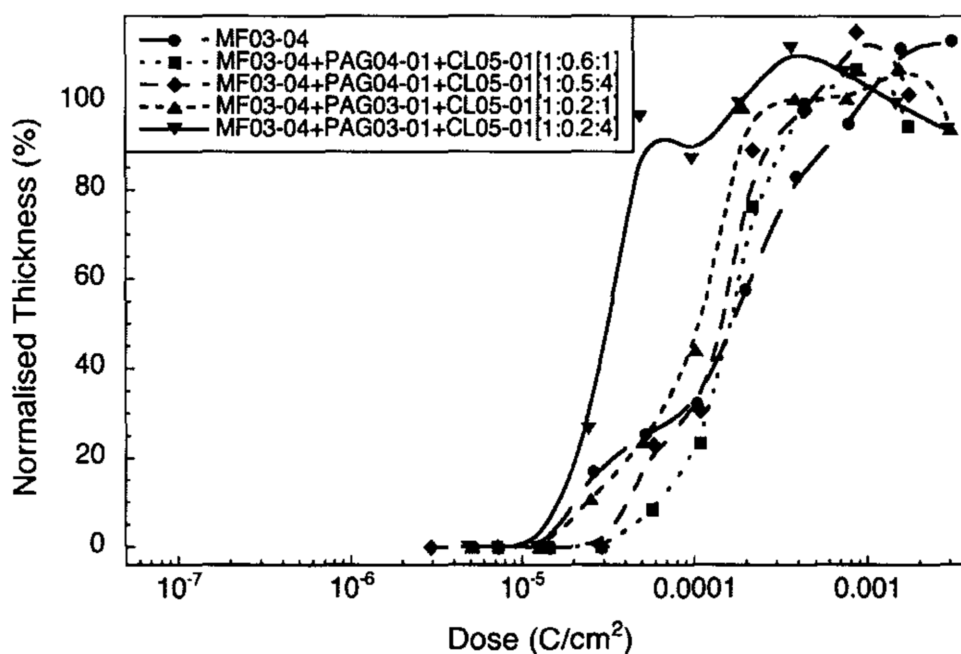

Figure 3.7 Response curve of various combination of MF03-04 and PAG04-01 or PAG03-01 and CL05-01 on exposure to 20 keV, PEB 100 °C for 60 s, and development in MCB.

Resist compositions were prepared using the epoxy crosslinker CL05-03, shown in figure 2.4(g), at crosslinker concentrations of 1 and 2 g, and photoinitiator PAG04-01

concentrations of 0.5 and 1 g, per g of derivative. Exposures were done at 20 keV electrons, followed by PEB of 100 °C for 60 s and development in MCB. The response curves in figure 3.8 show that increasing either crosslinker or photoinitiator concentrations gave better sensitivities. The composition with crosslinker and photoinitiator concentrations of 2 and 1 g per g of derivative respectively, gave the highest sensitivity of ~10 $\mu C/cm^2$. This ratio is equivalent to approximately 25 mol of CL05-03 and 1.5 mol of PAG04-01 per mol of MF03-04. Development using MCB, IPA:H_2O [7:3] (by volume) and MIBK:IPA gave similar sensitivity of ~10 $\mu C/cm^2$ whilst IPA:H_2O [1:1] (by volume), and MF322 (Shipley) were unsuccessful. Development in anisole gave the best sensitivity of 8 $\mu C/cm^2$ as shown in figure 3.9.

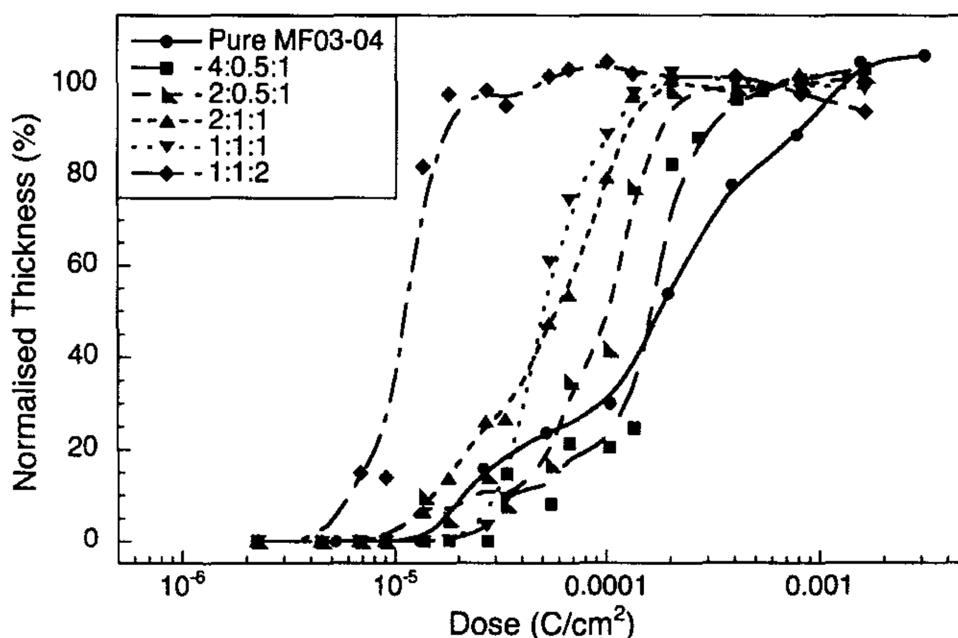

Figure 3.8 Response curve of CA MF03-04 at various ratios of MF03-04+PAG04-01+CL05-03 on exposure to 20 keV electrons, PEB of 100 °C for 60 s and development in MCB.

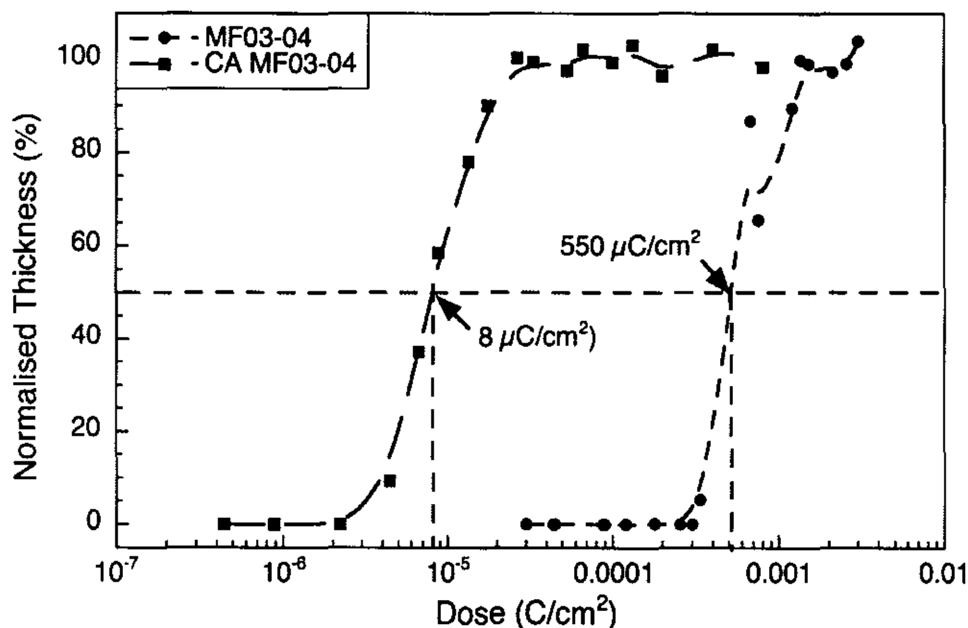

Figure 3.9 *Response curve of MF03-04+PAG04-01-CL05-03 [1:1:2] and pure MF03-04, exposed at 20 keV electrons, PEB 100 °C for 60 s, developed in anisole and MCB respectively.*

3.2.5 Other Fullerene Derivatives

MAF4 and MAF9 are shown in figures 3.1(b) and (d) respectively. They have similar structures to MF03-04. Chemical amplification using CL05-03 and PAG04-01 was investigated. Resist films comprising the derivatives, CL05-03 and PAG04-01 at concentrations of 2 g and 1 g, per g of derivative respectively were prepared. Films comprising MF03-01, CL05-03 and PAG04-01 at concentrations of [1:1:1] and [1:2:1], were also prepared. Sensitivity tests were carried out, applying PEBs of 100 °C for 60 s, and development in MCB for 20 s. The response curves in figure 3.10 showed sensitivities ranging from 50 to 200 μC/cm^2, an improvement compared to the non-chemically amplified derivatives, but not enough for commercial requirements. The results suggest that the high sensitivity achieved by the derivative MF03-04 was related to its multiple addends as well as the choice of crosslinker and photoinitiator.

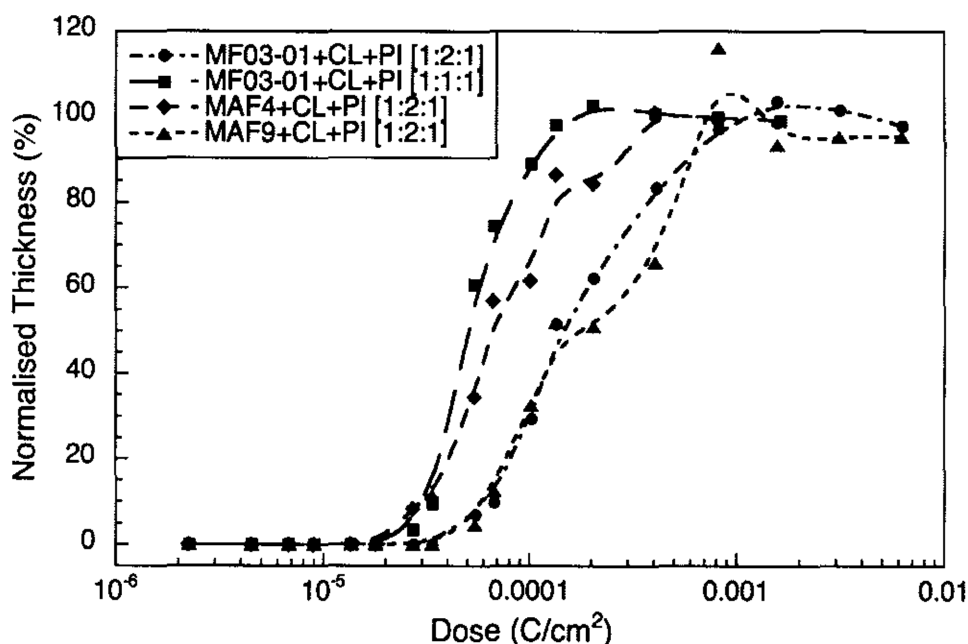

Figure 3.10 Response curve of various fullerene derivatives with CL05-03 and PAG04-01 incorporated on exposure to 20 keV electrons, PEB of 100 °C for 60 s and development in MCB.

3.3 Delay effects

Chemically amplified resists are known to be sensitive to environmental factors such as amines in the air. To investigate the effect of molecular contaminants, exposed samples of MF03-01+PAG03-01+CL03-01 were left in ambient cleanroom conditions. After taking the samples out of the SEM, they were left for periods between 10 s and 9 hours before PEB of 100 °C for 60 s and development in MCB for 10 s. Images of the samples were taken to measure the distortion due to contamination.

A control experiment was also conducted, in which the sample was left in the SEM vacuum for a delay of between 5 min and 9 hrs after exposure. A PEB of 100 °C for 60 s was applied before development in MCB for 10 s. Delays of less than 5 min were neglected because of the inconsistent time taken for venting. Figure 3.11 shows spots on samples that were held in

air before processing, while figure 3.12 shows spots on samples that were left in the SEM chamber. The samples delayed in air show obvious distortions of features. It could be seen that samples started to degrade between 1 and 10 minutes after exposure, whilst samples in vacuum lasted for at least 60 minutes before degrading. This showed that the change in shape was due to contamination and not to acid diffusion.

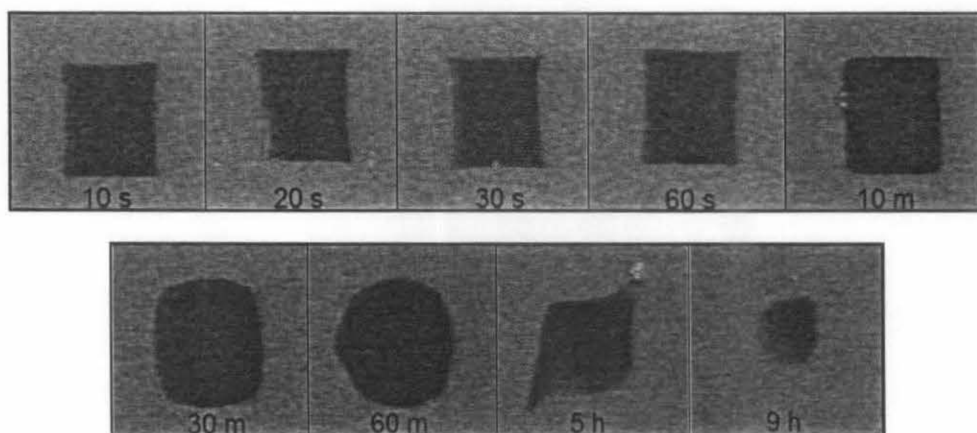

Figure 3.11 Exposure spot on samples subjected to delay in the cleanroom.

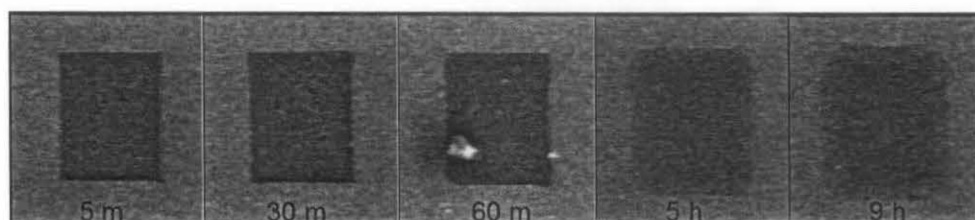

Figure 3.12 Exposure spot on samples subjected to delay in SEM vacuum

3.4 Etch Resistance

The etch durability of the CA MF03-04 resist was determined. Electron cyclotron resonance (ECR) microwave plasma etching was used to etch the samples. Etching was performed at ~25 °C with incident microwave power 250 W, RF power 20 W and a DC self-bias of 114 V. The etchant was SF_6, at a flow rate of 5 sccm and pressure of 1.0 mTorr. Rohm and Haas

SAL601, a conventional high durability novolac based negative resist, was used as a control. The etch was run for 5 minutes.

Results showed that the CA MF03-04 demonstrated a normalised etch durability of 2.55 to that of the silicon substrate, approaching that of SAL601 under the same etch conditions. [133]

3.5 Resolution

In order to determine its resolution, fine patterning was carried out in the CA MF03-04. Exposure was done at 30 keV using the pattern generator followed by a PEB of 100 °C for 60 s and development in MCB for 10 s. Lines as narrow as 50 nm were fabricated in the resist. However, the lines demonstrated a lot of swelling. Reducing the development time to 5 s improved the results slightly, as shown in figure 3.13.

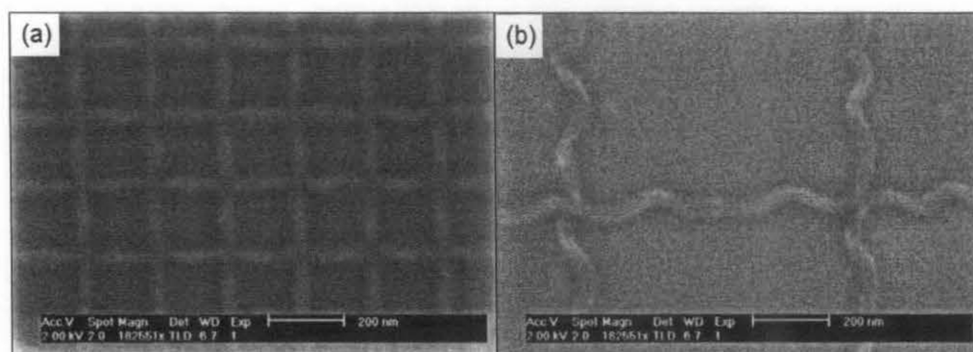

Figure 3.13 *SEM micrograph of patterns defined in CA MF03-04 resist at doses 200 pC/cm and 30 keV, PEB 100 °C for 60 s and development in MCB, showing (a) a mesh and (b) wavy lines.*

Swelling is often caused by penetration of developer into the resist, increasing its volume, and hence wavy lines. It is influenced by the type of developer, and the duration of development [51,134] as well as the resist composition. Further resolution tests were carried out applying PEBs of 90 °C for 3 min, and development in other developers such as anisole,

IPA:H_2O [7:3], anisole:IPA [1:1], and MCB:IPA [1:1]. The development time was reduced to 5 s to reduce the swelling. Development in MCB:IPA for 5 s gave a best resolution of 24 nm, as shown in figure 3.14, with reduced, but still evident, swelling.

Reducing the development time further using ultrasonic development was attempted, [51] but did not reduce the swelling. A PAB of 110 °C for 10 min reduced the smoothness of the film and did not improve fine patterning nor improve the sensitivity of the resist.

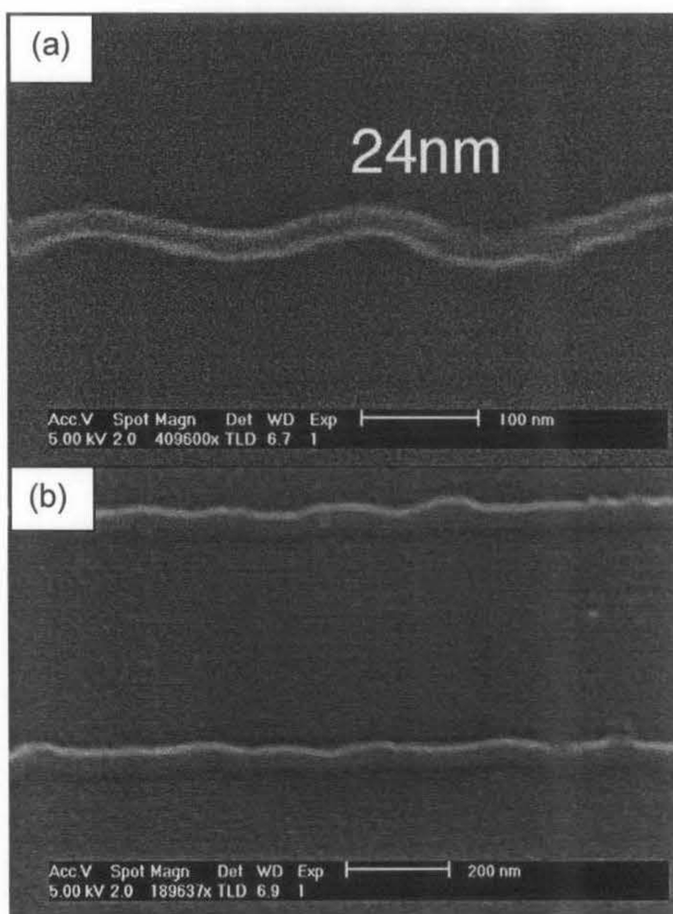

Figure 3.14 *SEM micrograph of lines defined in CA MF03-04 (a) at dose 200 pC/cm and (b) 800 pC/cm viewed at 30 °C angle. Exposure was at 20 keV, PEB of 90 °C for 3 min was applied and development was in MCB:IPA for 5 s.*

3.6 Conclusions

Chemical amplification of several fullerene derivatives using a number of crosslinkers and photoacid generators has been studied. The sensitivities of some derivatives have been greatly improved by the incorporation of crosslinkers and photoacid generators. However, most of these derivatives had problems with swelling, 'feathering' and acid-diffusion. The chemically amplified MF03-04 resist has a sensitivity of 8 $\mu C/cm^2$ when exposed to 20 keV electron beam, three orders of magnitude better than the pure MF03-04 resist, while maintaining a resolution below 30 nm. The CA resist also demonstrated good etch resistance comparable to commercial novolac resists.

The superior sensitivity of the chemically amplified MF03-04 compared to that of the other derivatives could be due to its addends. As a hexaadduct, it has more crosslinking sites compared to MAF4 or MAF9, which have only one addend, hence the higher sensitivity. Comparing MF03-04 with MF03-01, which is also a hexaadduct but with methyl termination, suggests that the OH termination in MF03-04 is also responsible for its crosslinking ability. MF03-04 with its high number of OH groups can be thought of as analogous to a polyol molecule commonly seen in epoxy crosslinker chemistry. The high number of epoxy groups in the crosslinker CL05-03 enabled it to work better in enhancing the sensitivities of the resists as compared to the other crosslinkers used.

4

Chemical Amplification of Triphenylene Derivatives

This chapter discusses the results of chemical amplification of the triphenylene derivative, 2,7,10-tri-pentyloxy-3,6,11-trihydroxytriphenylene, using the crosslinker hexamethoxymethyl melamine and the photoacid generator triphenylsulfonium triflate. The sensitivity of the negative tone pure triphenylene derivative when exposed to 20keV electrons is 6.5 mC/cm^2, which increases substantially to ~5 $\mu C/cm^2$ after chemical amplification. The effects of post-exposure bake (PEB) temperature and duration on the sensitivity of the resist were investigated. The chemically amplified resist demonstrates a high durability against SF_6 plasma in electron cyclotron resonance microwave plasma (ECR) etching, exhibiting a normalized etch durability of ~2.16 to the silicon substrate, approaching that of Rohm and Haas SAL601, a conventional novolac resist, under the same conditions.

It has been shown [70,80] that molecular resists based on triphenylene derivatives can be used as negative tone electron beam resists, enabling the fabrication of structure with sizes ~10 nm. The required electron dose of these derivatives is several mC/cm^2 at 20 keV and thus three orders of magnitude worse than those of standard chemically amplified resists. Results on the chemical amplification of these derivatives are discussed in this chapter.

4.1 Film Preparation

Three triphenylene derivatives, 2,3,6,7,10,11-hexakis(pentyloxy) triphenylene (C5/C5), hexa hydroxyl triphenylene (C0/C0) and 2,6,10-trihydroxy-3,7,11-tri(pentyloxy) triphenylene (C5/C0), the structures of which are shown in figure 2.2, were investigated. Resist films of C5/C5 and C5/C0 were prepared by spin coating using chloroform as the casting solvent. The pure molecular resist was prepared using solution concentrations in the range 1 to 20 g/l. Chemically amplified films were prepared by adding crosslinker and/or photoacid generator. Spin coating was done at speeds of between 600 and 3000 RPM, resulting in films from 10 to 120 nm thickness. In most cases, the films then received a post application bake (PAB) of 70 °C for 10 minutes.

The hexa hydroxy triphenylene, C0/C0, was not soluble in chloroform or in several other solvents tested, such as ethanol and anisole, and was not investigated further.

4.2 Sensitivity

4.2.1 C5/C5

Films of C5/C5 and PAG03-01 at various ratios, were prepared and exposed with 20keV electrons at a range of doses. A PEB of 100 °C or 110 °C for 60 s or 90 s was applied, and

samples were developed in MCB for 10 s and rinsed in IPA. However, response curves did not show any improvement in sensitivity compared to that of the pure derivative.

Samples with both PAG03-01 and crosslinker CL03-01 were prepared, starting at concentrations of 0.1 and 0.6 g per g of derivative, respectively. After exposure and development it was observed that pattern transfer was poor. Increasing the PAG03-01 and CL03-01 to 0.2 and 0.8 g respectively per g of derivative increased the sensitivity; even the spot receiving the lowest dose of ~6 $\mu C/cm^2$ was retained after development as shown in figure 4.1(a). Unfortunately, the exposed spots had ragged edges and rough, uneven surfaces as shown in figure 4.1(b). So as to exclude the possibility of incomplete crosslinking, samples with a higher ratio of crosslinker were prepared (up to 1.8 g crosslinker per g of derivative), but no improvement was seen on exposure.

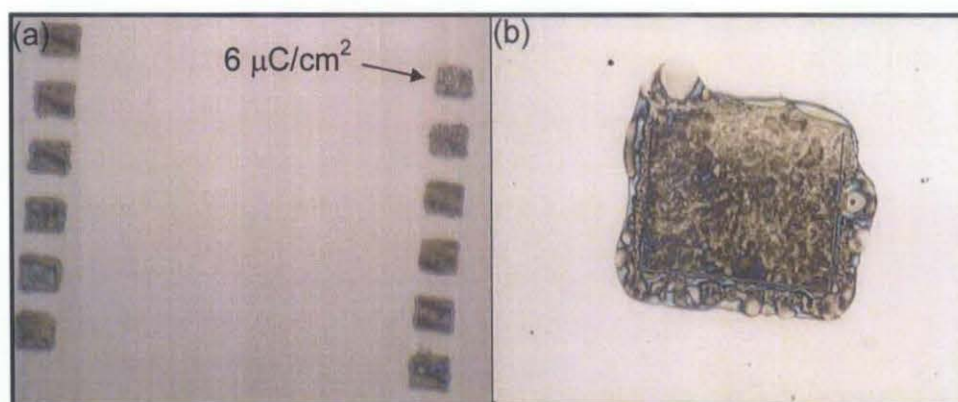

Figure 4.1 *Exposed and developed spots in CA C5/C5 (a) showing the spot with lowest dose and (b) a close up image of one of the spots.*

4.2.2 C5/C0

Samples of the triphenylene derivative C5/C0, and chemically amplified samples incorporating PAG03-01 and CL03-01 in various ratios were prepared by spin coating from chloroform. No PAB was applied. The films were exposed to 20 keV electrons. A PEB of 100 °C for 60 s was applied for both the pure and the mixed films, and development was in MCB for 10 s followed

by an IPA rinse. The response curves of a pure film and a CA film with PAG03-01 and CL03-01 at concentrations of 0.2 and 0.5 g per g of derivative respectively, is shown in figure 4.2. The sensitivity of the amplified resist is ~4.2 μC/cm², a substantial enhancement over the pure triphenylene derivative sensitivity of 5.5 mC/cm².

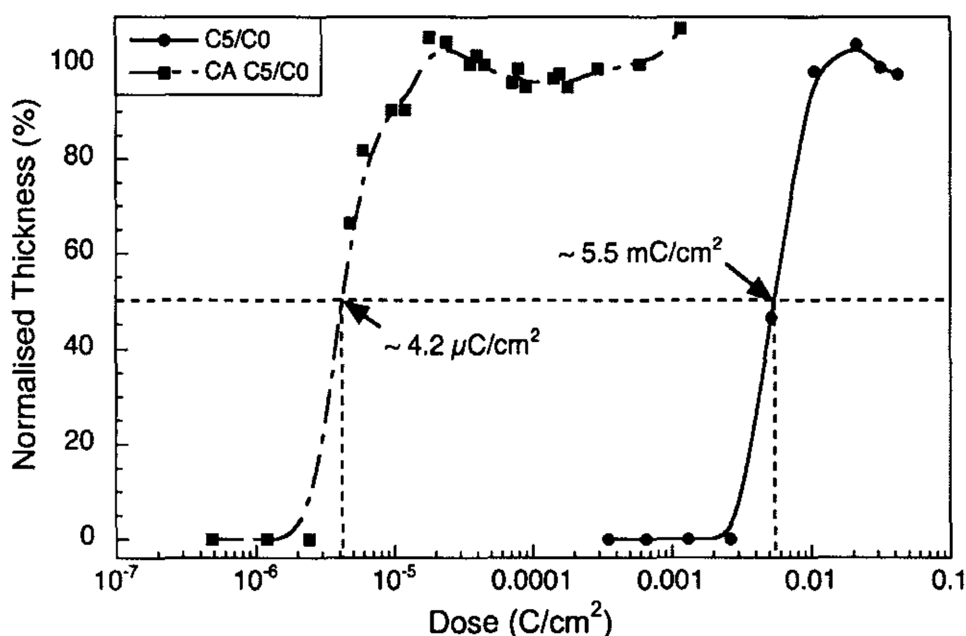

Figure 4.2 *Response curve of chemically amplified C5/C0 at [1:2:0.5] compared to that of pure C5/C0, on exposure to 20 keV electrons and development in MCB for 10 s.*

4.2.3 Sensitivity vs PAG and crosslinker concentration

The effects of PAG and crosslinker concentrations on the sensitivity of the resists were investigated. Resist films with the proportion of PAG varied from 0.2 to 0.4 g and crosslinker 1 g per g of derivative were prepared. Each sample was exposed to 20 keV electrons and a PEB of 100 °C for 60 s was applied. The developer was MCB for 10 s. Samples with the ratio of crosslinker varied from 0.6 to 1.5 g, whilst the PAG was kept constant at 0.2 g per g of derivative were prepared and exposed as before. The sensitivities are shown in Table 4.1. As

the PAG concentration increased, the sensitivity decreased. Although this is unexpected, the results suggest that a higher PAG concentration may reduce the efficiency of the acid generated as seen elsewhere. [106] It was also observed that for a crosslinker concentration of less than 1 g per g of derivative, the resist did not fully crosslink. Increasing the ratio from 1 to 1.5 g allowed full crosslinking but did not increase the resist sensitivity.

TABLE 4.1 The effect of PAG and crosslinker concentration (per g of derivative), on the sensitivity of the chemically amplified C5/C0 resist, exposed at 20 keV, with PEB of 100 °C and 60 s, and developed in MCB for 10 s.

PAG (g)	HMMM (g)	Sensitivity (μC/cm^2)
0.2	1.0	5.0
0.3	1.0	6.5
0.4	1.0	7.5
0.2	0.6	Incomplete crosslinking
0.2	0.8	Incomplete crosslinking
0.2	1.0	5.0
0.2	1.3	4.8
0.2	1.5	6.5

4.2.4 Sensitivity dependence on PEB conditions

The effect of PEB temperature and duration on the sensitivity of the resist conditions were investigated. Samples with PAG and crosslinker concentrations of 0.2 and 1 g per g of derivative were exposed at 20 keV. After exposure, one set of samples was baked for 60 s at temperature varying from 90 to 115 °C whilst a second received a PEB of temperature 100 °C with duration ranging from 45 to 90 s. Each sample was developed in MCB for 10 s.

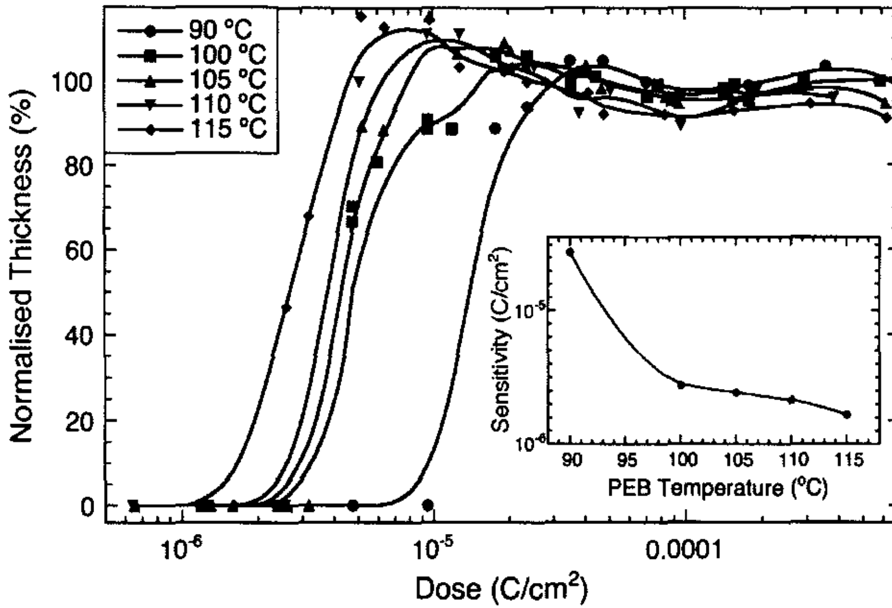

Figure 4.3 *The response of triphenylene derivative C5/C0+PAG03-01 +CL03-01 [1:0.2:1] exposed at 20 keV and developed in MCB as a function of PEB temperature (PEB time 60 s), with the sensitivity against temperature inset.*

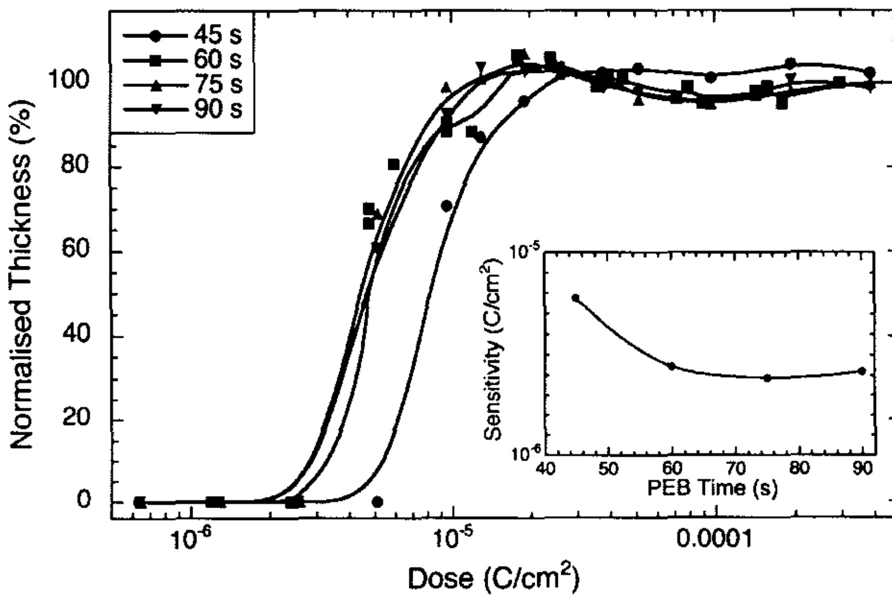

Figure 4.4 *The response of triphenylene derivative C5/C0+PAG03-01 +CL03-01 [1:0.2:1] exposed at 20 keV and developed in MCB as a function of PEB duration (PEB temperature 100 °C), with the sensitivity against time inset.*

The response curves presented in figure 4.3 show that, as expected, resist sensitivities improved with increased bake temperature, demonstrating that acid diffusion and/or the crosslinking reactions in this chemically amplified resist are thermally activated [46]. This is summarized in the insert to figure 4.3. Figure 4.4 shows that as PEB time is increased from 45 to 75 s, there is an increase in sensitivity, but that no further improvements are seen for PEB durations in excess of this. The insert to figure 4.4 summarizes the relationship between the PEB time and the sensitivity. The results point to an optimized resist sensitivity of at least 3 $\mu C/cm^2$.

4.3 Resolution

To examine the viability of the chemically amplified C5/C0 system for nanolithography, preliminary studies of fine patterning were conducted with the resist. Fine patterns were generated at 30 keV using the Raith pattern generator. Figure 4.5 shows an array of dots with a pitch of ~ 4 microns, patterned in a resist with PAG and crosslinker ratios of 0.2 and 1 g per g of derivative, at a dose of 1 fC/dot, with a PEB of 90 °C for 60 s and development in MCB for 10 s. The insert to figure 4.5 shows a single dot from the array, and it can be seen that the diameter is ~90 nm. However, it was found that the process latitude for fine patterning was extremely narrow. Figure 4.6(a) shows an array processed with the same conditions but at a dose of 2 fC/dot. It can be seen that whilst dots are clearly resolved at the edges of the pattern, the centre is extremely over-exposed. Furthermore, reducing the pitch to ~3 μm, and patterning at 1 fC/dot led to the same result, as shown in figure 4.6(b). Exposures of single features with slightly high doses, and longer PEB times or greater PEB temperatures also caused this apparent over-exposure, leading us to conclude that, rather than proximity effects, this is caused by extremely excessive acid diffusion in the thin films. No significant improvement was observed when a base compound was added to the resist mixture to reduce diffusion.

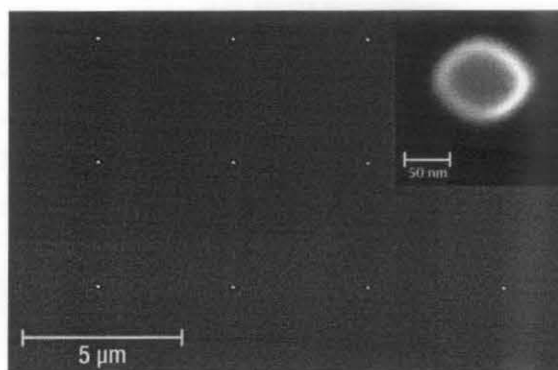

Figure 4.5 *SEM micrograph of an array of dot arrays, at a pitch of 4 microns, in CA triphenylene C5/C0 exposed at 30 keV with a dose of 1 fC/dot. Inset is a close up of one of the dots showing a feature size of 90 nm.*

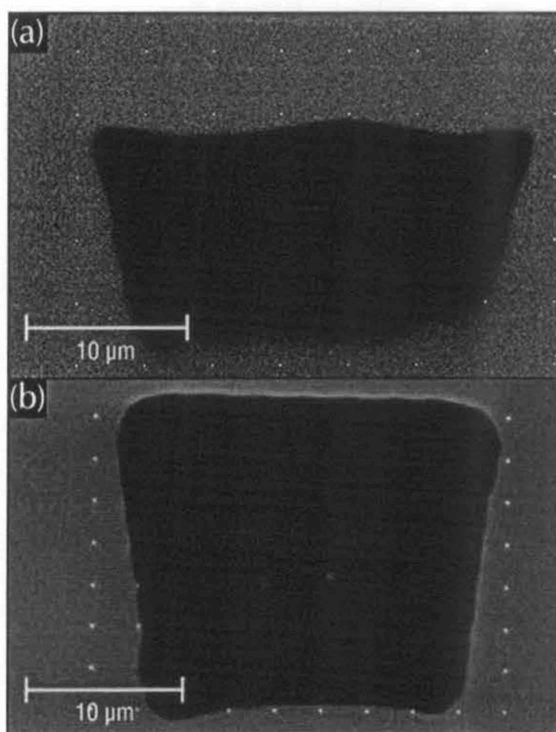

Figure 4.6 *SEM micrograph of (a) an array of 4 micron pitch dots exposed at 30 keV with a dose of 2 fC/dot and (b) an array of dots also exposed at 30 keV but with a dose of 1 fC/dot and a pitch of 3 microns, both showing significant acid diffusion..*

4.4 Etch Resistance

The etch resistance of the chemically amplified triphenylene was measured via electron cyclotron resonance microwave plasma (ECR) experiments. Etching was performed at ~25 °C with incident microwave power 250 W, RF power 20 W and a DC self-bias of 108 V. The etchant was SF_6, at a flow rate of 5 sccm and pressure of 1.0 mTorr. Rohm and Haas SAL 601, a conventional high durability novolac based negative resist, was used as a control. The normalized etch durability of the resist was found to be ~2.16 that of the silicon substrate for a range of component ratios and PEB conditions approaching that of SAL601 under the same conditions. [135]

4.5 Conclusions

We have explored chemical amplification of the triphenylene derivative, 2,6,10-trihydroxy-3,7,11-tri(pentyloxy) triphenylene, using triphenylsulfonium triflate as a photoacid generator, and hexamethoxymethyl melamine as a crosslinker. The chemically amplified mixture has a high sensitivity, increased by three orders of magnitude, compared with the pure material, to less than 5 $\mu C/cm^2$, in the optimal mixture and with the optimal PEB conditions. The optimal mixture was at 0.2 g and 1.0 g of PAG03-01 and CL03-01 per g of C5/C0. This is equivalent to ~0.26 mol PAG03-01 and ~1.37 mol CL03-01 per mol of C5/C0. Whilst the OH-rich derivative C0/C0 may have been more suitable for crosslinking, it was insoluble in $CHCl_3$, and therefore films could not be prepared. Chemical amplification of C5/C5 was unsuccessful. The observation suggests that the derivative C5/C0 provides a compromise between C0/C0 and C5/C5. The sensitivity enhancement of the chemically amplified C5/C0 compared to that of C5/C5 implies that the OH terminated addends in C5/C0 aided in the crosslinking of the resist during exposure and PEB.

The practicality of this CA molecular resist system as an etch mask was also demonstrated, with the material demonstrating a high durability against SF_6 plasma etching. However, a significant diffusion problem was seen, impairing the fine patterning capabilities, which must be addressed. This could be due to enhanced surface diffusion of the acid or incompatibility of the crosslinker and/or photoacid generator with the derivative leading to phase separation. This problem could be overcome by incorporating the crosslinker and/or photoacid generator into the resist structure.

5

Chemically Amplified Triphenylene Epoxide

This chapter discusses the results of chemical amplification of triphenylene derivative, 2,6,10-triethoxyoxirane-3,7,11-tris-pentyloxytriphenylene, a triphenylene with pendant epoxy groups to aid crosslinking. A cationic photoinitiator, bis[4-di(phenylsulfonio) phenyl]sulfide bis(hexafluorophoshate) was used for chemical amplification. The sensitivity of the negative tone pure triphenylene derivative, when exposed to an electron beam with energy 20 keV, is 600 $\mu C/cm^2$, which increases substantially to ~17 $\mu C/cm^2$ after chemical amplification. When used together with 2,6,10-trihydroxy-3,7,11-tri(pentyloxy) triphenylene, the sensitivity of the resist was further improved to ~7 $\mu C/cm^2$. The compound resist demonstrates a high durability against SF_6 plasma in electron cyclotron resonance microwave plasma etching, exhibiting a normalised etch durability of ~3.69 to the silicon substrate, better than that of Rohm and Haas SAL 601, a conventional novolac resist, under the same conditions. Patterns with a minimum feature size of ~40 nm were realized in the resist with a 30 keV electron beam.

The problem faced with the chemical amplification of C5/C0 discussed in chapter 4 could be due incompatibility of the crosslinker and/or photoacid generator used with the resist. To test this the derivative triphenylene epoxide (2,6,10-triethoxyoxirane-3,7,11-tris-pentyloxytriphenylene), shown in figure 2.3, with crosslinker incorporated into the structure of the resist was synthesised. Triphenylene epoxide (C5/epoxide) is similar to C5/C0 except that the OH addends has been replaced with three pendant epoxy groups – a commonly seen functionality in self crosslinking resists. C5/epoxide was developed specifically for this work to address concerns about the addition of a separate, possibly incompatible, crosslinker. [136] The photoacid generator triphenylsulfonium triflate, and photoinitiator, bis[4-di(phenylsulfonio) phenyl]sulfide bis(hexafluorophoshate), shown in figure 2.4 and figure 2.5 respectively, were used to sensitise the material for electron beam lithography.

5.1 Sensitivity

5.1.1 Sensitivity of C5/Epoxide

The C5/epoxide was dissolved in chloroform at a concentration of ~7 g/l and samples were prepared by spin coating on hydrogen-terminated silicon substrates. Film thickness was ~50 nm. The films were exposed at 20 keV and developed for 10 s in MCB. No PEB was applied. The response curve is shown in figure 5.1. The sensitivity of the pure C5/epoxide was measured to be ~600 $\mu C/cm^2$, an order of magnitude better than the pure triphenylene derivative, C5/C0, which has a sensitivity of 6.5 mC/cm^2.

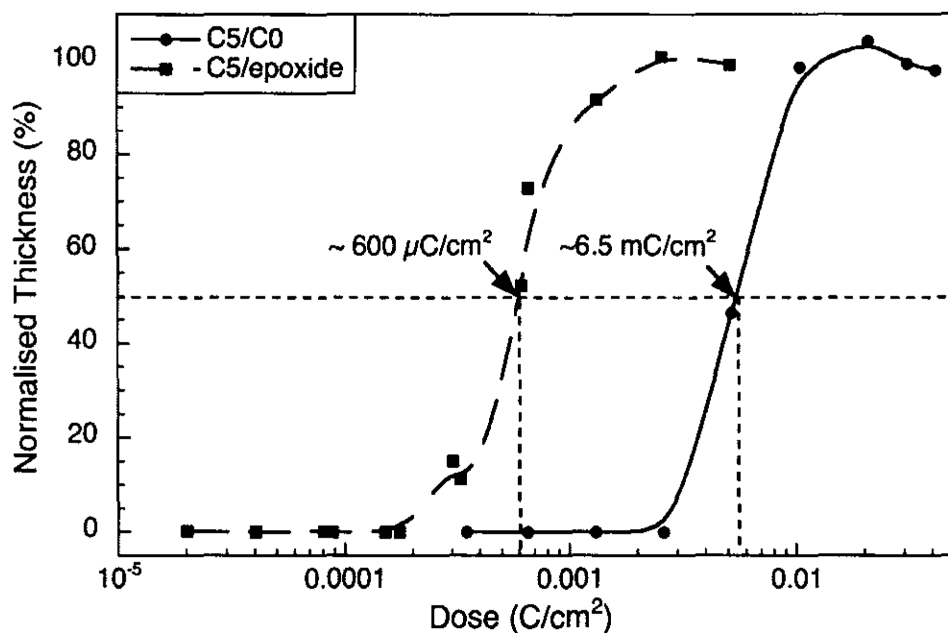

Figure 5.1 *Response curves of pure triphenylene derivative C5/C0 and C5/epoxide on exposure to 20 keV electrons and development in MCB.*

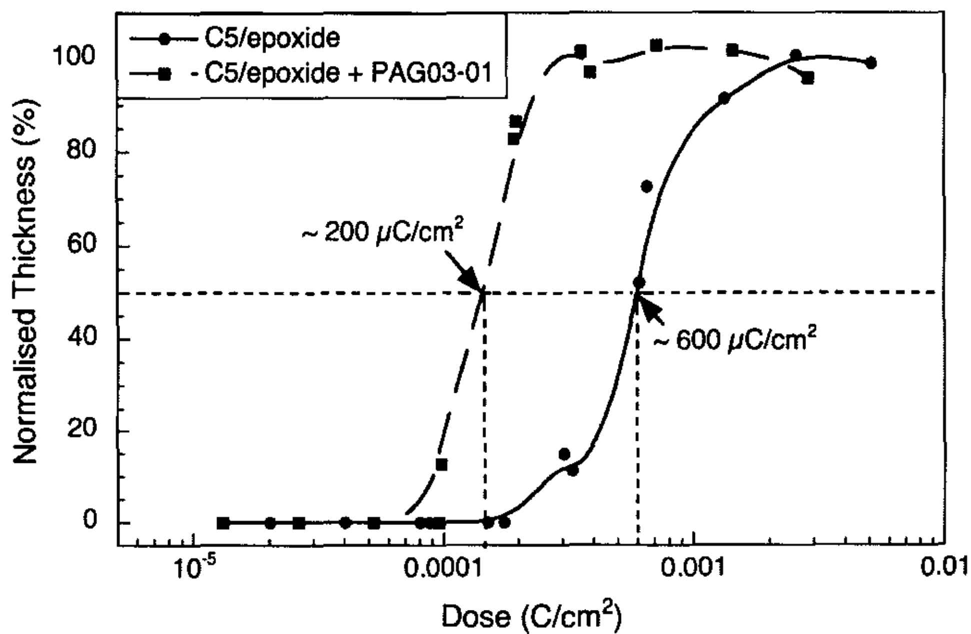

Figure 5.2 *Response curves of C5/epoxide and C5/epoxide+PAG03-01 on exposure to 20 keV electrons, PEB of 100 ℃ for 60 s (C5/epoxide+PAG03-01 only) and development in MCB.*

5.1.2 Sensitivity of C5/Epoxide + Photoacid generator

The photoacid generator PAG03-01 was added to C5/epoxide at a ratio of 0.3 g per g of derivative. Smooth films were prepared by spin coating on hydrogen-terminated silicon and were irradiated at 20 keV. A PEB of 100 °C for 60 s was applied, and development was in MCB. The response curve is plotted in figure 5.2. The sensitivity of the CA resist was ~200 $\mu C/cm^2$ a slight improvement compared to the pure derivative. Increasing the PAG to derivative mass ratio, up to 0.5 g per g of derivative gave no significant improvement in sensitivity. Increasing the PEB temperature and duration, up to 110 °C and 90 s respectively, was also ineffective.

5.1.3 Sensitivity of C5/Epoxide + Photoinitiator

The photoinitiator bis[4-di(phenylsulfonio) phenyl]sulfide bis(hexafluorophoshate), (PAG04-01), shown in figure 2.6, is commonly used for epoxide curing. The photoinitiator was combined with at 0.2 g per g of derivative. Films were spin coated on hydrogen terminated silicon and in this case a PAB of 70 °C for 10 min was applied. The films were irradiated at 20 keV, followed by a PEB of 100 °C for 60 s and development in MCB. The response curve is shown in figure 5.3. The sensitivity of the CA composition, ~90 $\mu C/cm^2$, is significantly better than the pure derivative. Increasing the photoinitiator concentration from 0.2 to 0.5 g per g of derivative improved the sensitivity further, but beyond that the sensitivity dropped. It can be seen from figure 5.3 that the resist with photoinitiator concentration of 0.5 g per g of derivative gives the best sensitivity at 15 $\mu C/cm^2$. This combination ratio is equivalent to ~0.2 mol PAG04-01 per mol C5/epoxide. The insert to figure 5.3 summarizes the relationship between the photoinitiator concentration and the sensitivity.

Further tests were carried out on this composition, applying various PEB temperatures and times. The highest sensitivity observed of ~12 μC/cm^2 was achieved with a PEB of 100 °C for 5 min.

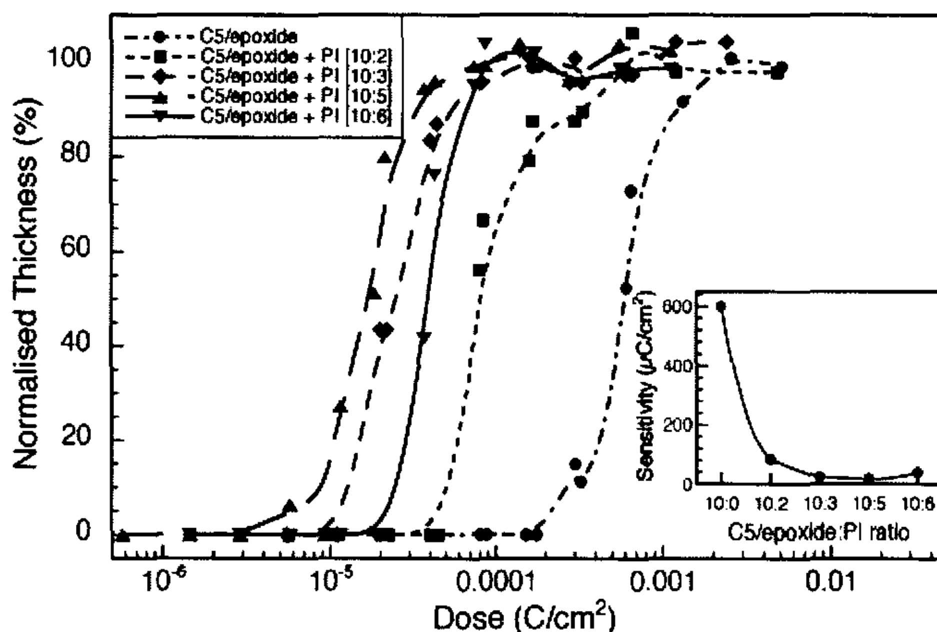

Figure 5.3 Response curves of C5/epoxide+photoinitiator at various ratios on exposure to 20 keV and development in MCB.

A proposed reaction scheme showing the mechanism for sensitivity enhancement is given in figure 5.4. Upon irradiation, the photoinitiator forms a Lewis acid, which initiates ring opening of the pendant epoxide chain on the C5/epoxide. This provides an electrophilic site for a crosslinking reaction with the benzene ring in the main triphenylene structure. This reaction also generates a hydrogen cation, which induces a further ring opening event.

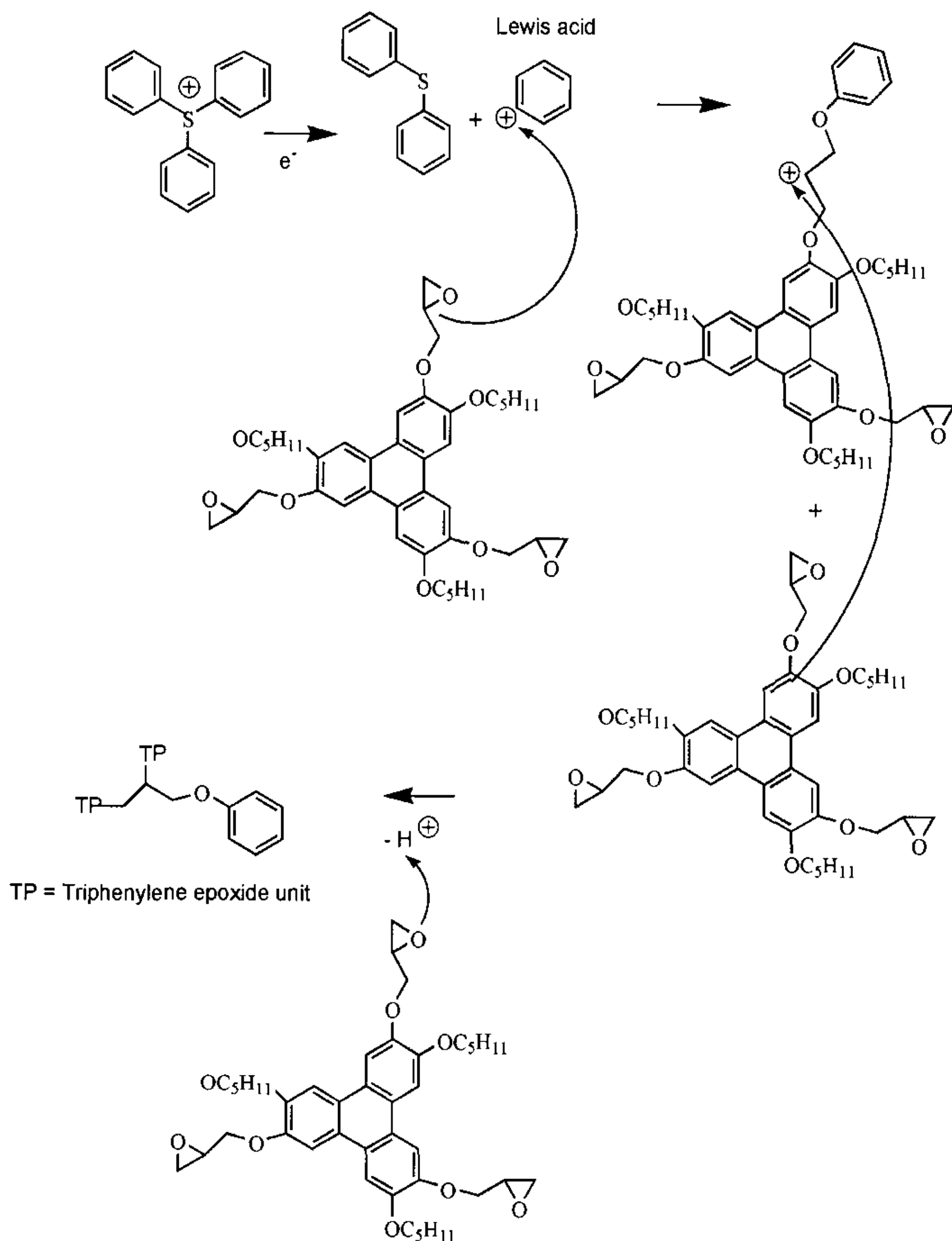

Figure 5.4 Chemical amplification scheme of the triphenylene epoxide using the photoinitiator, PAG04-01

5.1.4 Sensitivity of C5/Epoxide + C5/C0 + Photoinitiator

C5/C0, described in chapter 4, has somewhat better film formation properties than C5/epoxide. To improve the performance of the CA C5/epoxide resist, a composition incorporating C5/epoxide, C5/C0 and the photoinitiator at C5/C0 and photoinitiator concentrations of 0.7 and 1 g per g of C5/epoxide respectively, was prepared. The solution was spin coated on hydrogen terminated silicon, followed by a PAB of 70 °C for 5 min. Smooth films of ~40 nm thickness were produced. The films were irradiated at 20 keV, received a PEB of 100 °C for 60 s and were developed in MCB for 10 s. The response curve is shown in figure 5.5. The sensitivity of the 3 component resist was ~7.6 μC/cm^2.

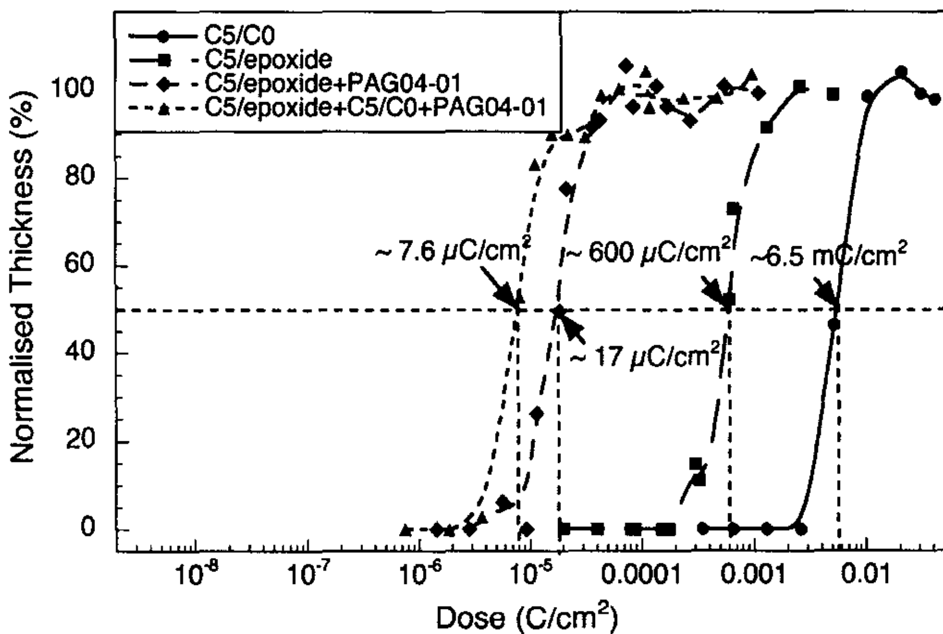

Figure 5.5 *Response curve of the composite resist C5/epoxide+C5/C0+photoinitiator compared to those of C5/epoxide+photoinitiator, C5/epoxide and C5/C0, on exposure to 20 keV and development in MCB. PEBs of 100 °C for 60 s were applied to C5/epoxide+C5/C0+photoinitiator and C5/epoxide+photoinitiator combinations.*

5.1.5 Sensitivity vs Beam Energy

The sensitivity of a resist is usually lower at higher beam energy, as discussed in section 1.5.3. To determine the relationship between sensitivity and beam energy for the composite C5/epoxide+C5/C0+PAG04-01, samples were exposed to 10, 20, 25 and 30 keV electrons. A PEB of 100 °C for 60 s was applied to all the samples, and development was in MCB. The response curves are shown in figure 5.6.

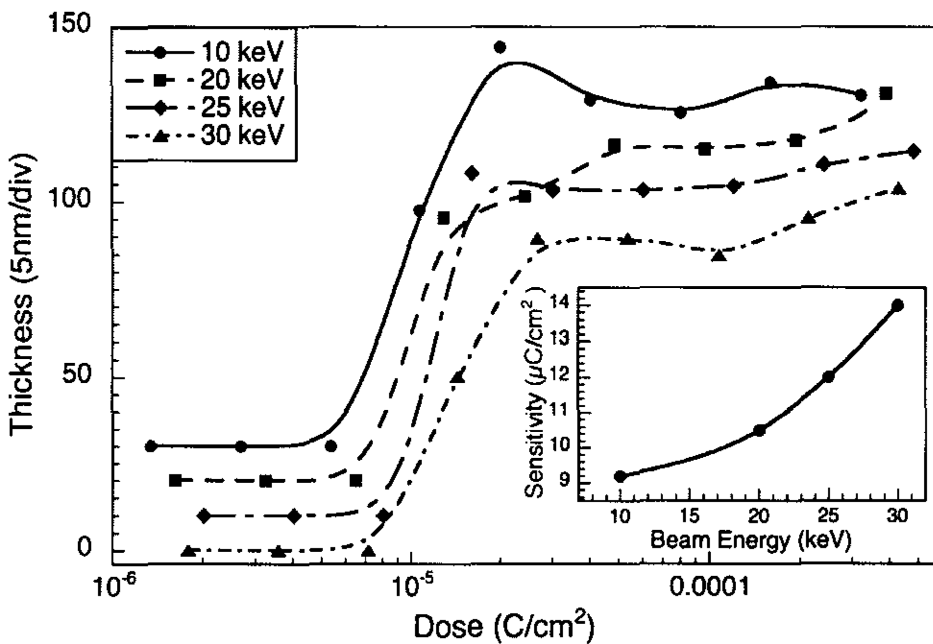

Figure 5.6 *Response curves of composite resist C5/epoxide+C5/C0 +PAG04-01 at various beam energies. PEB of 100 °C for 60 s was applied and development was in MCB. The curves have been distributed along the y-axis for clarity.*

5.2 Resolution

To ensure that chemical amplification of the resist improves sensitivity without sacrificing the triphenylene high-resolution capability, fine patterning was performed with the chemically

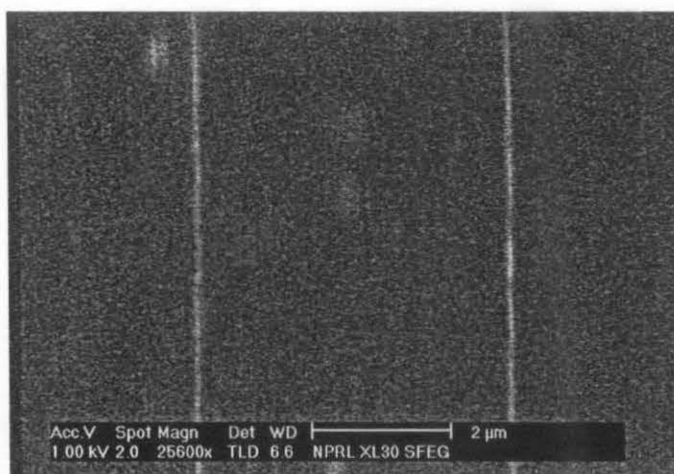

Figure 5.7 *SEM micrograph of line patterns after irradiation with electron dose of 600 pC/cm on C5/epoxide film with 0.5 g photoinitiator per g of derivative.*

amplified resist. C5/epoxide+PAG04-01 [2:1] (the highest sensitivity composition) was used. Patterning was done at 30 keV. A PEB of 100 °C for 2 min was applied, followed by development in MCB for 20 s and an IPA rinse. Linewidths of ~95 nm were fabricated using a dose of 600 pC/cm, as shown in figure 5.7.

Fine patterning was also performed in the C5/epoxide+C5/C0+PAG04-01 composite. The previously applied PAB compromised the patterning by roughening the film. When the PAB was discarded, linewidths of ~40 nm were achieved as shown in figure 5.8. PEB was 100 °C for 60 s, and development was in MCB for 10 s.

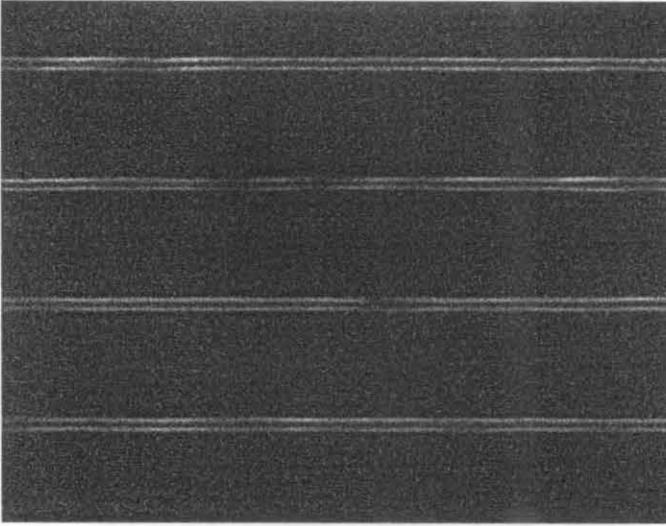

Figure 5.8 *SEM micrograph of line pattern after irradiation with line dose of 400 pC/cm on C5/epoxide+C5/C0+photoinitiator composite resist. Exposure was at 30 keV, PEB of 100 °C for 60 s was applied and development was in MCB.*

5.3 Etch Resistance

The etch durability of the composite resist was measured using electron cyclotron resonance (ECR) microwave plasma etching. The etching gas was SF_6 (flow rate: 5 sccm), with an incident microwave power of 250 W, and RF power 20 W. The DC bias was 114 V. The etch was run for 5 minutes. Rohm and Haas SAL601, a conventional high durability novolac based negative resist, was etched simultaneously as a control. It was found that the normalized etch durability of the resist is ~3.69 that of the silicon substrate, better than that of SAL 601 under the same conditions. [137]

5.4 Conclusions

The chemical amplification of a triphenylene derivative, 2,6,10-triethoxyoxirane-3,7,11-tris-pentyloxytriphenylene, using a cationic photoinitiator, bis[4-di(phenylsulfonio) phenyl]sulfide bis(hexafluorophoshate) was investigated. The epoxides on the derivative structure act as crosslinkers and the photoinitiator catalyses the crosslinking process on exposure to radiation. It was observed that having epoxides incorporated into the structure of the derivates improved the patterned images significantly as compared to using chemical amplification of C5/C0 using a separate crosslinker. Phase separation, which occurs when chemically dissimilar molecules within a material separated into homogeneous region could also be avoided. It was shown that chemical amplification increased the sensitivity of the derivative significantly to ~17 $\mu C/cm^2$. When the derivative C5/C0 was added to the resist system, its performance was further improved. The composite resist, comprising C5/epoxide and C5/C0 together with PAG04-01, was found to give the best combination of sensitivity and resolution. This results could be due to the OH addends in the C5/C0 providing more sites for crosslinking. The material is a negative tone resist with a sensitivity of ~7 $\mu C/cm^2$. A minimum feature size of ~40 nm was realized. The etch durability of the material is better than that of SAL601 under ECR etching.

6

Discussion and Outlook

Chemical amplification of several fullerene and triphenylene derivatives using a number of crosslinkers and photoacid generators has been studied. The sensitivities of some derivatives have been greatly improved by the incorporation of crosslinkers and photoacid generators. The chemically amplified MF03-04 fullerene resist has a sensitivity of 7 $\mu C/cm^2$ when exposed to 20 keV electrons, three orders of magnitude improvement over pure MF03-04, while maintaining a resolution below 30 nm. The chemically amplified C5/epoxide triphenylene resist also shows significant sensitivity enhancement to ~12 $\mu C/cm^2$ after chemical amplification. The composite C5/epoxide:C5/C0 triphenylene resist has a sensitivity of 7 $\mu C/cm^2$ and is capable of 40 nm linewidth.

6.1 Discussion and Conclusion

Chemical amplification of nine fullerene derivatives and three triphenylene derivatives was investigated. The response of the resists, in pure form, and chemically amplified, to electron beam irradiation was examined. Patterns were written in the chemically amplified resist films to determine their resolution. The effect of environmental contamination on exposed CA MF03-01 resists prior to PEB and development was investigated by varying the interval between exposure and PEB. The best PEB conditions for the CA C5/C0 resists were also determined by varying the temperature and time of post-exposure bake.

Pure MF02-01 resist shows a quite low sensitivity of ~460 μC/cm^2. Incorporation of both PAG and HMMM crosslinker increase its sensitivity by about 2 orders of magnitude. However, 'feathering' of the edges and roughing of the surface made it unsuitable for high resolution patterning. MAF5 with PAG and crosslinker showed an increase in sensitivity to ~150 μC/cm^2, compared to ~3 mC/cm^2 for pure MAF5. However, this is still a factor of 15 too low for industrial application. MF03-01 with PAG and HMMM demonstrates encouraging sensitivities as high as 9 μC/cm^2. This high sensitivity could be due to the number of addends in MF03-01, which is six times that of MAF5, which provides more crosslinking sites. Unfortunately, fine patterning of the film showed rounding of feature edges, which could be due to acid diffusion. The effects of environmental contamination on the sensitivity and features of the resist were demonstrated by increasing the interval between exposure and PEB. It was shown that the fidelity of the patterned features was reduced with increased delay. A control experiment, wherein the sample delayed under vacuum rather than in air, showed that the degradation was most likely due to molecular contaminants in the air than by acid diffusion during the interval, since the samples in air started to degrade between 1 and 10 minutes after exposure, whilst samples in vacuum last for at least 60 minutes before degrading.

Chemical amplification of the derivative MF03-04, demonstrated a significant sensitivity enhancement when the epoxy novolac crosslinker, CL05-03, and photoinitiator PAG04-01 were added. It was shown that increasing the crosslinker and photoinitiator concentration increased the sensitivity, reaching a maximum of 8 $\mu C/cm^2$ when 2 g crosslinker and 1 g photoinitiator per g of derivative were used. This CA resist also showed a high resolution, enabling linewidths of 24 nm to be fabricated in the resist, albeit with some swelling. ECR etching of the CA MF03-04 demonstrated a normalised etch durability of 2.55 that of the silicon substrate, approaching that of SAL601 under the same etch conditions. Although similar ombinations of CL05-03 and PAG04-01 with other fullerene derivatives MF03-01, MAF4 and MAF9 did increase their sensitivities, they are still low compared to that of the chemically amplified MF03-04. This results suggest that the improved sensitivity of the CA MF03-04 is influenced by the number of addends in the derivative, which is six times that of MAF4 or MAF5, providing more crosslinking sites, and to its functional groups (OH termination), which is not found in MF03-01 (also a hexaadduct) and not just the crosslinker and photoinitiator themselves. The success of CL05-03 in enhancing the sensitivity of MF03-04 could be due to the high number of epoxy groups in the crosslinker.

With the triphenylene derivatives, sensitivity enhancement was successful for the C5/C0 using CL03-01 as crosslinker and PAG03-01 as photoacid generator. The sensitivity of the CA resist was improved by more than 3 orders of magnitude from 6500 to ~5 $\mu C/cm^2$. However, fabrication of fine patterns in the resist was unsuccessful. Although sparse dot patterns close to 90 nm in diameter were realized, patterns with dense features and lines could not be defined. This is probably due to excessive diffusion of the acid. This problem was resolved by synthesizing a derivative with epoxide chains incorporated into the structure, C5/epoxide, together with the use of a different PAG. The pure C5/epoxide had a sensitivity of 600 $\mu C/cm^2$. Addition of the photoinitiator PAG04-01 improved its sensitivity to ~17 $\mu C/cm^2$, and linewidths of 100 nm were defined in the resist. The performance of the CA C5/epoxide as

compared to that of CA C5/C0 suggests that incorporating epoxide chains into the structure of the derivatives is more effective than using a separate crosslinker possibly since it helps to prevent phase separation. Incorporation of C5/C0 into the resist not only improved the smoothness of the films, but also improved the resolution to 40 nm and the sensitivity to ~7 $\mu C/cm^2$. This suggests that the OH functionality in C5/C0 aided in crosslinking. It was also found that the normalized etch durability of the resist is ~3.69 that of the silicon substrate, better than SAL601 under the same conditions.

The chemical amplification of fullerene derivatives has been demonstrated, with chemical amplification of methanofullerene MF03-04 using crosslinker CL05-03 and photoinitiator PAG04-01 giving the best sensitivity of 8 $\mu C/cm^2$ and a resolution of less than 30 nm. With the triphenylenes, a CA resist consisting of C5/epoxide, C5/C0 and the photoinitiator PAG04-01, a sensitivity of ~7 $\mu C/cm^2$, resolution of ~40 nm and a high etch durability was demonstrated. These characteristics are comparable if not better than most commercially available resists, as shown in Table 6.1.

6.2 Future Work

Further work on the chemically amplified resists could be done to improve their performance. Other developers should be investigated with the aim of improving sensitivity and resolution.

The effectiveness of chemical amplification of MF03-04 using epoxide crosslinker and photoinitiator suggest the possibility of similar schemes for other fullerene derivatives. It has also been shown that these derivatives have good etch resistance comparable to conventional novolac resists. Addition of epoxide pendants, as in the triphenylene derivative C5/epoxide, has shown its role in sensitivity enhancement for molecular resists whilst maintaining resolution. It may therefore be advantageous to attempt synthesis of fullerene derivatives with pendant epoxy functionality.

TABLE 6.1 Comparison of Resists

Resists	Tone	Sensitivity (e-beam energy)	Resolution	Etch Resistance	PAB
PMMA (non-CAR)	Positive	90 μC/cm² (20 keV)	5 nm	Very poor	Yes
SAL601	Negative	4 μC/cm² (20 keV)	20 nm	Good	Yes
SU-8	Negative	4 μC/cm² (20 keV)	30 nm	Moderate	Yes
UVIII	Positive	~40 μC/cm² (50 keV)	60 nm	-	Yes
UVN-2	Negative	30 μC/cm² (50 keV)	50 nm	-	Yes
UV-5	Positive	12 μC/cm² (50 keV)	50 nm	-	Yes
CA calixarene TOMCA4	Negative	15 μC/cm² (25 keV)	40 nm	Poor	Yes
CA MF03-04	Negative	~8 μC/cm² (20 keV)	24 nm	Good	No
CA C5/epoxide + C5/C0	Negative	~7 μC/cm² (20 keV)	40 nm	Very Good	No

Appendix A

This appendix provides the full chemical names of the methanofullerene and polysubstituted triphenylene derivatives described in this dissertation.

C_{60} Derivative Acronyms

MAF1	3'H-cyclopropa[1,9][5,6]fullerene-C_{60}-I_h-3',3'-carboxylic{2-(2-(2-(tetrahydropyran-2-yloxy)ethoxy)ethoxy)ethyl}ester
MAF4	3'*H*-Cyclopropa[1,9][5,6]fullerene-C_{60}-I_h-3',3'-carboxylic[2-(2-hydroxyethoxy) ethyl]ester
MAF5	3'H-cyclopropa[1,9][5,6]fullerene-C_{60}-I_h-3',3'-carboxylic{2-(2-methoxyethoxy) ethyl}ester
MAF9	3'H-cyclopropa[1,9][5,6]fullerene-C_{60}-I_h-3',3'-carboxylic{2-(2-chloroethoxy) ethyl}ester
MF02-01	3' H-cyclopropa [1, 9, 5, 6] fullerene-C60-Ih - 3', 3'- carboxylic [5-pentapentyloxyl triphenylene-2-yloxyl] pentyl ester: its mixture of adducts
MF03-01	3' H-cyclopropa [1, 9, 5, 6] fullerene-C60-Ih - 3', 3'-carboxylic [2-(2-methoxyethoxy) ethyl] ester: its mixture of adducts
MF03-04	3' H-cyclopropa [1, 9, 5, 6] fullerene-C60-Ih - 3', 3'- carboxylic [2-2-(2-hydroxyethoxy) ethoxyl ethyl] ester: its mixture of adducts
MF04-01	bis[2-(1-piperazinyl)pyridine C60monoepoxide
MF04-02	tetrakis[2-(1-piperazinyl)pyrimidine C60monoepoxide

Polysubstituted Triphenylene Derivative Acronyms

C0/C0	Hexa hydroxy triphenylene
C5/C0	2,6,10-trihydroxy-3,7,11-tri(pentyloxy) triphenylene
C5/C5	2,3,6,7,10,11-hexakis(pentyloxy) triphenylene
C5/epoxide	2,6,10-triethoxyoxirane -3,7,11-tris-pentyloxytriphenylene

List of Publications

1. H. Mohd Zaid, A.P.G. Robinson, R.E. Palmer, M. Manickam, and J.A. Preece, "Chemically amplified triphenylene derivative as a high sensitivity electron-beam resist". Submitted J. Vac. Sci. Technol. B.
2. A.P.G. Robinson, H. Mohd Zaid, F. Gibbons, R.E. Palmer, M. Manickam, J.A. Preece, R. Brainard, T. Zampini, K. O'Connell, "Chemically amplified molecular resists for electron beam lithography". MNE 2005
3. H. Mohd Zaid, A.P.G. Robinson, R.E. Palmer, M. Manickam, and J.A. Preece, "Chemical amplification of molecular triphenylene resists". To be submitted.
4. A.P.G. Robinson, H. Mohd Zaid, F. Gibbons, R.E. Palmer, M. Manickam, J.A. Preece, "Chemical amplification of fullerene resists". To be submitted

References:

[1] H. Ito, Jpn. J. Appl. Phys., **31**, 4273 (1992)

[2] M.C. Peckerar, F.K. Perkins, E.A. Dobisz, and O.J. Glembocki, *Handbook of Microlithography, Micromachining and Microfabrication Vol. 1*, P.Rai Chaudhury, ed., (IEE, London, 1997), p. 683

[3] G.E. Moore, Electronics, **38**, 114 (1965)

[4] K.F. Brennan, A.S. Brown, *Theory of Modern Electronic Semiconductor Devices*, (Wiley, New York, 2002), p. 1

[5] R.P. Feynman, Engineering and Science, **23**, 22 (1960)

[6] H.J. Levinson, W.H. Arnold, *Handbook of Microlithography, Micromachining, and Microfabrication Vol. 1*, P.Rai Chaudhury, ed., (IEE, London, 1997), p. 13

[7] A. Ledwith, *The Chemistry of The Semiconductor Industry,* S.J. Moss and A. Ledwith eds., (Blackie and Son Ltd, London, 1987), p. 175

[8] K. Ronse, Microelectron. Eng., **67/68**, 300, (2003)

[9] B.J. Lin, P. Rai-Choudhury, *Handbook of Microlithography, Micromachining, and Microfabrication Vol 1*, P. Rai Chaudhury, ed., (IEE, London, 1997), p. 4

[10] A.P.G. Robinson, Private Communication, (2003)

[11] G.M. Wallraff and W. D. Hinsberg, Chem. Rev., **99**, 1801 (1999)

[12] L. R. Harriott, Proc. IEEE, **89**, 366 (2001)

[13] R.L. Brainard, G.G. Barclay, E.H. Anderson, L.E. Ocola, Microelectron. Eng., **61/62**, 707 (2002)

[14] L.W. Liebmann, S.M. Mansfield, A.K. Wong, M.A. Lavin, W.C. Leipold, T.G. Dunham, IBM J. Res. Dev., **45**, 651 (2001)

[15] International Technology Roadmap for Semiconductors 2004 at http://public.itrs.net/

[16] T. Ito, S. Okazaki, Nature, **406**, 1027 (2000)

[17] S. Chan, Y. Li, L.J. Rothberg, B.L. Miller, P.M. Fauchet, Mat. Sci. Eng. C-Biomim., **15**, 277 (2001)

[18] P. Takhistov, Biosens. Bioelectron., **19**, 1445 (2004)

[19] J. Mulkens, J. McClay, B. Tirri, M. Brunotte, B. Mecking, H. Jasper, SPIE Proceedings, **5040**, 753 (2003)

[20] M. Rothschild, A.R. Forte, R.R. Kunz, S.C. Palmateer, J.H.C. Sedlacek, IBM J. Res. & Dev., **41**, 49 (1997)

[21] M. Switkes, R.R. Kunz, M. Rothschild, R.F. Sinta, M. Yeung, and S.-Y. Baek, J. Vac. Sci. Technol. B, **21**, 2794 (2003)

[22] B. Smith, OEmagazine, **4**, 22 (2004)

[23] D. Gil, T.A. Brunner, C. Fonseca, N. Seong, B. Streefkerk, C. Wagner, M. Stavenga, J. Vac. Sci. Technol. B, **22**, 3431 (2004)

[24] C.W. Gwyn, R. Stulen, D. Sweeney and D. Attwood, J. Vac. Sci. Technol. B, **16**, 3142 (1998)

[25] R.H. Stulen, Microelectron. Eng., **46**, 19 (1999)

[26] S. Vaidya, D. Sweeney, R. Stulen, D. Attwood, *Inter. Symposium on VLSI Technol., Systems, and Applications*, 1999, p127

[27] R.D. Piner, J. Zhu, F. Xu, S. Hong, C.A. Mirkin, Science, **283**, 661 (1999)

[28] L.J. Guo, J. Phys. D. Appl. Phys. **37**, R123 (2004)

[29] M.D. Austin, H. Ge, W. Wu, M. Li, Z. Yu, D. Wasserman, S.A. Lyon, S.Y. Chou, Appl. Phys. Lett., **84**, 5299 (2004)

[30] J. Melngailis, A.A. Mondelli, I.L. Berry III and R. Mohondro, J. Vac. Sci. Technol. B, **16**, 927 (1998)

[31] F. Cerrina, *Handbook of Microlithography, Micromachining and Microfabrication Vol. 1*, P.Rai Chaudhury, ed., (IEE, London, 1997), p. 253

[32] G. Simon, A.M. Haghiri-Gosnet, J. Bourneix, D. Decanini, Y. Chen, F. Rousseaux, H. Launois and B. Vidal, J. Vac. Sci. Technol. B, **15**, 2489 (1997)

[33] J.P. Silverman, J. Vac. Sci. Technol. B, **15**, 2117 (1997)

[34] M.A. McCord and M.J. Rooks, *Handbook of Microlithography, Micromachining, and Microfabrication Vol 1*, P.Rai Chaudhury, ed., (IEE, London, 1997), p. 142

[35] E.D. Roberts, *The Chemistry of the Semiconductor Industry*, S.J. Moss and A. Ledwith eds., (Blackie and Son Ltd, London, 1987), p. 197

[36] S.D. Berger, J.M. Gibson, R.M. Camarda, R.C. Farrow, H.A. Huggins, J.S. Kraus and J.A. Liddle, J. Vac. Sci. Technol. B, **9**, 2996 (1991)

[37] L.R. Harriott, J. Vac. Sci. Technol. B, **15**, 2130 (1997)

[38] T.F. Teepen, A.H.V. van Veen, A. van Zuuk, C.Th.H. Heerkens, M.J. Wieland and P. Kruit, *Micro and Nano Eng. 2004 International Conference* (2004), p. 412

[39] B.J. Kampherbeek, M.J. Wieland, A. van Zuuk and P. Kruit, Microelectron. Eng., **53**, 279 (2000)

[40] R.S. Dhaliwal et al, IBM J. Res. Dev., **45**, 615 (2001)

[41] H.C. Pfeiffer, R.S. Dhaliwal, S.D. Golladay, S.K. Doran, M.S. Gordon, T.R. Groves, R.A. Kendall, J.E. Lieberman, P.F. Petric, D.J. Pinckney, R.J. Quickle, C.F. Robinson, J.D. Rockrohr, J.J. Senesi, W. Stickel, E.V. Tressler, A. Tanimoto, T. Yamaguchi, K. Okamoto, K. Suzuki, T. Okino, S. Kawata, K. Morita, S.C. Suziki, H. Shimizu, S. Kojima, G. Varnell, W.T. Novak, D.P. Stumbo and M. Sogard, J. Vac. Sci. Technol. B., **17**, 2840 (1999)

[42] H.C. Pfeiffer, Microelectron. Eng., **53**, 61 (2000)

[43] T. Utsumi, Jpn. J. Appl. Phys., **38**, 7046 (1999)

[44] T. Utsumi, J. Vac. Sci. Technol. B, **17**, 2897 (1999)

[45] CASINO, Monte Carlo Simulation Software, at http://www.gel.usherbrooke.ca/casino/index.html

[46] S. Manako, J. Fujita, Y. Ochiai, E. Nomura and S. Matsui, Jpn. J. Appl. Phys., **36**, 7773 (1999)

[47] A.P.G. Robinson, PhD thesis, University of Birmingham, UK, 1999

[48] W. Henschel, Y.M. Georgiev, and H. Kurz, J. Vac. Sci. Technol. B, **21**, 2018 (2003)

[49] N.P. Hacker, MRS Bull., **22**, 33 (1997)

[50] M. Aktary, M.O. Jensen, K.L. Westra, M.J. Brett and M.R. Freeman, J. Vac. Sci. Technol. B, **21**, L5 (2003)

[51] S. Yasin, D.G. Hasko, and H. Ahmed, Appl. Phys. Lett., **78**, 2760 (2001)

[52] D.R. Medeiros, A. Aviram, C.R. Guarnieri, W.-S. Huang, R. Kwong, C.K. Magg, A.P. Mahorowala, W. M. Moreau, K.E. Petrillo, M, Angelopoulos, IBM J. Res. & Dev. **45**, 639 (2001)

[53] S. Matsuda, Polym. Eng. Sci., **17**, 410 (1977)

[54] T. Tada and T. Kanayama, J. Vac. Sci. Technol. B, **13**, 2801 (1995)

[55] M.J. Word, H. Adesida and P.R. Berger, J. Vac. Sci. Technol B, **21**, L12 (2003)

[56] M. Peuker, M.H. Lim, H.I. Smith, R. Morton, A.K. van Langen-Suurling, J. Romijn, E.W.J.M. van der Drift, F.C.M.J.M. van Delft, Microelectron. Eng., **61/62**, 803 (2002)

[57] I. Junarsa, M.P. Stoykovich, P.F. Nealey, Y. Ma, F. Cerrina and H.H. Solak, J. Vac. Sci. Technol B, **23**, 138 (2005)

[58] F.C.M.J.M. van Delft, J.P. Weterings, A.K. van Langen-Suurling and H. Romijn, J. Vac. Sci. Technol. B, **18**, 3419 (2000)

[59] C-C. Yang and W-C. Chen, J. Mater. Chem., **12**, 1138 (2002)

[60] T. Ishii, T. Tamamura, and K. Shigehara, Jpn. J. Appl. Phys., **39**, L1068 (2000)

[61] T. Ishii, Y. Murata, and K. Shigehara, Jpn. J. Appl. Phys., **40**, L478 (2001)

[62] G.P. Patsis, E. Gogolides and K. Van Werden, Jpn. J. Appl. Phys., **44**, 6341 (2005)

[63] J. Fujita, Y. Ohnishi, Y. Ochiai, E. Nomura, and S. Matsui, J. Vac. Sci. Technol. B, **14**, 4272 (1996)

[64] S. Yasin and D.G. Hasko, J. Vac. Sci. Technol. B, **19**, 311 (2001)

[65] S. Manako, Y. Ochiai, H. Yamamoto, T. Teshima, J. Fujita, and E. Nomura, J. Vac. Sci. Technol. B, **18**, 3424 (2000)

[66] N. Kihara, S. Saito, T. Ushirogouchi, M. Nakase, J. Photopolym. Sci. Technol. **11**, 553 (1998)

[67] T. Tada and T. Kanayama, Jpn J. Appl. Phys., **35**, L63 (1998)

[68] A.P.G. Robinson, R.E. Palmer, T. Tada, T. Kanayama, J.A. Preece, D. Philp, U. Jonas, F. Deiderich, Chem. Phys. Lett., **289**, 586 (1998)

[69] A.P.G. Robinson, R.E. Palmer, T. Tada, T. Kanayama, J.A. Preece, Appl. Phys. Lett., **72**, 1302 (1998)

[70] T. Tada, T. Kanayama, A.P.G. Robinson, R.E. Palmer, M.T. Allen, J.A. Preece, and K.D.M. Harris, Microelectron. Eng., **53**, 425 (2000).

[71] A.P.G. Robinson, R.E. Palmer, T. Tada, T. Kanayama, M.T. Allen, J.A. Preece, K.D.M. Harris, J. Vac. Sci. Technol. B, **18**, 2730 (2000)

[72] H. Sailer, A. Ruderisch, D.P. Kern, V. Schurig, J. Vac. Sci. Technol. B, **20**, 2958 (2002)

[73] A. Ruderisch, H. Sailer, V. Schurig, D.P. Kern, Microelectron. Eng., **67-68**, 292 (2003)

[74] J. Fujita, Y. Ohnishi, S. Manako, Y. Ochiai, E. Nomura, T. Sakamoto, S. Matsui, Jpn. J. Appl. Phys., **36**, 7769 (1997)

[75] N. Kihara, S. Saito, T. Ushirogouchi, M. Nakase, J. Photopolym. Sci. Technol., **11**, 553 (1998)

[76] S. Saito, N. Kihara, T. Ushirogouchi, Microelectron. Eng., **61/62**, 777 (2002)

[77] H.W. Kroto, J.R. Heath, S.C. O'Brien, R.F. Curl and R.E. Smalley, Nature, **318**, 162 (1985)

[78] A.P.G. Robinson, R.E. Palmer, T. Tada, T. Kanayama, E.J. Shelley, D. Philp, J.A. Preece, Chem. Phys. Lett., **312**, 469 (1999)

[79] T. Tada, K. Uekusa, T. Kanayama, T. Nakayama, R. Chapman, W. Y. Cheung, L. Eden, I. Hussain, M. Jenning, J. Perkins, M. Phillips, J. A. Preece, E. Shelley, Microelectron. Eng., **61-62**, 737 (2002)

[80] A.P.G. Robinson, R.E. Palmer, T. Tada, T. Kanayama, M.T.Allen, J.A. Preece, and K.D.M. Harris, J. Phys. D. Appl. Phys., **32**, L75 (1999)

[81] H. Ito, J. Polym. Sci., **41**, 3863 (2003)

[82] H. Ito, IBM J. Res. Dev., **41**, 69, (1997)

[83] W.D. Hinsberg, G.M. Wallraff, R.D. Allen et al, *Kirk-Othmer Encyclopedia of Chemical Technology*, *Vol 15*, (John Wiley & Sons Inc., 1998), p 10

[84] H. Liu, M.P. deGrandpre, W.E. Feely, J. Vac. Sci. Technol. B, **6**, 379 (1988)

[85] T. Yoshimura, Y. Nakayama, and S. Okazaki, J. Vac. Sci. Technol. B, **10**, 2615 (1992)

[86] P.M. Dentinger and J.W. Taylor, J. Vac. Sci. Technol. B, **15**, 2632 (1997)

[87] P.M. Dentinger, C.M. Nelson, S.J. Rhyner, J.W. Taylor, T.H. Fedynyshyn and M.F. Cronin, J. Vac. Sci. Technol. B, **14**, 4239 (1996)

[88] N. Glezos, G.P. Patsis, A. Rosenbusch and Z. Cui, Microelectron. Eng., **41/42**, 319 (1998)

[89] G.P. Patsis and N. Glezos, J. Vac. Sci. Technol. B, **20**, 1303 (2002)

[90] I. Raptis, Jpn. J. Appl. Phys., **36**, 6562 (1997)

[91] T. Azuma, K. Masui, Y. Takigami, H. Sasaki, K. Sakai, T. Nomaki, Y. Kato, and I. Mori, Jpn. J. Appl. Phys., **30**, 3138 (1991)

[92] Z.C.H. Tan, T. Stivers, H. Lem, N. DiGiacomo, D. Wood, J. Vzc. Sci. Technol. B, **13**, 2539 (1995)

[93] V. Kudryashov, X.-C. Yuan, W.-C. Cheong, K. Radhakrishnan, Microlectron. Eng., **67-68**, 306 (2003)

[94] A. Pépin, V. Studer, D. Decanini, Y. Chen, Microelectron. Eng., **73-74**, 233 (2004)

[95] F.C.M.J.M. van Delft and F.G. Holthuysen, Microelectron. Eng., **46**, 383 (1999)

[96] D. Macintyre and S. Thoms, Microelectro. Eng., **35**, 213 (1997)

[97] Z. Cui and P. Prewett, Microelectron. Eng., **46**, 255 (1999)

[98] Z. Cui, A. Gerardino, M. Gentili, and E. DiFabrizio, J. Vac. Sci. Technol. B, **16**, 3284 (1998)

[99] H. Sailer, A. Ruderisch, W. Henschel, V. Schurig, J. Vac. Sci. Technol. B., **22**, 3485 (2004)

[100] H. Sailer, A. Ruderisch, D.P. Kern, V. Schurig, Microelectronic Engineering, **73/74**, 228 (2004)

[101] S. Saito, N. Kihara and T. Ushirogouchi, *Proc. Int. Conf. Microprocess. Nanotechnol.*, 1999, p82

[102] K. Hashimoto, Akiko Katsuyama, Masayuki Endo and Masaru Sasago, J. Vac. Sci. Technol. B, **12**, 37 (1994)

[103] T. Yoshimura, H. Shiraishi and S. Okazaki, Jpn. J. Appl. Phys., **34**, 6786 (1995)

[104] E. Reichmanis, F. M. Houlihan, 0. Nalamasu, and T. X. Neenan, Chem. Mater., **3**, 394 (1991)

[105] K. E. Petrillo, A.T.S. Pomerene, E.D. Babich, D.E. Seeger, D. Hofer, G. Breyta, H. Ito, J. Vac. Sci. Technol. B, **12**, 3863 (1994)

[106] A.R. Pawloski and P.F. Nealey, J. Vac. Sci. Technol. B, **20**, 2413 (2002)

[107] H. Wu and K.E. Gonsalves, Adv. Funct. Mater., **11**, 271 (2001)

[108] M.A. Ali, K.E. Gonzales, A. Agrawal, A. Jeyakumar, and C.L. Henderson, Microelectron. Eng., **70**, 19 (2003)

[109] L. Schlegel, T. Ueno, N. Hayashi and T. Iwayanagi, J. Vac. Sci. Technol. B, **9**, 278 (1991)

[110] E. Ainley, K. Nordquist, D. Resnick, D. Carr, and R. Tiberio, Microelectron. Eng., **46**, 375 (1999)

[111] S. Manako, Y. Ochiai, J. Fujita, N. Samoto, and S. Matsui, Jpn. J. Appl. Phys., **33**, 6993 (1994)

[112] W. Henshel, Y. M. Georgiev, H. Kurz, J. Vac. Sci. Technol. B, **21**, 2018 (2003)

[113] J-B. Kim, J-H Choi, Y-G Kwon, M-H Jung, K-H Chang, Polym. Commun., **40**, 1087 (1999)

[114] K. Petrillo, J. Bucchignano, M. Angelopoulos, K. Cornett and W. Brunsvold, J. Vac. Sci. Technol. B, **16**, 3709 (1998)

[115] F.W. Sears, M.W. Zemansky and H.D. Young, *College Physics, Seventh Edition,*, (Addison-Wesley, Reading, Mass., 1991), p. 469

[116] L. Pain, B. Scarfogliere, S. Tedesco, C. Gourgon, J.P. Coulomb, M. Morin and M. Riberio, Microelectron. Eng., **57-58**, 511 (2001)

[117] J. Nakamura, H. Ban and A. Tanaka, Jpn. J. Appl. Phys., **31**, 4294 (1992)

[118] M. Cheng, E. Croffie, L. Yuan, and A. Neureuther, J. Vac. Sci. Technol. B, **18**, 3318 (2000)

[119] M. Cheng, L. Yuan, E. Croffie, and A. Neureuther, J. Vac. Sci. Technol. B, **20**, 734 (2002)

[120] M.A. McCord, T.H. Newman, J. Vac. Sci. Technol. B, **10**, 3083 (1992)

[121] P.A. Peterson, Z.J. Radzimski, S.A. Schwalm, and P.E. Russell, J. Vac. Sci. Technol. B, **10**, 3088 (1992)

[122] S. Yasin, D.G. Hasko, and H. Ahmed, J. Vac. Sci. Technol. B, **17**, 3390 (1999)

[123] T. Ishii, H. Nozawa, T. Tamamura, Appl. Phys. Lett., **70**, 1110 (1997)

[124] S. Migitaka, J. Yamamoto, S-i. Uchino, M. Hashimoto, F. Murai and H. Shiraishi, Jpn. J. Appl. Phys., **39**, 1387 (2000)

[125] S. Saito, N. Kihara, T. Naito, M. Nakase, T. Nakasugi and Y. Kato, SPIE Proceedings, **3049**, 659 (1997)

[126] H. Ito, M. Ueda, and R. Schwalm, J. Vac. Sci. Technol. B, **6**, 2259 (1988)

[127] T. Watanabe, Y. Yamashita, T. Kozawa, Y. Yoshida, and S. Tagawa, J. Vac. Sci. Technol. B, **12**, 3879 (1994)

[128] T. Asakura, H. Yamato, A. Matsumoto, P. Murer, and M. Ohwa, SPIE Proceedings, **5039**, 1155 (2003)

[129] T. Ueno, H. Shiraishi, N. Hayashi, K. Tadano, E. Fukuma, and T. Iwayanagi, SPIE Proceedings, **1262**, 26 (1990)

[130] The Philips XL FEG SEM Operating Manual, Philips, section 2-1

[131] Dektak3ST Surface Profiler Manual, Veeco Systems, p. 13

[132] J.M. Shaw, J.D. Gelorme, N.C. LaBianca, W.E. Conley, and S.J. Holmes, IBM J. Res. Dev., **41**, 81 (1997)

[133] Unnormalised etch rate was 1/2.52 that of silicon for CA MF03-04 and 1/2.96 that of silicon for SAL601

[134] H. Ito, IBM J. Res. Dev., **45**, 683 (2001)

[135] Unnormalised etch rate was 1/2.3 that of silicon for CA C5/C0 and 1/3.2 that of silicon for SAL601

[136] H. Mohd Zaid, A.P.G. Robinson, R.E. Palmer, M. Manickam, and J.A. Preece, Submitted J. Vac. Sci. Technol. B.

[137] Unnormalised etch rate was 1/3.64 that of silicon for CA C5/epoxide and 1/2.96 that of silicon for SAL601